

**EVALUATING LEAD CHEMISTRY UNDER VARIABLE WATER
QUALITY CONDITIONS**

by

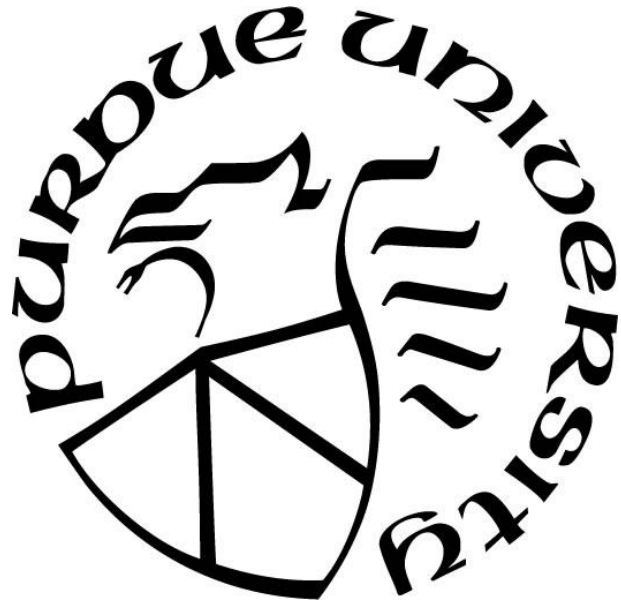
Mackenzie Davies

A Thesis

Submitted to the Faculty of Purdue University

In Partial Fulfillment of the Requirements for the degree of

Master of Science in Engineering



Division of Environmental and Ecological Engineering

West Lafayette, Indiana

May 2020

THE PURDUE UNIVERSITY GRADUATE SCHOOL
STATEMENT OF COMMITTEE APPROVAL

Dr. Inez Hua, Co-chair

Lyles School of Civil Engineering &
Division of Environmental & Ecological Engineering

Dr. Amisha Shah, Co-chair

Lyles School of Civil Engineering &
Division of Environmental & Ecological Engineering

Dr. Chad Jafvert

Lyles School of Civil Engineering &
Division of Environmental & Ecological Engineering

Approved by:

Dr. John Sutherland

*To my family
Distance is no match for the heart*

ACKNOWLEDGMENTS

I would like to thank my advisors, Dr. Inez Hua and Dr. Amisha Shah, for your support and guidance. You have taught me so much about professionalism, how to lead a classroom, and how to be a good researcher.

Thank you to my lab mates and office mates. I'm thankful for the friendships we have formed, and I know that we all helped each other get to where we are today. Holly, Rachel, Kun, Mahsa, Calvin, Omar, Kelsey, and Marya – I appreciate all the joy and struggles we have gone through together.

Thank you to the other staff and faculty members in EEE, especially Dr. Nadezhda Zyaykina, Dr. Larry Nies and Dr. Chad Jafvert. I appreciated the opportunity to learn from and teach under you all. Thank you for the lab, engineering, and life lessons.

Book Club, Sojos, and God of Covenant family - You have been so supportive amidst your own work and it's been fun to grow with each other. Thanks for teaching me about myself and the Lord.

Thank you to my family who have kept up support through distance. You are so important to me and my sanity. Thanks for your patience and love during these past few years. Morgan, you have been one of my biggest supporters. Your friendship, support, and loyalty have meant so much to me. Sisterhood has been good for us. I love you all immensely!

- Philippians 1:6 –

“And I am certain that God, who began the good work within you, will continue his work until it is finally finished on the day when Christ Jesus returns.”

TABLE OF CONTENTS

LIST OF TABLES	8
LIST OF FIGURES	11
LIST OF ABBREVIATIONS	14
ABSTRACT	15
1. INTRODUCTION	16
1.1 Lead regulations in drinking water	16
1.2 Lead contamination: Case studies	16
1.3 Lead speciation in a distribution system	18
1.3.1 Oxidation States of Lead	18
1.3.2 Lead Complexation Chemistry in the Dissolved Phase	18
1.3.3 Precipitation Reactions of Lead	19
1.3.4 Effect of pH and Alkalinity	20
1.3.5 Effect of ORP	21
1.3.6 Impact of ionic strength	22
1.4 Water heaters	22
1.5 Water softeners	24
1.6 Quantification of Dissolved Lead	26
1.7 Study Objectives	27
1.8 References	27
2. TEMPERATURE AND pH DEPENDENCE OF SOLUBLE LEAD	33
2.1 Introduction	33
2.2 Materials & Methods	33
2.2.1 Standards, Reagents, and Preparation of Stocks	33
2.2.2 Experimental Procedure	34
2.2.3 Analytical Methods	35
2.3 Equilibrium Thermodynamic Parameters	38
2.4 Results & Discussion	40
2.4.1 Effect of nitrogen sparging	40

2.4.2	Effect of pH and temperature on soluble lead in kinetic experiments.....	41
2.4.3	Effect of pH and temperature on soluble lead at equilibrium.....	47
2.5	Conclusions.....	55
2.6	Future Work.....	56
2.7	References.....	56
3.	IONIC STRENGTH DEPENDENCE OF SOLUBLE LEAD	59
3.1	Introduction.....	59
3.2	Materials & Methods	60
3.2.1	Standards, Reagents, & Preparation of Stocks	60
3.2.2	Experimental Procedure and Sample Analysis	60
3.3	Results & Discussion	61
3.3.1	Effect of ionic strength on kinetic experiments	61
3.3.2	Effect of ionic strength on equilibrium experiments	63
3.4	Conclusions.....	74
3.5	References.....	74
4.	CARBONATE DEPENDENCE OF SOLUBLE LEAD	76
4.1	Introduction.....	76
4.2	Methods & Materials	77
4.2.1	Standards, Reagents & Preparation of Stocks	77
4.2.2	Experimental Procedure.....	78
4.3	Results & Discussion	78
4.3.1	Effect of carbonate concentration on kinetic experiments	78
4.3.2	Effect of carbonate concentration on equilibrium experiments.....	80
4.4	Conclusion	93
4.5	References.....	93
5.	METHOD TO DETERMINE LEAD DIOXIDE CONCENTRATION	95
5.1	Introduction.....	95
5.2	Methods & Materials	96
5.2.1	Standards, Reagents, & Preparation of Stocks	96
5.2.2	Experimental Procedure.....	96
5.3	Results & Discussion	97

5.4 Conclusions & Future Work	100
5.5 References.....	101
6. CONCLUSIONS	103
6.1 Future work & application	104
APPENDIX A: TABULATED THERMODYNAMIC & EQUILIBRIUM VALUES	105
APPENDIX B: DETERMINATION OF ICP-OES ANALYSIS WAVELENGTH.....	107
APPENDIX C: EXPERIMENTAL KINETIC & EQUILIBRIUM DATA.....	109
APPENDIX D. IODOMETRIC METHOD.....	123

LIST OF TABLES

Table 1.1. Relevant reactions of lead (Pb) oxidation states.....	18
Table 1.2. Complexation reactions of lead (Pb) with relevant species & ions.	19
Table 1.3. Precipitation reactions of lead (Pb) with relevant species & ions.	20
Table 2.1. Standard Pb curve data. Raw intensity (output) was compared to the known Pb in vial (input).....	35
Table 2.2. Enthalpy of reaction (ΔH), and equilibrium constants (K) for a variety of relevant Pb compounds in drinking water. Sections labeled with a dash (-) refer to unavailable data.	40
Table 2.3. Ionic strength calculation for speciation model with $Pb_{Total} = 9.7 \times 10^{-7}$ at pH 7.0....	48
Table 2.4. Activity coefficients calculated for speciation model.....	49
Table 2.5. Equilibrium constants and β values for relevant complexes of Pb in a Pb-H ₂ O system.	51
Table 2.6. * K_{s0} values for relevant solids used in the speciation model for the Pb-H ₂ O system.	52
Table 2.7. Long-term equilibrium experiment recovery as a function of temperature and pH. ...	54
Table 3.1. Ionic strength calculations for speciation at I = 0.02 M, pH 7.0, T = 25°C.....	61
Table 3.2. Activity coefficients for Pb-H ₂ O-NaCl system at I = 0.02-0.15 M, pH 7.0, T = 25°C.	64
Table 3.3. Equilibrium and complexation constants for relevant Pb species in Pb-H ₂ O-NaCl closed system.	67
Table 3.4. Equilibrium solubility constants for relevant solids used in the speciation model.....	69
Table 3.5. Average factors of change for each lead complex (right) with predominating solid (top) when comparing system at $I = 8.5 \times 10^{-6}$ M to 0.02 M. No chloride complexes included because NaCl present at low ionic strength.....	70
Table 3.6. Average factors of change for each lead complex (right) with predominating solid (top) when comparing system at I = 0.02 M to 0.15 M.	70
Table 3.7. Long-term equilibrium Pb recovery as a function of ionic strength.....	73
Table 4.1. Activity coefficients for Pb-H ₂ O-CO ₂ system at C _t = 0.01-0.14 M (I = 0.01-0.21 M), pH° 7.0, T = 25°C.....	81
Table 4.2. Equilibrium and complexation constants for relevant Pb species in Pb-H ₂ O-CO ₂ closed system with changes in I due to varying C _t	83
Table 4.3. Equilibrium solubility constants for relevant solids used in the speciation model.....	85

Table 4.4. Average factors of change for each lead complex (right) with predominating solid (top) when comparing system at $C_t = 0$ M to 0.07 M ($I = 8.5 \times 10^{-6}$ M to 0.09 M). No carbonate complexes included because no carbonate was present at low ionic strength.....	88
Table 4.5. Average factors of change for each lead complex (right) with predominating solid (top) when comparing system at $C_t = 0.07$ M to 0.14 M ($I = 0.09$ M to 0.21 M).	88
Table 4.6. Long-term equilibrium Pb recovery as a function of carbonate concentration.	91
Table 5.1. Summary of experimental input parameters and results comparing Zhang et al. (2010) and this work [6].....	99
Table A.1. Thermodynamic data for relevant Pb species: standard enthalpy of formation.....	105
Table A.2. Thermodynamic data for relevant Pb species: standard Gibbs free energy of formation.	106
Table B.1. ICP-OES output data at various wavelengths. Sixteen (16) replicates of eight (8) standards ranging from 1.0-20 ppb Pb were analyzed to determine the most accurate wavelength for Pb analysis. Standard deviation (STD Dev), relative standard deviation (RSD), limit of quantitation (LOQ), and instrument detection limit (IDL) were determined from the output data.	107
Table C.1. Kinetic data output from ICP-OES at pH 5.0, T = 25°C within glovebox.....	109
Table C.2. Kinetic and equilibrium data output from ICP-OES at pH 2.9-3.1, T = 25°C.....	109
Table C.3. Kinetic and equilibrium data output from ICP-OES at pH 3.0-3.1, T = 55°C.....	110
Table C.4. Kinetic and equilibrium data output from ICP-OES at pH 4.8-5.6, T = 25°C.....	111
Table C.5. Kinetic and equilibrium data output from ICP-OES at pH 4.0-5.2, T = 55°C.....	112
Table C.6. Kinetic and equilibrium data output from ICP-OES at pH 5.5-7.4, T = 25°C.....	112
Table C.7. Kinetic and equilibrium data output from ICP-OES at pH 4.1-6.8, T = 55°C.....	113
Table C.8. Kinetic and equilibrium data output from ICP-OES at pH 6.5-8.4, T = 25°C.....	114
Table C.9. Kinetic and equilibrium data output from ICP-OES at pH 4.9-8.9, T = 55°C.....	114
Table C.10. Kinetic and equilibrium data output from ICP-OES at pH 7.0-9.8, T = 25°C.....	115
Table C.11. Kinetic and equilibrium data output from ICP-OES at pH 4.4-9.5, T = 55°C.....	115
Table C.12. Kinetic and equilibrium data output from ICP-OES at $I = 0.02$ M, pH 7.0, T = 25°C.	117
Table C.13. Kinetic and equilibrium data output from ICP-OES at $I = 0.07$ M, pH 7.0, T = 25°C.	117
Table C.14. Kinetic and equilibrium data output from ICP-OES at $I = 0.15$ M, pH 7.0, T = 25°C	118

Table C.15. Kinetic and equilibrium data output from ICP-OES at $C_t = 0.01 \text{ M}$, $I = 0.01 \text{ M}$, $\text{pH}^{\circ} 7.0$, $T = 25^{\circ}\text{C}$. Not included in final data set.	120
Table C.16. Kinetic and equilibrium data output from ICP-OES at $C_t = 0.07 \text{ M}$, $I = 0.09 \text{ M}$, $\text{pH}^{\circ} 7.0$, $T = 25^{\circ}\text{C}$	121
Table C.17. Kinetic and equilibrium data output from ICP-OES at $C_t = 0.14 \text{ M}$, $I = 0.21 \text{ M}$, $\text{pH}^{\circ} 7.0$, $T = 25^{\circ}\text{C}$	122
Table D.1. Summary of results from iodometric method experiments. Organized by original mass added of $\text{PbO}_{2(\text{s})}$. Recovery ranged from 53-103% of original mass, with average $81 \pm 10.8\%$, excluding over-recovered samples.....	124

LIST OF FIGURES

Figure 1.1. Schematic of residential electric tank water heater.	23
Figure 1.2. Schematic of residence with water softener and water heater. Lead (Pb) enters residential plumbing through distribution system.....	24
Figure 1.3. Schematic of residential ion-exchange water softener system.	25
Figure 2.1. Standard curve with ICP-OES lead samples with linear correlation between Pb in vial (ppb) vs. ICP-OES response (cps).	36
Figure 2.2. Comparison of soluble lead (Pb) at pH 4.8-5.6 under variable atmospheric conditions: open to atmosphere with nitrogen sparging (black points) or in a nitrogen-sparged glovebox (“GB”, red points). $Pb_{Total} = 9.7 \times 10^{-7}$ M and low $I = 8.5 \times 10^{-6}$ M.	41
Figure 2.3. Changes in soluble lead (Pb) concentration (left axis, squares) and pH reported (right axis, triangles) for pH 3.0 over 48 hours. Kinetic data compared against temperature at (A) 25°C, pH 2.9-3.1 and (B) 55°C, pH 3.0-3.1.	42
Figure 2.4. Changes in soluble lead (Pb) concentration (left axis, square) and pH reported (right axis, triangle) for pH 4.4-5.3 over 48 hours. Kinetic data compared against temperature at (A) 25°C, pH 4.8-5.3 and (B) 55°C, pH 4.4-5.2.	43
Figure 2.5. Changes in soluble lead (Pb) concentration (left axis, square) and pH reported (right axis, triangle) for pH 4.0-5.3 over 48 hours. Kinetic data compared against temperature at (A) 25°C, pH 5.7-7.4 and (B) 55°C, pH 4.8-6.8.	44
Figure 2.6. Changes in soluble lead (Pb) concentration (left axis, square) and pH reported (right axis, triangle) for pH 5.6-8.9 over 48 hours. Kinetic data compared against temperature at (A) 25°C, pH 6.8-8.1 and (B) 55°C, pH 5.6-8.9.	45
Figure 2.7. Changes in soluble lead (Pb) concentration (left axis, square) and pH reported (right axis, triangle) for pH 6.8-9.8 over 48 hours Kinetic data compared against temperature (A) 25°C, pH 7.3-9.8 and (B) 55°C, pH 6.8-9.5.	46
Figure 2.8. Soluble lead concentration over time. Comparison at T = 25°C from pH 2.9-9.8. Error bars removed for readability.	46
Figure 2.9. Soluble lead concentration over time. Comparison at T = 55°C from pH 3.0-9.5. Error bars removed for readability.	47
Figure 2.10. pC-pH diagram for the Pb-H ₂ O system at 25°C when either PbO _(s) or Pb(OH) _{2(s)} predominates. $Pb_{Total} = 9.7 \times 10^{-7}$ M and low $I = 8.5 \times 10^{-6}$ M.	53
Figure 2.11. Comparison of experimental equilibrium solubility of Pb at various pH values with speciation model. Total dissolved Pb (Pb_{TOT}^{II} , M) over range of pH with PbO _(s) and Pb(OH) _{2(s)} predominating at 25°C with $Pb_{Total} = 9.7 \times 10^{-7}$ M and low $I = 8.5 \times 10^{-6}$ M.	54

Figure 3.1. Measurement of soluble lead (Pb_{TOT}^{II}) over time at pH 7.0, 25°C with (A) $I = 8.5 \times 10^{-6}$ M, (B) $I = 0.02$ M, (C) $I = 0.07$ M, (D) $I = 0.15$ M.....	62
Figure 3.2. Comparison of soluble Pb measured in experimental reactors for 48 hours; $I = 8.5 \times 10^{-6}$ to 0.15 M at pH = 7.0, T = 25°C.....	63
Figure 3.3. pC-pH diagram for the Pb-H ₂ O system at pH = 7.0, 25°C when either $PbO_{(s)}$ or $Pb(OH)_{2(s)}$ predominates. $Pb_{Total} = 9.7 \times 10^{-7}$ M and $I = 8.5 \times 10^{-6}$ M.....	71
Figure 3.4. pC-pH diagram for the Pb-H ₂ O-NaCl system at pH = 7.0, 25°C when either $PbO_{(s)}$ or $Pb(OH)_{2(s)}$ predominates. $Pb_{Total} = 9.7 \times 10^{-7}$ M and $I = 0.02$ M.....	71
Figure 3.5. pC-pH diagram for the Pb-H ₂ O-NaCl system at pH = 7.0, 25°C when either $PbO_{(s)}$ or $Pb(OH)_{2(s)}$ predominates. $Pb_{Total} = 9.7 \times 10^{-7}$ M and $I = 0.15$ M.....	72
Figure 3.6. Long-term equilibrium model for all controlling solids in Pb-H ₂ O-NaCl system under different ionic strength conditions, ranging from 8.5×10^{-6} M to 0.15 M. Experimental points taken at 6 weeks are plotted on model lines.....	73
Figure 4.1. Measurement of soluble lead (Pb_{TOT}^{II}) over time at pH 7.0, 25°C with (A) $C_t = 0$ M, $I = 8.5 \times 10^{-6}$ M, (B) $C_t = 0.07$ M, $I = 0.09$ M (C) $C_t = 0.14$ M, $I = 0.21$ M.....	79
Figure 4.2. Soluble Pb in reactor with varying C_t from 8.5×10^{-6} M to 0.14 M. $Pb_{Total} = 9.7 \times 10^{-7}$ M at 25°C and pH = 7.0.....	80
Figure 4.3. pC-pH diagram for the Pb-H ₂ O-CO ₂ system at pH = 7.0, 25°C when either $PbO_{(s)}$ or $Pb(OH)_{2(s)}$ predominates at $C_t = 0$ M. $Pb_{Total} = 9.7 \times 10^{-7}$ M and $I = 8.5 \times 10^{-6}$ M.....	86
Figure 4.4. pC-pH diagram for the Pb-H ₂ O-CO ₂ system at pH = 7.0, 25°C when either $PbO_{(s)}$ or $Pb(OH)_{2(s)}$ predominates at $C_t = 0.07$ M. $Pb_{Total} = 9.7 \times 10^{-7}$ M and $I = 0.09$ M.....	87
Figure 4.5. pC-pH diagram for the Pb-H ₂ O-CO ₂ system at pH = 7.0, 25°C when either $PbO_{(s)}$ or $Pb(OH)_{2(s)}$ predominates at $C_t = 0.14$ M. $Pb_{Total} = 9.7 \times 10^{-7}$ M and $I = 0.21$ M.....	87
Figure 4.6. pC-pH diagram for the Pb-H ₂ O-CO ₂ system at pH = 7.0, 25°C when $PbCO_3{}_{(s)}$ predominates at $C_t = 0.07$ M. $Pb_{Total} = 9.7 \times 10^{-7}$ M and $I = 0.09$ M.....	89
Figure 4.7. pC-pH diagram for the Pb-H ₂ O-CO ₂ system at pH = 7.0, 25°C when $PbCO_3{}_{(s)}$ predominates at $C_t = 0.14$ M. $Pb_{Total} = 9.7 \times 10^{-7}$ M and $I = 0.21$ M.....	89
Figure 4.8. pC-pH diagram for the Pb-H ₂ O-CO ₂ system at pH = 7.0, 25°C when $Pb_3(CO_3)_2(OH)_{2(s)}$ predominates at $C_t = 0.07$ M. $Pb_{Total} = 9.7 \times 10^{-7}$ M and $I = 0.09$ M.....	90
Figure 4.9. pC-pH diagram for the Pb-H ₂ O-CO ₂ system at pH = 7.0, 25°C when $Pb_3(CO_3)_2(OH)_{2(s)}$ predominates at $C_t = 0.14$ M. $Pb_{Total} = 9.7 \times 10^{-7}$ M and $I = 0.21$ M.....	91
Figure 4.10. Long-term equilibrium model plotted as pC-pH diagram for all solids in Pb-H ₂ O-CO ₂ system under various C_t conditions (listed in legend). Experiments measured at 6 weeks plotted as points on model lines. $Pb_{Total} = 9.7 \times 10^{-7}$ M, $C_t = 0-0.14$ M with corresponding $I = 8.5 \times 10^{-6}-0.21$ M.....	92

Figure 5.1. Results of iodometric experiment with 7.05 mg/L (3.4×10^{-5} M) Pb shown as the dashed line with 0.5 mg/L Cl ₂ . Recovery over time shown as points. Maximum recovery of 85% original Pb at 20 minutes.....	98
Figure 5.2. Plot showing the recovery of PbO ₂ from 0.06-15.0 mg/L Pb with free chlorine = 0.5 mg/L as Cl ₂ , KI = 2.0 g/L, temp = 25°C, pH = 2.0. Specific experiment recoveries are reported in Table D.1 in Appendix D.....	100
Figure B. 1. Experimental set to determine accurate wavelength for ICP-OES analysis of Pb. Due to consistency and accuracy of measurement, the author chose 220.353 nm.....	108
Figure D.1. Determination of PbO _{2(s)} via triiodide measurement using the iodometric method. Experiment duration of 60 minutes to ensure full recovery of Pb over time.....	123

LIST OF ABBREVIATIONS

C _p	Heat capacity
H	Enthalpy
I	Ionic strength
K	Equilibrium constant
ppb	Part(s) per billion
ppm	Part(s) per million
STP	Standard temperature and pressure

ABSTRACT

Lead has long been identified as a health issue in the United States. Government regulations limit the amount of lead allowed in distribution pipes, fittings and residential plumbing systems, but lead leaching problems persist as water quality changes or new technologies are implemented. In this work, experiments were developed to determine the effect of temperature, ionic strength, and carbonate concentrations on soluble lead concentrations over relevant pH ranges. Equilibrium models were developed to predict changes in soluble lead and the predominating solid(s) that form under these varied water quality conditions. Additional experiments were also performed to verify how effectively $\text{PbO}_{2(\text{s})}$, a lead(IV) solid, could be measured using a colorimetric method. Results for the kinetic experiments tested over a period of 48 hours found that an increase in temperature from 25°C to 55°C brought a decrease in soluble lead (i.e. increased lead precipitation) across a pH range of 3.0-9.8. Increasing ionic strength (NaCl) as well as increasing the total carbonate concentrations in these solutions at 25°C resulted in higher measured soluble lead over 48 hours at pH 7.0 than the same kinds of experiments without these variables. In the solutions containing lead with and without NaCl and NaHCO_3 , no solid was modeled to predominate in equilibrium (6 week analysis). Since several of the 6-week experiments measured lower levels of soluble lead than originally added, the systems were unlikely to be at equilibrium. Additionally, the previously developed iodometric method proved to be a feasible method of quantifying $\text{PbO}_{2(\text{s})}$ in water with 80-88% accuracy. These findings may have important implications towards how lead behaves in in-home water heaters or softeners.

1. INTRODUCTION

1.1 Lead regulations in drinking water

In spite of its presence in potable water distribution systems, lead (Pb) has long been known as a toxicant [1]. Health-related research concerning drinking water contamination in the past few decades has revealed more about the toxicity of Pb. In response, the United States Environmental Protection Agency (USEPA) established the Safe Drinking Water Act (SDWA) of 1974 [2]. Exposure may lead to cognitive and development issues, as well as infant mortality and stillbirths [1],[3],[4]. Pb contamination in drinking water accounts for approximately 14-20% of Pb exposures in the U.S. [5]. The SDWA limited newly-constructed water systems with leaded components, where “Pb free” materials had no more than 0.2% Pb solder and flux and no more than 8% Pb in pipes themselves. Further revisions have lowered the Pb-free content in wetted surfaces from 8% to 0.25% and also restricted non-Pb free pipes, solder and joints from entering the market [2]. The 1986 amendments to the SDWA included passing additional regulations for communities and non-transient non-community water systems in order to ensure safe water to people in both urban and rural areas. The main source of Pb in potable distribution systems today is a result of leaching either from preexisting Pb pipes (Pb service lines), solder, fittings, and joints or the small percentage of Pb in pipes and components installed after 1986 [6]–[10]. As of this amendment, new construction does not include fully leaded components.

The Lead and Copper Rule (LCR, 1991) was a follow-up regulation by the USEPA to limit the amount of lead and copper in drinking water by adding 15 ppb as the action level [5]. The action level is defined as the contaminant level at which the water distribution authority is required to act to inhibit corrosion and inform the public about safe preventative measures [5]. They must minimize Pb levels below the action level using corrosion controls, additional treatment, or full line replacement [5]. Additionally, the LCR reduced the 50 ppb maximum contaminant level goal (MCLG) for Pb to zero to further limit adverse health effects and corrosion hot spots [5].

1.2 Lead contamination: Case studies

Several incidents in the U.S. exemplify how lead can contaminate drinking water systems. In one example, Washington, D.C. residents experienced long-term exposure to Pb in water due to a

change in disinfectant. Typical disinfectants used in the US include chlorine and chloramines. Free chlorine has high oxidation-reduction potential (ORP) but a shorter residence time than one type of chloramine, monochloramine, which is comprised of chlorine and ammonia. Washington, D.C.'s utility had been using free chlorine but switched to chloramines in 2000 when disinfectant byproducts began to be a concern [11]. When using free chlorine, the pipe layers passivated with insoluble Pb chlorides and other highly oxidized Pb solids (i.e. PbO_2) [12],[13]. Once the free chlorine was no longer keeping the electrochemical potential of the water in the higher range, the solids began to break down [12]. Soluble Pb leached from the pipes and entered people's homes, resulting in elevated blood lead levels (BLLs) in children, up to four times the amount found in children drinking uncontaminated water [14],[15].

In another case study, elevated BLLs in Greenville and Durham, North Carolina were a result of high amounts of particulate Pb found in the water in 2006. In this case, the utilities had changed the chemical coagulant from alum to ferric chloride, disrupting the steady state chloride to sulfate mass ratio (CSMR) [16],[17]. A year passed between detecting the alarming BLLs in children and the authorities responding in proper corrective action. One child's lead test in Greenville, NC returned 20 $\mu\text{g}/\text{dL}$ Pb in his blood (compared to the CDC's limit of concern at the time, 10 $\mu\text{g}/\text{dL}$) [16],[18] .

From each of these scenarios, water quality played a large role on the changes in Pb speciation. Any number of changes – from disinfectant to corrosion inhibitor, pH to alkalinity – affected these distinct systems in dramatic ways. One of the most recent examples of Pb contamination in the U.S. occurred in Flint, MI in 2014. The city changed its water source from a Detroit water district to save money, but the new source was a naturally more corrosive water [19]. The new source water, the Flint River, had an overall lower pH than the older source [20]. Additionally, the new district did not add in any phosphate buffer for corrosion control while the previous one had [19]. The internal pipe lining, a passivating layer of phosphate that distanced the water from the pipe material, degraded over time without continuing addition [20]. Within a few months of the changing to the Flint River water, residents of Flint were complaining of discolored and foul-tasting water. The lack of a passivating layer along with acidic water created ideal conditions for Pb leaching from the pipes [20]. The problem escalated with Pb levels measured over 25 ppb across the city, with some reaching concentrations over 1,000 ppb [21]. BLLs of children in Flint increased significantly after the exposure [22].

1.3 Lead speciation in a distribution system

1.3.1 Oxidation States of Lead

Pb speciation in water is highly dependent on water quality conditions; therefore, a considerable amount of literature has investigated how Pb chemical speciation is affected by these water quality conditions. Pb exists naturally in the environment as Pb(II) and Pb(IV), but its various forms include both solid and dissolved species (Table 1.1, Table 1.2, Table 1.3) Additionally, Pb tends to exist in the Pb(II) oxidation state in water distribution systems, which is mostly due to the high ORP required to change Pb(II) into Pb(IV) [23].

Table 1.1. Relevant reactions of lead (Pb) oxidation states.

#	Reaction	log K _{eq}	Source
1.1	$\text{Pb}_{(\text{s})}^0 \rightleftharpoons \text{Pb}_{(\text{aq})}^{2+} + 2\text{e}^-$	-0.13	[24]
1.2	$\text{Pb}_{(\text{aq})}^{4+} + 2\text{e}^- \rightleftharpoons \text{Pb}_{(\text{aq})}^{2+}$	28.64	[25]

References: [24] MINEQL+, [25] Benjamin

1.3.2 Lead Complexation Chemistry in the Dissolved Phase

As a positively charged ion, lead readily binds with anionic hydroxides, oxides, chlorides, phosphates, sulfates and carbonates in potable water systems. The following reactions form the foundation for models that are documented in later chapters to determine speciation of Pb over varied pH. In relevant pH ranges with good aeration, Pb in drinking water tends to form oxide, hydroxide and carbonate species, outlined in Table 1.2 below [26]. While water does not attack lead, aerated water allows the formation of many Pb(II) compounds.

Soluble hydroxide complexes form in water at neutral to high pH values. Additionally, higher alkalinity can contribute to hydroxide concentration, whether natural or added chemically at a treatment plant. Alkalinity is defined as acid neutralizing capacity and is outlined in the following equation:

$$\text{Alk}_t = [\text{HCO}_3^-] + 2[\text{CO}_3^{2-}] + [\text{OH}^-] - [\text{H}^+]$$

Eq. 1.1

Chlorination for disinfection can form soluble Pb chloride complexes. This set of complexation reactions (1.9-1.12) is a direct result of chlorination (HOCl/OCl^-), which increases the amount of available chloride ions in the water. Water containing atmospheric carbon dioxide can allow the reaction forming Pb(II) bicarbonate. Another source of carbonaceous compounds is due to alkalinity.

Table 1.2. Complexation reactions of lead (Pb) with relevant species & ions.

#	Reaction	$\log K_{\text{eq}}$	Source
1.3	$\text{H}_2\text{O} \leftrightarrow \text{H}^+ + \text{OH}^-$	-14	[24]
Hydroxides			
1.4	$\text{PbOH}_{(\text{aq})}^+ \rightleftharpoons \text{Pb}_{(\text{aq})}^{2+} + \text{OH}^-$	6.4	[24],[25],[27]
1.5	$\text{Pb}(\text{OH})_2^0_{(\text{aq})} \rightleftharpoons \text{Pb}_{(\text{aq})}^{2+} + 2\text{OH}^-$	4.5	[27]
1.6	$\text{Pb}(\text{OH})_3^-_{(\text{aq})} \rightleftharpoons \text{Pb}_{(\text{aq})}^{2+} + 3\text{OH}^-$	3.0	[25],[27],[28]
1.7	$\text{Pb}(\text{OH})_4^{2-}_{(\text{aq})} \rightleftharpoons \text{Pb}_{(\text{aq})}^{2+} + 4\text{OH}^-$	-11.9	[25]
Chlorides			
1.8	$\text{HOCl} \rightleftharpoons \text{OCl}^- + \text{H}^+$	-7.60	[25]
1.9	$\text{PbCl}_{(\text{aq})}^+ \rightleftharpoons \text{Pb}_{(\text{aq})}^{2+} + \text{Cl}^-$	1.550	[29]
1.10	$\text{PbCl}_2_{(\text{aq})} \rightleftharpoons \text{Pb}_{(\text{aq})}^{2+} + 2\text{Cl}^-$	0.650	[29]
1.11	$\text{PbCl}_3^-_{(\text{aq})} \rightleftharpoons \text{Pb}_{(\text{aq})}^{2+} + 3\text{Cl}^-$	-0.400	[29]
1.12	$\text{PbCl}_4^{2-}_{(\text{aq})} \rightleftharpoons \text{Pb}_{(\text{aq})}^{2+} + 4\text{Cl}^-$	-0.340	[29]
Carbonates			
1.13	$\text{H}_2\text{CO}_3^- \rightleftharpoons \text{H}^+ + \text{HCO}_3^-$	-6.35	[24]
1.14	$\text{HCO}_3^- \rightleftharpoons \text{H}^+ + \text{CO}_3^{2-}$	-10.33	[24]
1.15	$\text{PbCO}_3^0_{(\text{aq})} \rightleftharpoons \text{Pb}_{(\text{aq})}^{2+} + \text{CO}_3^{2-}$	6.478	[24]
1.16	$\text{Pb}(\text{CO}_3)_2^-_{(\text{aq})} \rightleftharpoons \text{Pb}_{(\text{aq})}^{2+} + 2\text{CO}_3^{2-}$	3.460	[24]
1.17	$\text{PbHCO}_3^+_{(\text{aq})} \rightleftharpoons \text{Pb}_{(\text{aq})}^{2+} + \text{CO}_3^{2-} + \text{H}^+$	13.20	[25]

References: [24] MINEQL+, [25] Benjamin, [27] Lind, [28] Bilinski, [29] Brezonik

1.3.3 Precipitation Reactions of Lead

Given the right conditions, lead may settle out to form solids listed in Table 1.3. The literature cited below elucidates these relationships more thoroughly, citing the effects of various water quality conditions on the formation of different lead solids.

Table 1.3. Precipitation reactions of lead (Pb) with relevant species & ions.

#	Reaction	$\log K_{eq}$	Source
Oxides			
1.18	$PbO_{(s)(yellow)} + 2H^+ \rightleftharpoons Pb_{(aq)}^{2+} + H_2O$	12.91	[24]
1.19	$PbO_{2(s)} + 4H^+ + 2e^- \leftrightarrow Pb^{2+} + H_2O + \frac{1}{2}O_{2(aq)}$	-8.91	[23],[24]
Hydroxide			
1.20	$Pb(OH)_{2(s)}^0 \rightleftharpoons Pb_{(aq)}^{2+} + 2OH^-$	8.15	[30]
Carbonates			
1.21	$PbCO_{3(s)}^0 \rightleftharpoons Pb_{(aq)}^{2+} + CO_3^{2-}$	-13.13	[28]
1.22	$Pb_3(CO_3)_2(OH)_{2(s)} + 2H^+ \rightarrow 3Pb^{2+} + 2CO_3^{2-} + 2H_2O$	-18.77	[31]

References: [23] Delahay, [24] MINEQL+, [28] Bilinski, [30] Smith, [31] Schock

1.3.4 Effect of pH and Alkalinity

Due to various sources of water, a range of pH values and alkalinity can be seen in water distribution systems. Schock (1980) modeled the trends of varying alkalinity with formation of lead(II) carbonate compounds (reactions 1.21 and 1.22 in Table 1.3) [31]. He compared experiments from Patterson and O'Brien and saw correlation between high alkalinity and scale formation on Pb coupons [32]. Results showed that carbonate levels 30-40 mg/L as $CaCO_3$ were ideal to precipitate lead on the coupons and decrease total Pb concentrations in water below the then-MCL 50 $\mu g/L$ Pb for pH 8.0-9.5. However, additional carbonate actually increased the formation of soluble Pb carbonate complexes, and local points of increased pH may have served to create more permeable scale. Noel et al. (2010) also found that hydrocerussite ($Pb_3(CO_3)_2(OH)_{2(s)}$) solubility was pH- and DIC-dependent, with dissolution rates decreasing with increased pH [33]. Adding in DIC (10, 50 mg C/L) decreased the dissolution rate at each pH tested.

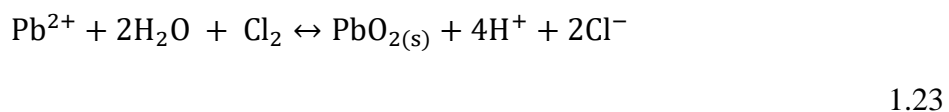
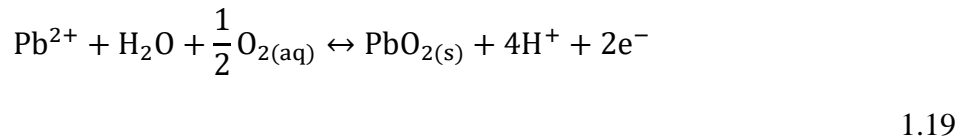
Lead(IV) dioxide ($PbO_{2(s)}$) has long been established as a corrosion-controlling lead solid due to its highly insolubility [23],[31]. Wang et al. (2010) postulated that DIC and pH could affect the formation of PbO_2 polymorphs from Pb(IV) solids - α - PbO_2 , scrutinyite and β - PbO_2 , plattnerite (reaction 1.19 in Table 1.3). A matrix of tests with a range of pH, DIC, and free chlorine proved that various mechanisms caused of formation of $PbO_{2(s)}$ from $PbCl_{2(aq)}$ and solids $PbO_{(s)}$ (massicot, yellow), hydrocerussite, and cerussite ($PbCO_{3(s)}$) [34]. Complex mechanisms characterize these interactions, and assumptions could not be uniformly applied to all situations. Another researcher reported water in Cincinnati, OH with high disinfectant concentrations over time, relatively high pH (8.5-9.2) resulted in formation of $PbO_{2(s)}$ and traces of $PbCO_{3(s)}$ in service lines [35]. However,

pipes from Madison, WI with low organic carbon but high alkalinity and neutral pH had only a thin layer of $\text{PbO}_{2(s)}$ with the majority of the Pb as $\text{PbCO}_{3(s)}$.

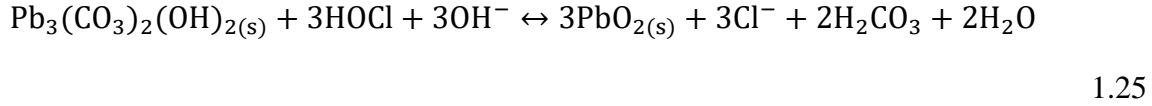
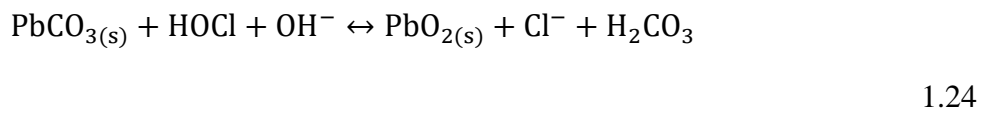
Xie et al. (2010) determined that varying pH and dissolved inorganic carbon (DIC) impacted the slow dissolution rates of $\text{PbO}_{2(s)}$ [36]. Dissolution rates were higher at lower pH values but increased with increasing DIC concentrations. A change from 0 to 50 mg C/L DIC accelerated the formation of soluble Pb(II) carbonate complexes more than an increase in pH (from 7.5 to 10). Higher pH resulted in increased formation of Pb hydroxide complexes, which also increased the dissolution rate of $\text{PbO}_{2(s)}$, even at lower DIC.

1.3.5 Effect of ORP

Moderate oxidation-reduction potentials (ORP) favor the formation of Pb(II) solids and complexes. Research has shown that at environmentally-relevant pH values (5-10) and more oxidizing conditions at higher (ORP), Pb tends to form $\text{PbO}_{2(s)}$ [23],[35]. The following reactions show that $\text{PbO}_{2(s)}$ can form from the oxidation of Pb(II) salts in the presence of a strong oxidizer such as chlorine [37].



Additionally, Pb(II) solids such as cerussite ($\text{PbCO}_{3(s)}$) and hydrocerussite ($\text{Pb}_3(\text{CO}_3)_2(\text{OH})_{2(s)}$), can exist in systems with moderate to high alkalinity [38]. They can also oxidize to $\text{PbO}_{2(s)}$ when free chlorine is added to the system [38],[39].



1.3.6 Impact of ionic strength

Limited research has considered ionic strength as a factor in lead solubility. Holm and Schock (1991) determined that chloropyromorphite ($\text{Pb}_5(\text{PO}_4)_3\text{Cl}_{(s)}$) solubility is dependent on ionic strength. Solubilities of Pb solids chloropyromorphite and hydrocerussite were estimated to decrease with higher ionic strength (0.005 M versus 0.1 M) [40].

1.4 Water heaters

Whether by seasonal variations, locations, or anthropological changes (i.e. residential water heaters), temperature of water is consistently changing. Residential water heaters have been in use since the early 1900s. Today, both tank and tankless water heaters are prevalent in U.S. homes with 8 million sold in the U.S. in 2009 and 118.2 million in use in 2015 [41],[42]. Energy sources for water heaters include electric, natural gas, and solar power.

The schematic below shows an upflow electric water heater, holding 30-50 gallons of water (Figure 1.1). Water from the distribution system enters the water through the bottom of the tank via the cold water supply valve. One or two (pictured) heating elements supply heat to the system and begin warming the water up to 45-60°C, depending on the set temperature. The anodic rod or sacrificial anode is present to prevent corrosion of the heating elements and is generally made of zinc, aluminum, or magnesium. The metal tank has an inner vitreous lining, non-reactive with the water entering it. Water continues to fill the tank as heats to the set temperature, and then is

dispensed out the hot water outflow pipe to the rest of the premises plumbing system as residents use hot water.

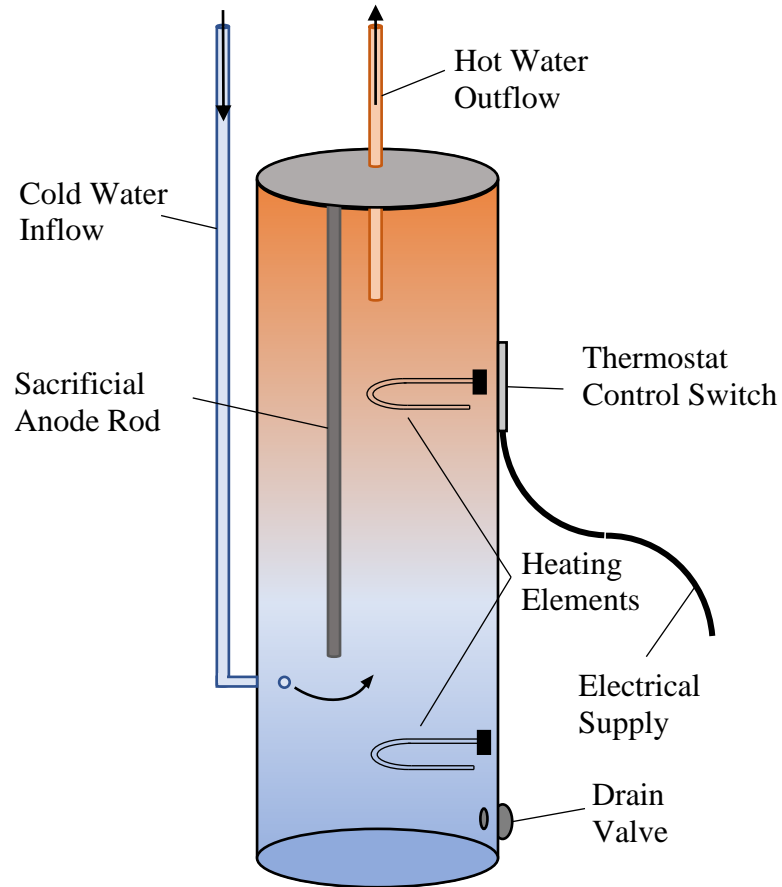


Figure 1.1. Schematic of residential electric tank water heater.

Current water heater literature is primarily concerned with the formation of harmful bacteria and pathogens [43]–[47] or flushing protocols to remove contaminants [48],[49]. Masters et al. noted that lead release proved to be related to temperature where increasing the temperature (4°C to 20°C) as a function of seasonal variations tended to increase solubility of common Pb solids as well as total Pb release [50]. Dissolution of Pb dioxide increased by a factor of 35 when the temperature increased from 4°C to 20°C in the presence of NOM [50]. At this point, lead (Pb) response has not been measured as a function of higher temperature water from water heaters.

1.5 Water softeners

Natural freshwater has an ionic strength (I) ranging from 10^{-4} to 10^{-2} M, where continental rainfall has ionic strength of approximately 10^{-4} M and hard water from groundwater sources approaches the upper limit [29]. In ideal solutions, concentration is equivalent to activity, denoted with brackets ($\{ \}$). However, actual solutions account for ionic strength using activity coefficients, γ ($\gamma = 1.0$ at $I = 0$ M; otherwise, $\gamma < 1.0$). Water softeners are used in residential and industrial applications to soften water. In 2011, the EPA estimated that 6-10 million cation exchange water softeners were in use in residences across the U.S. [51]. Ion-exchange softening is the most common type of system for residences, especially in areas with very hard water. Figure 1.2 shows a schematic of simplified residential pipe network where water softeners are installed upstream of the water heaters and the residence so that all inflow runs through it.

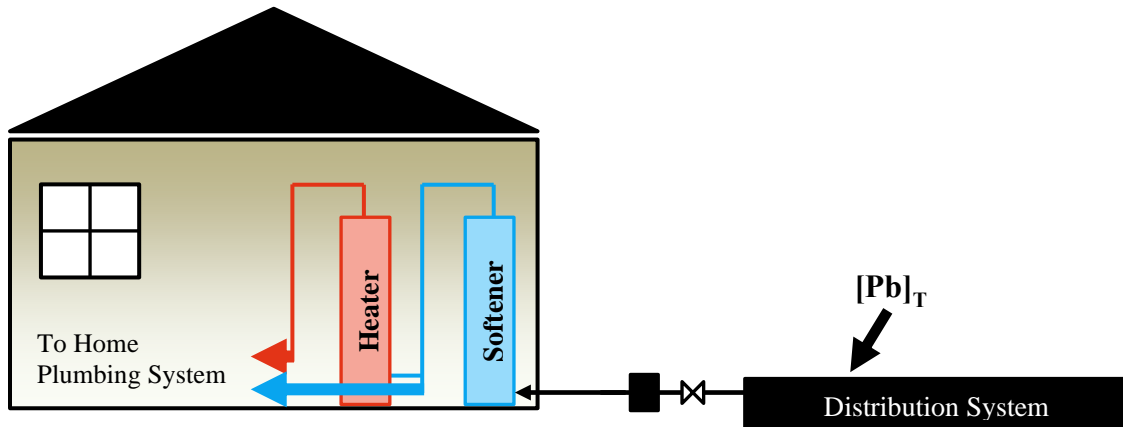


Figure 1.2. Schematic of residence with water softener and water heater. Lead (Pb) enters residential plumbing through distribution system.

A model of a home water softener system is shown below in Figure 1.3. The user fills a brine tank (used to hold salt and keep up the required sodium concentrations in the resin tank) with a salt and then fills it with water. The brine mixture is pumped into the main softening tank and salt cations (Na^+) coat the resin inside the tank. The resin inside the softener is now covered by sodium ions from salt, which are exchanged for the more favorable Ca^{2+} and Mg^{2+} hardness ions. This exchange is especially pertinent when the hard water percolates down through the resin. The ions exchanging on the resin can change the ionic strength of the water passing through the softener. Other softeners can use potassium as the exchange ion, but sodium is the most common. Cation exchange technology allows the exchange of hardness cations (Ca^{2+} , Mg^{2+} , Fe^{2+}) for other cations

like Na^+ or K^+ in salts. In some cases, iron, manganese, and other ions could be also taken up in the resin.

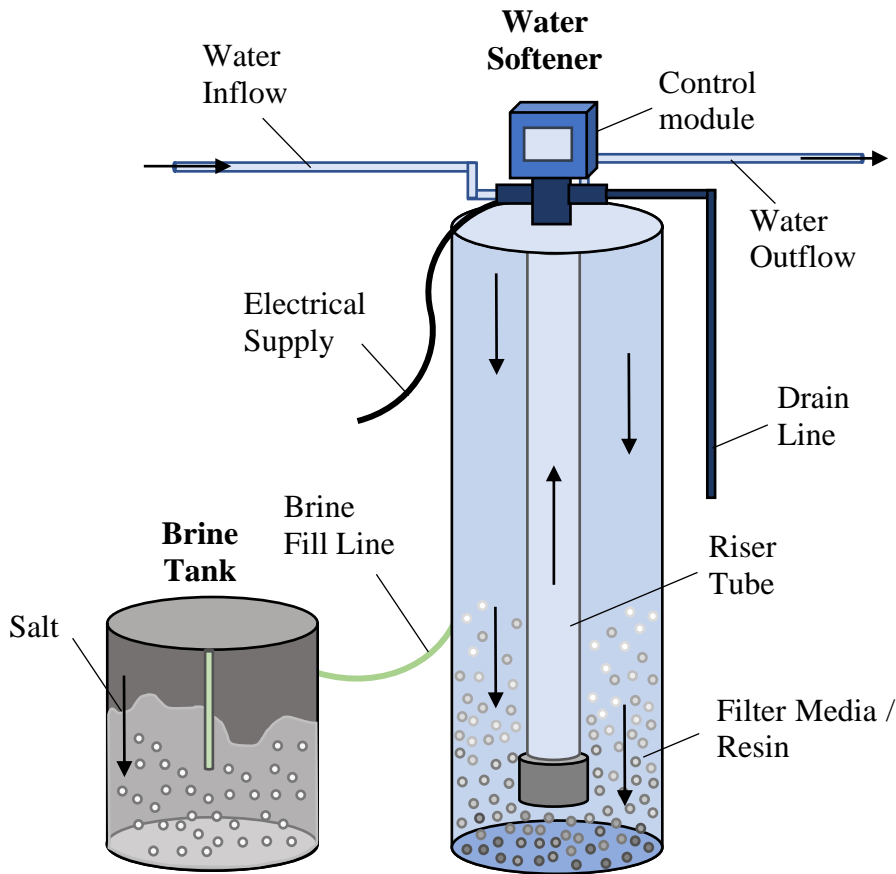


Figure 1.3. Schematic of residential ion-exchange water softener system.

However, research indicates that softeners could also be used to remove harmful contaminants such as lead, cadmium, or copper. Research in this area has been focused on determining effective resins, optimizing the ion-exchange process, or determining if a resin could assist in heavy metal removal [52]–[54]. Manufacturers employ different resins, like zeolite mineral or carbon-based materials, that exchange hardness cations out of the water and onto the resin. Some of these resins have shown potential for removal of particulate lead with both anionic and cationic resins. One study that measured lead concentrations across a range of temperatures and reported that 25–96% of the known value(s) of lead sequestered to the resin [53]. Another study used coal as a resin and determined that lower pH (0–3) resulted in lower Pb(II) removal [54]. Pb uptake on the coal resin was inversely proportional to the temperature, where the higher

temperatures were less effective at Pb(II) removal. In all of this, there is still a lack of knowledge as to how the water quality changes due to the use of water softeners could affect lead.

1.6 Quantification of Dissolved Lead

Due to varied water quality and the impact of water quality on speciation, Pb exists in a variety of forms. Parameters such as pH, alkalinity, water temperature and ionic strength vary immensely and can alter which Pb species exist at any one time. Determining speciation is critical to make assessments for environmental and human health. The USEPA standard method 200.8 measuring total Pb in an aqueous sample requires full sample acidification with 0.15% HNO₃. Samples have at least a 16-hour holding period for all lead analyses using an ICP-MS (or OES) [55]. Proper acidification is required for total Pb analysis. However, Triantafyllidou, Parks, and Edwards (2007) determined that the analysis by EPA Standard Method 200.8 resulted in only recovering 20% or less of pure Pb_(s), Pb(IV), and solder particles [56]. Dissolution increased by 20-33% when the samples were introduced to 2% HNO₃ and higher temperatures for 3 hours. Additionally, follow-up experiments of full acid digestion with 2% HNO₃ and heating the sample to 85-90°C recovered 90-100% of Pb after 1 week of digestion.

Measurement of Pb(IV) is difficult because of the tendency of lead to be in the Pb(II) oxidation state in natural conditions. The reactions in Table 1.1-Table 1.3, in conjunction with natural water ORP from Delahay et al. [23], show that given a significant decrease in pH, most lead solids tends to undergo dissolution along with a reversion from Pb(IV) to Pb(II). While effective for measuring total lead in a sample, the EPA Standard Method 200.8 acidification for Pb analysis means all the lead in the sample will likely be in the Pb(II) form. Therefore, determining the speciation of Pb by oxidation states (II or IV) remains a challenge. Various methods of filtration, chemical tracers, or solids analysis (x-ray diffraction) are available, but require more materials or analytical machinery. There are some researched methods in development to determine Pb(IV) solids using indirect measurement [57], but procedures have yet to be standardized.

1.7 Study Objectives

Based on this literature, there are some clear knowledge gaps even with a plethora of information concerning lead chemistry. The complex kinetics and lack of established equilibrium data make it difficult to properly characterize lead under different water quality conditions. Research has yet to determine a strong connection between the kinetics of lead speciation changes and temperatures reached in a water heater. Additionally, current research focused on water softeners are not associated with the impact on lead chemistry.

Core chapters discuss experimental kinetic data that was collected, as well as several long-term equilibrium points that will be compared to a mathematical model. To simulate a residential water heater affecting water temperature, Chapter 2 examines the effect of temperature on lead (Pb) speciation, addressing (1) how variation in temperature affects the speciation of Pb. In Chapter 3, the effect of ionic strength is discussed to explore how residential water softeners could impact lead (Pb) chemistry, addressing (2) how variation in ionic strength affects the speciation of Pb. Chapter 4 focuses on addressing (3) how carbonate concentration affects the speciation of Pb. Another challenge to determine the speciation of lead is (4) to separate Pb(IV) from Pb(II), as well as accurately quantify the Pb(IV) solid PbO₂. Indirect lead(IV) dioxide measurement and analysis is confirmed and applied in Chapter 5. The last chapter summarizes the final results from the previous chapters and concludes with application points about the significance of using these traditional in-home devices and their effect on Pb speciation.

1.8 References

- [1] Agency for Toxic Substances & Disease Registry, “Toxicological Profile for Lead,” 2019.
- [2] United States Senate, *Safe Water Drinking Act, 1974*. U.S.A., 1974.
- [3] W. Troesken, “Lead Water Pipes and Infant Mortality in Turn-of-the-Century Massachusetts,” *J. Chem. Inf. Model.*, 2003.
- [4] M. Edwards, “Fetal death and reduced birth rates associated with exposure to lead-contaminated drinking water,” *Environ. Sci. Technol.*, vol. 48, no. 1, pp. 739–746, Jan. 2014.
- [5] United States EPA, *Lead and Copper Rule*. U.S.A, 1991.
- [6] United States Senate, *Safe Drinking Water Act, 1986 amendment*. U.S.A, 1986.

- [7] C. S. Wong and P. Berrang, “Contamination of tap water by lead pipe and solder,” *Bull. Environ. Contam. Toxicol.*, vol. 15, no. 5, pp. 530–534, May 1976.
- [8] E. Deshommes, L. Laroche, S. Nour, C. Cartier, and M. Prévost, “Source and occurrence of particulate lead in tap water,” *Water Res.*, vol. 44, no. 12, pp. 3734–3744, Jun. 2010.
- [9] C. Cartier *et al.*, “Investigating dissolved lead at the tap using various sampling protocols,” *J. / Am. Water Work. Assoc.*, vol. 103, no. 3, pp. 55–67, Mar. 2011.
- [10] C. Cartier, S. Nour, B. Richer, E. Deshommes, and M. Prévost, “Impact of water treatment on the contribution of faucets to dissolved and particulate lead release at the tap,” *Water Res.*, 2012.
- [11] M. Triantafyllidou, Simoni; Lambrinidou, Y.; Edwards, “Lead exposure through Drinking Water: Lessons to be learned from recent U.S. experience,” *Glob. NEST JournalGlobal NEST Int. J.*, vol. 11, no. 3, pp. 341–348, 2009.
- [12] M. R. Schock and R. Giani, “Oxidant/Disinfectant Chemistry and Impacts on Lead Corrosion,” in *In Proceedings, Sunday Workshop Getting the Lead Out: Analysis and Treatment of Elevated Lead Levels in DC’s Drinking Water*, 2004.
- [13] M. Edwards and D. Abhijeetdudi, “Role of chlorine and chloramine in corrosion of lead-bearing plumbing materials,” 2004.
- [14] M. Edwards, S. Triantafyllidou, and D. Best, “Elevated blood lead in young children due to lead-contaminated drinking water: Washington, DC, 2001-2004,” *Environ. Sci. Technol.*, 2009.
- [15] M. Reel and S. Cohen, “Little Action on Lead Warnings,” *Washington Post*, Washington, D.C., 14-Mar-2004.
- [16] R. Renner, “Out of Plumb.,” *Environ. Health Perspect.*, 2009.
- [17] M. Edwards and S. Triantafyllidou, “Chloride-to-sulfate mass ratio and lead leaching to water,” *J. / Am. Water Work. Assoc.*, 2007.
- [18] Agency for Toxic Substances & Disease Registry, “Lead Toxicity: What Are U.S. Standards for Lead Levels?,” 2017. [Online]. Available: <https://www.atsdr.cdc.gov/csem/csem.asp?csem=34&po=8>. [Accessed: 05-Jun-2019].
- [19] M. A. Del Toral, “High Lead Levels in Flint, Michigan - Interim Report. WG-15J; Region 5,” Chicago, IL, 2015.

- [20] K. J. Pieper, M. Tang, and M. A. Edwards, “Flint Water Crisis Caused by Interrupted Corrosion Control: Investigating ‘ground Zero’ Home,” *Environ. Sci. Technol.*, vol. 51, no. 4, pp. 2007–2014, 2017.
- [21] M. Edwards, J. O. Falkingham, and A. Pruden, “RAPID: Synergistic Impacts of Corrosive Water and Interrupted Corrosion Control on Chemical/Microbiological Water Quality: Flint, MI,” 2015.
- [22] M. Hanna-Attisha, J. LaChance, R. C. Sadler, and A. C. Schnepf, “Elevated blood lead levels in children associated with the flint drinking water crisis: A spatial analysis of risk and public health response,” *Am. J. Public Health*, vol. 106, no. 2, pp. 283–290, Feb. 2016.
- [23] P. Delahay, M. Pourbaix, and P. Van Rysselberghe, “Potential-pH Diagram of Lead and its Applications to the Study of Lead Corrosion and to the Lead Storage Battery,” *J. Electrochem. Soc.*, vol. 98, no. 2, pp. 57–64, 1951.
- [24] W. D. . Schecher and D. C. McAvoy, “MINEQL+: A Chemical Speciation Modeling for the Real World.” Environmental Research Software, 2015.
- [25] M. M. Benjamin, *Water Chemistry*, 1st ed. New York, NY: McGraw-Hill, 2002.
- [26] J. D. Hopwood, R. J. Davey, M. O. Jones, R. G. Pritchard, P. T. Cardew, and A. Booth, “Development of chloropyromorphite coatings for lead water pipes,” *J. Mater. Chem.*, 2002.
- [27] C. J. Lind, “Polarographic Determination of Lead Hydroxide Formation Constants at Low Ionic Strength,” *Environ. Sci. Technol.*, 1978.
- [28] H. Bilinski and P. Schindler, “Solubility and equilibrium constants of lead in carbonate solutions (25°C, I = 0.3 mol dm⁻³),” *Geochim. Cosmochim. Acta*, vol. 46, no. 6, pp. 921–928, 1982.
- [29] W. A. Brezonik, Patrick L.; Arnold, *Water Chemistry: An Introduction to the Chemistry of Natural and Engineered Aquatic Systems*, 1st ed. Oxford University Press, 2011.
- [30] R. M. Smith and A. E. Martell, “Critical Stability Constants,” in 4: *Inorganic Complexes*, New York, NY: Springer Science + Business Media, 1976, pp. 10–38.
- [31] M. R. Schock, “Response of lead solubility to dissolved carbonate in drinking water,” *Am. Water Work. Assoc.*, vol. 72, no. 12, pp. 695–704, 1980.
- [32] J. W. Patterson and J. E. O’Brien, “Water Technology Control of Lead Corrosion,” *J. Am. Water Work. Assoc.*, vol. 71, no. 5, pp. 264–271, 1979.

- [33] J. D. Noel, Y. Wang, and D. E. Giammar, “Effect of water chemistry on the dissolution rate of the lead corrosion product hydrocerussite,” *Water Res.*, vol. 54, pp. 237–246, May 2014.
- [34] Y. Wang, Y. Xie, W. Li, Z. Wang, and D. E. Giammar, “Formation of lead(IV) oxides from lead(II) compounds,” *Environ. Sci. Technol.*, vol. 44, no. 23, pp. 8950–8956, Dec. 2010.
- [35] D. A. Lytle and M. R. Schock, “Formation of Pb(IV) oxides in chlorinated water,” *Journal /American Water Works Association*, vol. 97, no. 11. Nov-2005.
- [36] Y. Xie, Y. Wang, V. Singhal, and D. E. Giammar, “Effects of pH and carbonate concentration on dissolution rates of the lead corrosion product PbO₂,” *Environ. Sci. Technol.*, 2010.
- [37] A. F. Wiberg, Egon; Holleman, “Inorganic Chemistry,” in *Inorganic Chemistry*, 34th ed., N. Wiberg, Ed. Berlin: Academic Press, 1995, pp. 912–928.
- [38] H. Liu, G. V. Korshin, and J. F. Ferguson, “Investigation of the kinetics and mechanisms of the oxidation of cerussite and hydrocerussite by chlorine,” *Environ. Sci. Technol.*, vol. 42, no. 9, pp. 3241–3247, 2008.
- [39] Y. Zhang and Y. P. Lin, “Determination of PbO₂ formation kinetics from the chlorination of Pb(II) carbonate solids via direct PbO₂ measurement,” *Environ. Sci. Technol.*, vol. 45, no. 6, pp. 2338–2344, Mar. 2011.
- [40] T. R. Holm and M. R. Schock, “Potential effects of polyphosphate products on lead solubility in plumbing systems,” *J. / Am. Water Work. Assoc.*, 1991.
- [41] D. Ryan, R. Long, D. Lauf, M. Ledbetter, and A. Reeves, “Energy Star Water Heater Market Profile,” Silver Spring, MD, 2009.
- [42] U.S. Energy Information Administration, “Residential Energy Consumption Survey 2015,” 2015..
- [43] R. H. Brazeau and M. A. Edwards, “Role of Hot Water System Design on Factors Influential to Pathogen Regrowth: Temperature, Chlorine Residual, Hydrogen Evolution, and Sediment,” *Environ. Eng. Sci.*, 2013.
- [44] H. Wang, M. A. Edwards, J. O. Falkingham, and A. Pruden, “Probiotic approach to pathogen control in premise plumbing systems? A review,” *Environ. Sci. Technol.*, vol. 47, no. 18, pp. 10117–10128, 2013.

- [45] W. J. Rhoads, P. Ji, A. Pruden, and M. Edwards, “Water heater temperature set point and water use patterns influence Legionella pneumophila and associated microorganisms at the tap,” *Microbiome*, 2015.
 - [46] P. Ji, W. J. Rhoads, M. A. Edwards, and A. Pruden, “Impact of water heater temperature setting and water use frequency on the building plumbing microbiome,” *ISME J.*, vol. 11, no. 6, pp. 1318–1330, 2017.
 - [47] J. O. Falkingham, E. D. Hilborn, M. J. Arduino, A. Pruden, and M. A. Edwards, “Epidemiology and Ecology of Opportunistic Premise Plumbing Pathogens: Legionella pneumophila, *Mycobacterium avium*, and *Pseudomonas aeruginosa*,” *Environ. Health Perspect.*, vol. 123, no. 8, pp. 749–758, 2015.
 - [48] J. K. Hawes, E. A. Conkling, K. S. Casteloes, R. H. Brazeau, M. Salehi, and A. J. Whelton, “Predicting contaminated water removal from residential water heaters under various flushing scenarios,” *Journal - American Water Works Association*. 2017.
 - [49] S. Chowdhury, F. Kabir, M. A. J. Mazumder, and M. H. Zahir, “Modeling lead concentration in drinking water of residential plumbing pipes and hot water tanks,” *Sci. Total Environ.*, 2018.
 - [50] S. Masters, G. J. Welter, and M. Edwards, “Seasonal Variations in Lead Release to Potable Water,” *Environ. Sci. Technol.*, vol. 50, no. 10, pp. 5269–5277, May 2016.
 - [51] S. Tanner, “Cation Exchange Water Softener Notification of Intent (NOI),” 2011.
 - [52] E. Maliou, M. Malamis, and P. O. Sakellarides, “Lead and cadmium removal by ion exchange,” in *Water Science and Technology*, 1992, vol. 25, no. 1, pp. 133–138.
 - [53] K. Vaaramaa and J. Lehto, “Removal of metals and anions from drinking water by ion exchange,” *Desalination*, vol. 155, pp. 157–170, 2003.
-
- [54] F. Aydin, F. Yasar, I. Aydin, and F. Guzel, “Determination of lead separated selectively with ion exchange method from solution onto BCW in Sirnak, East Anatolia of Turkey,” *Microchem. J.*, vol. 98, no. 2, pp. 246–253, Jul. 2011.
 - [55] United States EPA, *EPA Method 200.8: Determination of Trace Elements in Waters and Wastes by Inductively Coupled Plasma-Mass Spectrometry*. U.S.A., 1994.
 - [56] S. Triantafyllidou, J. Parks, and M. Edwards, “Lead particles in potable water,” *J. / Am.*

Water Work. Assoc., 2007.

- [57] Y. Zhang, Y. Zhang, and Y. P. Lin, “Fast detection of lead dioxide (PbO₂) in chlorinated drinking water by a two-stage iodometric method,” *Environ. Sci. Technol.*, 2010.

2. TEMPERATURE AND pH DEPENDENCE OF SOLUBLE LEAD

2.1 Introduction

Characterizing lead speciation within distribution systems and residences has become more prominent in the last few decades. Using several pipe loop studies, Masters, Welter and Edwards (2014) found that temperature fluctuations from 20°C to 4°C affected lead solids' dissolution very little on its own [1]. When considered in the presence of natural organic matter, lead release increased by factors of 2-36 concerning various lead species. Research has been performed on the development of *Legionella pneumophila* and other microbial growth in water heaters [2]-[4]. However, minimal experimental research has been performed in the area linking lead speciation specifically with high water temperature. One study developed a set of models to predict the concentration of lead in water heaters, a premise plumbing network, and the external distribution system [5]. The model in that study was based on inputs from water samples at a nearby housing complex but was not specifically chemistry based. This work will attempt to close the gap on characterizing lead speciation in water at high temperatures that are achieved by a residential water heater.

2.2 Materials & Methods

2.2.1 Standards, Reagents, and Preparation of Stocks

All solutions were prepared with ultrapure deionized water from a THERMO Barnstead GenPure Pro water system with a resistivity of 18.0-18.2 MΩ-cm, sparged with nitrogen. Concentrated nitric acid (67-70%, trace metal grade, Fisher Scientific) was used for all sample acidification. All stock solutions of lead were 4.8×10^{-3} M (1000 ppm) Pb(NO₃)₂ as Pb dissolved in 2% HNO₃ purchased from EXAXOL Chemical Corp. or 4.8×10^{-3} M Pb(NO₃)₂ as Pb dissolved in 0.5% HNO₃ purchased from Inorganic Ventures. pH control was achieved with the addition of solutions made from NaOH pellets from ACROS Organics at a purity of 98.5% for analysis or dilutions of concentrated HNO₃. Stock Yttrium (1.1×10^{-4} M, 10 ppm) in 2% HNO₃ from EXAXOL Chemical Corp. was used as an internal standard for the ICP-OES analysis.

Stock solutions for sample preparation were prepared by diluting the 4.8×10^{-3} M Pb standard solution to 4.8×10^{-5} M (10 ppm) Pb in sparged DI water. Stock solutions for ICP-OES

standards preparation were prepared by diluting the stock solution to 4.8×10^{-5} M (10 ppm) and 4.8×10^{-7} M Pb (100 ppb) in 2% HNO₃. ICP-OES lead standards were created in concentrations ranging from 2.4×10^{-8} M to 4.8×10^{-6} M (5-1000 ppb) from stock solutions. Standards were periodically remade, and samples were calibrated to these standards when run on the ICP-OES. Stock solutions of 4% HNO₃, 10^{-3} M NaOH, and 10^{-1} M NaOH were used for pH control and added in small volumes to avoid dilution of lead.

2.2.2 Experimental Procedure

Ultrapure water was sparged with nitrogen (N₂) gas prior to formulating any solutions to exclude all other gases. All experiments were conducted in 15 or 50 mL metal-free, non-sterile polypropylene (PP) centrifuge tubes. To initiate the reaction, 15 mL plastic vials were filled with 7.35 mL of N₂ sparged water and were adjusted with acid or base to reach the target pH. The lead stock solution (4.8×10^{-5} M) was then added to the solution to reach a total volume of 7.50 mL, which led the reactor to contain a final concentration of 9.7×10^{-7} M Pb (200 ppb Pb). All weighing was performed using a Mettler Toledo, NewClassic MS balance. Select samples were used for pH measurement using a Mettler Toledo SevenCompact, pH/ion InLab® Routine Pro-ISM glass electrode. Experiments were conducted at two temperatures, 25°C and 55° C. All 25°C samples were kept at a constant temperature on the benchtop in the lab space. All higher temperature samples were placed in the constant temperature oven (Thermo Scientific Heratherm OGS60) set to 55°C.

Each data point was tested in triplicate. Samples were taken at half hour increments for the first 3 hours, and then at 4, 6, 10, 12, 24, 48 hours for kinetic tests. Sample pH was taken prior to filtration and acidification for at least half of the samples in each condition to determine a trend over time. A benchtop recirculating bath was used to keep high temperature samples at 55°C during transitional phases as pH values were taken, until they were filtered. Total Pb concentrations were determined using an iCAP 7400 Duo inductively coupled plasma optical emission spectroscopy (ICP-OES, Thermo Scientific). Abiding by ICP-OES analysis requirements, solids were filtered into another 15 mL vial using surfactant-free cellulose acetate (SFCA) 0.45µm syringe filters and the entire sample was acidified to 2% HNO₃ (pH = 0.2-1.0). Using a 1:1 dilution. Y stock was added (0.150 mL) to the final 15 mL sample for a final concentration of 1.1×10^{-6} M Y (100 ppb Y, corresponding to the maximum final analyzed mass concentration of lead, 100 ppb

Pb). One set of triplicate samples from each experiment was processed for total recovery after creation to verify the total starting concentration of lead. In this case, the sample procedure reversed - first acidified to 2% HNO₃ and then filtered. Internal standard Y was added for a final concentration of 1.1×10⁻⁶ M Y. Another set of triplicate samples from each experiment was left undisturbed for a 6-week analysis (about 1000 hours). These samples followed the same experimental procedure as the traditional kinetic samples. It was believed that these ~1000 hour samples likely represented conditions where equilibrium was met in the system, and thus, the data were directly compared to the developed equilibrium models.

2.2.3 Analytical Methods

Lead was measured by ICP-OES analysis. This method is described below and is the same for all subsequent chapters where Pb was measured. In general, raw intensities from the ICP-OES were used to back-calculate the concentration of Pb (ppb) in sample vials. Originally, internal standard Y intensities were used to standardize both the standard curve and sample readings using an intensity ratio of Pb/Y (Table 2.1). Due to inconsistency of the Y readings over time in the kinetic experiments, the Pb/Y ratio was no longer a usable value. Instead, raw Pb intensities were converted to concentration using Eq. 2.1.

Table 2.1. Standard Pb curve data. Raw intensity (output) was compared to the known Pb in vial (input).

Standard	Pb in Vial (Calculated) ppb	Average ICP-OES Pb Response cps	Average ICP-OES Y Response cps	Pb/Y Intensity Ratio
STD 0 ppb	0.00	6.13	494.74	0.01
STD 5 ppb	5.00	10.79	496.60	0.02
STD 50 ppb	50.39	63.21	479.31	0.13
STD 100 ppb	101.84	126.45	491.62	0.26
STD 250 ppb	250.46	296.11	469.64	0.63
STD 500 ppb	500.04	606.22	489.65	1.24
STD 1000 ppb	1003.26	1181.96	473.03	2.50

$$\text{ICP-OES Avg Pb Response (cps)} = (\text{slope} \times \text{Calculated Pb Concentration (ppb)}) + \text{y-intercept}$$

Eq. 2.1

Concentrations of Pb were first determined mathematically by weight (Table 2.1). Plotting the known concentrations of standard curve (0-1000 ppm) against the output intensities (0-1200 cps) results in Figure 2.1 below, establishing a relationship that allowed the calculation of lead concentration when given intensity (Eq. 2.2).

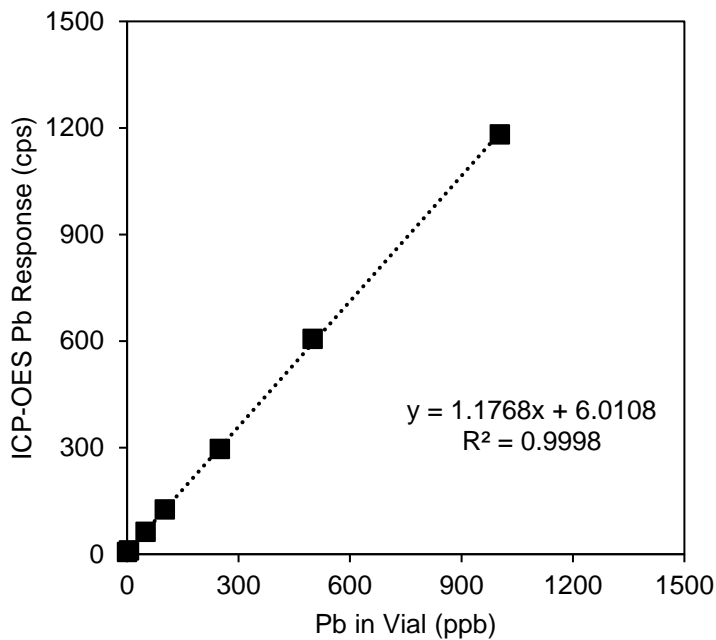


Figure 2.1. Standard curve with ICP-OES lead samples with linear correlation between Pb in vial (ppb) vs. ICP-OES response (cps).

$$\text{Calculated Pb concentration (ppb)} = \frac{[\text{ICP} - \text{OES Pb Response(cps)} - \text{y-intercept}]}{\text{slope}}$$

Eq. 2.2

Standards were always run on the ICP-OES for every sample analysis. Every 5-6 weeks, standards were remade to ensure accurate readings; therefore, several individual sample data sets have different standard curves that correspond to different sections of the data if data sets were run on multiple days. Samples corresponding to different time points were made in triplicate, injected into the ICP-OES three (3) times, and analyzed in triplicate to ensure accuracy of the readings, especially without the implementation of an internal standard. This resulted in at least 9 data points per sample (1 vial) and 27 data points for each time point (set of 3 vials). If sample intensity showed significant variation, they were remade, reanalyzed, and the new data was added to the set.

Averages and standard deviations of lead concentrations reported in tables and graphs take all intensities into consideration.

Percentages of measured lead are reported using Eq. 2.3 to show the amount of lead that was measured on the ICP-OES in relation to the concentration of lead that was added to an individual reactor. Though each sample was prepared with the same process, there was still variability and error per reactor. Every reactor had a total lead of approximately 9.7×10^{-7} M, but specific values within each reactor were used for accuracy in reporting.

$$\frac{\text{Measured soluble lead (ppb)}}{\text{Total added lead (ppb)}} \times 100\% = \text{Percent Pb (\%)}$$

Eq. 2.3

Limits of detection and quantitation were determined mathematically from a single run with low lead concentrations. Eight (8) standards with lead concentrations ranging from 1.0-20 ppb were run with 16 injections against 4 wavelengths (168.215 nm, 182.205 nm, 216.999 nm, 220.353 nm). Data measured against 220.353 nm performed with the highest accuracy and all subsequent lead studies used this wavelength (Table B.1 in Appendix B). Standard deviation (σ) was determined for each of the standards based on all 16 of the injections (x) and sample average (\bar{x}) then correlated to a relative standard deviation (RSD):

$$\text{Sample Standard Deviation } (\sigma) = \sqrt{\frac{\sum_{i=1}^n (x_i - \bar{x})^2}{n - 1}}$$

Eq. 2.4

$$\text{RSD(\%)} = \frac{\sigma(\text{ppb})}{\bar{x}(\text{ppb})}$$

Eq. 2.5

Recovery of the standards was measured against the calculated lead concentration (from mass measurements). If the recovery was within 10% of the calculated amount (90-110%), the limit of quantitation (LOQ) could be calculated using the following equation:

$$\text{LOQ} = 10\sigma$$

Eq. 2.6

The instrument detection limit (IDL) was also determined for standards that recovered within 10% of the calculated amount. With 16 injections and a 99% confidence interval, a t-value of 2.947 was determined:

$$\text{IDL} = 2.947\sigma$$

Eq. 2.7

With this analysis, LOQ = 2.5×10^{-8} M (5.15 ppb) and IDL = 7.3×10^{-9} M (1.52 ppb). Sample data that read as negative intensity after data manipulation was recorded as a zero (0). Intensity data that fell below the IDL but above zero (0) was replaced with the IDL (7.3×10^{-9} M). Previous research suggested that values below the LOQ were not able to accurately quantify the data; however, no approximation would gain any accuracy. Therefore, all data above the IDL is the originally reported value. Refer to Table B.1 in Appendix B for the raw LOQ and IDL data as well as additional data concerning the chosen wavelength (220.353 nm).

2.3 Equilibrium Thermodynamic Parameters

A thermodynamic model was also developed to predict the equilibrium concentration of soluble Pb and potential solid Pb formations with an increase temperature from equilibrium conditions. The van't Hoff equation (Eq. 2.8) quantifies the temperature dependence of equilibrium constants. The integrated form of the equation, with the assumption that $\Delta H^\circ_{\text{rxn}}$ is constant, is shown below

$$\ln \frac{K_{\text{eq},T_2}}{K_{\text{eq},T_1}} = \frac{\Delta H^\circ_{\text{rxn}}}{R} \left(\frac{1}{T_1} - \frac{1}{T_2} \right)$$

Eq. 2.8

where $T_1 = 25^\circ\text{C}$ (298.15 K) to represent STP conditions and $T_2 = 55^\circ\text{C}$ (328.15 K) to represent the average temperature of water within a residential water heater. Applying Eq. 2.8 to all the possible Pb species in each of the conditions specified in the following work results in the following system inputs in Table 2.2. With the assumption that $\Delta C^\circ p = 0 \text{ J mol}^{-1} \text{ K}^{-1}$, then it can be assumed that there is no change in the enthalpy of a reaction with temperature; therefore, $\Delta H^\circ_{1,\text{rxn}} = \Delta H_{2,\text{rxn}}$. Based on the experimental conditions for the system, lead oxides, hydroxides, or nitrates could form. Additional data for lead carbonates, bicarbonate, and chlorides were included to further characterize a traditional potable water distribution system.

From the initial equilibrium constant and enthalpy data reported in Table 2.2, a thermodynamic equilibrium model was compiled that predicted changes in log K values from 25°C to 55°C. All equilibrium K_{eq} values were written as functions of dissolution reactions. Therefore, an increase in K_{eq} would suggest that the species is more likely to dissociate, favoring the products. Because lead(IV) species are uncommon in many systems as well as the performed experiments, those reactions were not included. Hydrocerussite ($Pb_3(CO_3)_2(OH)_2(s)$) and $PbO(s)$ were modeled to slightly increase solubility with an increase in temperature. Most of the other species considered showed little to no change in the equilibrium constant, meaning that solubility models would remain relatively unchanged by incorporating the thermodynamic data.

Table 2.2. Enthalpy of reaction (ΔH), and equilibrium constants (K) for a variety of relevant Pb compounds in drinking water. Sections labeled with a dash (-) refer to unavailable data.

#	Reaction	ΔH°_{rxn} at 25°C (kJ/mol)	$\log K_{eq}$ at 25°C	$\log K_{eq}$ at 55°C
Aqueous				
1.1	$Pb_{(s)}^0 \rightleftharpoons Pb_{(aq)}^{2+} + 2e^-$	1.02	-0.13	-0.13
1.4	$PbOH_{(aq)}^+ \rightleftharpoons Pb_{(aq)}^{2+} + OH^-$	-	6.40	
1.5	$Pb(OH)_{2(aq)}^0 \rightleftharpoons Pb_{(aq)}^{2+} + 2OH^-$	-	4.5	
1.6	$Pb(OH)_{3(aq)}^- \rightleftharpoons Pb_{(aq)}^{2+} + 3OH^-$	-	3.0	
1.7	$Pb(OH)_{4(aq)}^{2-} \rightleftharpoons Pb_{(aq)}^{2+} + 4OH^-$	-	-11.9	
1.9	$PbCl_{(aq)}^+ \rightleftharpoons Pb_{(aq)}^{2+} + Cl^-$	12.10	1.550	1.550
1.10	$PbCl_{2(aq)} \rightleftharpoons Pb_{(aq)}^{2+} + 2Cl^-$	-323.06	0.650	0.650
1.11	$PbCl_{3(aq)}^- \rightleftharpoons Pb_{(aq)}^{2+} + 3Cl^-$	-340.14	-0.40	-0.40
1.12	$PbCl_{4(aq)}^{2-} \rightleftharpoons Pb_{(aq)}^{2+} + 4Cl^-$	-188.09	-0.34	-0.34
1.14	$HCO_3^- \leftrightarrow H^+ + CO_3^{2-}$	-	13.20	
1.15	$PbCO_{3(aq)}^0 \rightleftharpoons Pb_{(aq)}^{2+} + CO_3^{2-}$	23.15	6.48	6.48
1.16	$Pb(CO_3)_{2(aq)}^{2-} \rightleftharpoons Pb_{(aq)}^{2+} + 2CO_3^{2-}$	-	3.46	3.46
Solid				
1.18	$PbO_{(s)(yellow)} + 2H^+ \rightleftharpoons Pb_{(aq)}^{2+} + H_2O$	217.05	-15.11	-15.23
1.20	$Pb(OH)_{2(s)}^0 \rightleftharpoons Pb_{(aq)}^{2+} + 2OH^-$	54.41	8.15	8.17
1.21	$PbCO_{3(s)}^0 \rightleftharpoons Pb_{(aq)}^{2+} + CO_3^{2-}$	-13.74	-13.13	-13.12
1.22	$Pb_3(CO_3)_2(OH)_{2(s)} + 2H^+ \rightarrow 3Pb^{2+} + 2CO_3^{2-} + 2H_2O$	-101.86	-18.77	-18.70

2.4 Results & Discussion

2.4.1 Effect of nitrogen sparging

The glovebox experimental results were compared with those performed outside the glovebox at pH 4.8-5.6 at 25°C to determine the effect of CO₂ sequestration from the atmosphere and potential formation of lead carbonate solids. All the same procedures were followed as in the temperature comparison experiments. Both experiments confirmed the total initial Pb concentration at 9.7×10^{-7} M Pb, and subsequently, soluble lead concentrations decreased after t = 0 hours. While maintaining the same pH, the soluble lead concentrations over 6 hours measured just under 50% of the added lead value were not significantly different between the two experiments, as shown in

Figure 2.2. These results indicated that eliminating all CO₂ from the reaction in the glovebox did not change the soluble lead concentrations significantly. Since the data from both experiments performed similarly, it was unlikely that additional (carbonate) solid was forming under normal benchtop conditions. Any data differences were not significant enough to require all subsequent samples to be made under glovebox conditions. ICP-OES soluble lead concentrations and pH data can be found in Table C.1 and

Table C.4 in Appendix C.

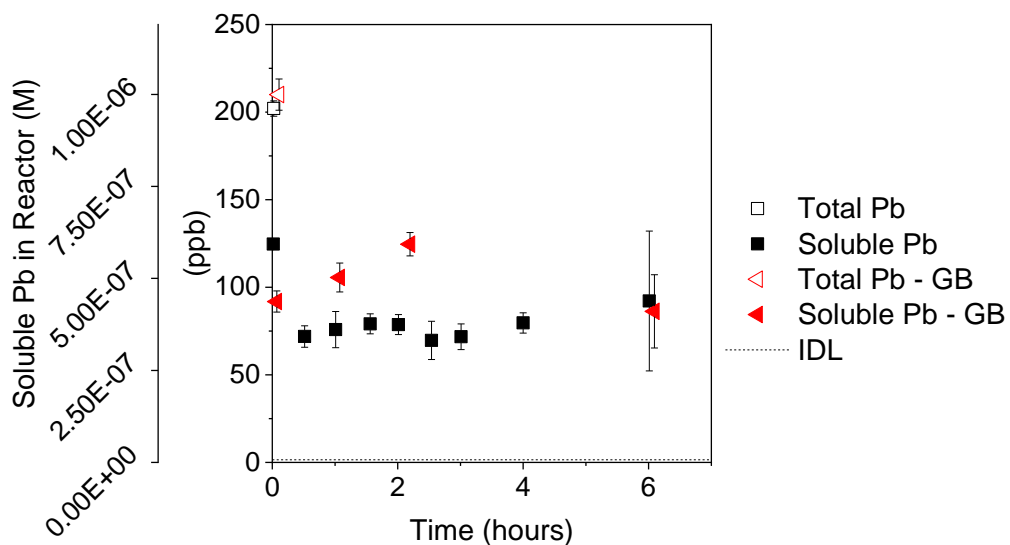


Figure 2.2. Comparison of soluble lead (Pb) at pH 4.8-5.6 under variable atmospheric conditions: open to atmosphere with nitrogen sparging (black points) or in a nitrogen-sparged glovebox (“GB”, red points). Pb_{Total} = 9.7×10⁻⁷ M and low I= 8.5×10⁻⁶ M.

2.4.2 Effect of pH and temperature on soluble lead in kinetic experiments

Experiments were conducted over a range of pH values (2.9-9.8) at 25°C to characterize a traditional drinking water system at both standard conditions and at 55°C to simulate the difference higher temperatures can have. ICP-OES soluble lead concentrations and pH data can be found in Appendix C.

First, for the pH 3.0 experiment, the pH at both 25°C and 55°C experiments remained relatively constant throughout the 48-hour experiment. This similarly enabled the Pb trends at these different temperatures to be directly compared to each other (Figure 2.3). Total lead was verified at the beginning of each experiment at 25°C and 55°C as 1.1×10^{-6} M (227 ppb) and 1.0×10^{-6} M (210 ppb), respectively (Figure 2.3). As expected, the pH 2.9-3.1 at 25°C soluble lead concentrations remained relatively constant, with a slight dip under 100% recovery at approximately 9 hours (9.34×10^{-7} M, 94%) (Figure 2.3(A)). At 55°C, pH 3.0-3.1 soluble lead concentrations consistently recovered just under half of the total lead (90-100.1 ppb) originally in the reactors (Figure 2.3(B)). The higher temperature experiment did not follow the expected trend that there would be equal or greater soluble lead of species at higher temperature. Conditions between the two experiments remained constant except for the temperature variation, but the measured soluble lead clearly differed.

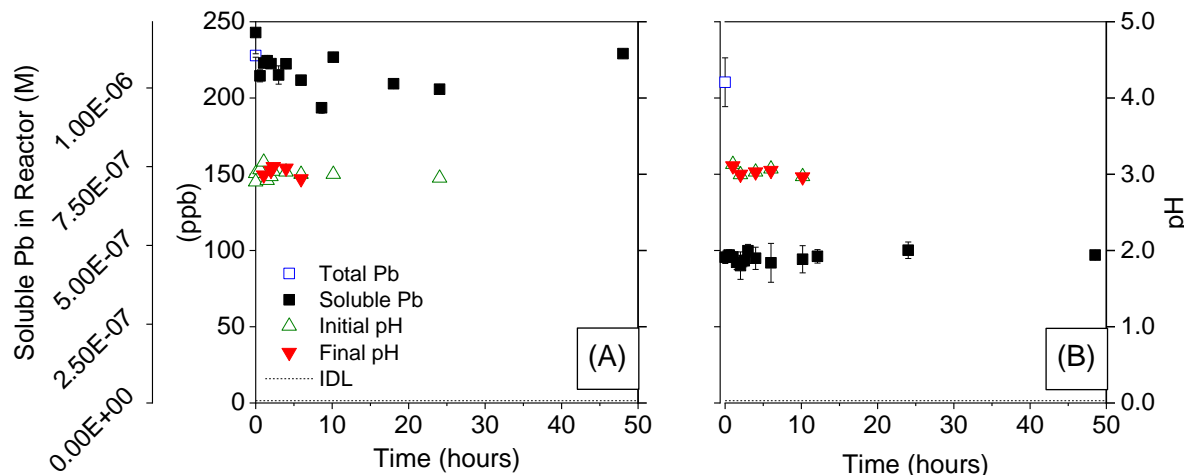


Figure 2.3. Changes in soluble lead (Pb) concentration (left axis, squares) and pH reported (right axis, triangles) for pH 3.0 over 48 hours. Kinetic data compared against temperature at (A) 25°C, pH 2.9-3.1 and (B) 55°C, pH 3.0-3.1.

However, as the pH was increased, the experiments were more difficult to interpret because the pH did not remain constant as a function of reaction time. This issue also became exacerbated with higher temperature experiments and at higher starting pH values.

With a similar trend at each temperature, kinetic experiments at pH 4.4-5.3 and at a temperature of 25°C and 55°C showed variable soluble lead concentrations from 3.36×10^{-7} to

6.1×10^{-7} M (34-63% of original Pb) within the first 10 hours (Figure 2.4). However, the 25°C experiment had lower average soluble lead concentration (4.5×10^{-7}) than the 55°C experiment (5.4×10^{-7}) until 48 hours. While maintaining a smaller pH range of 4.8-5.3, lower temperature specimens also had higher variance of single timepoint samples, shown in Figure 2.4(A). Higher temperature experimental data in this lower pH range in Figure 2.4(B) had a greater variation in samples at different time points as well as a larger pH range at lower values (4.4-5.2). As the systems approached the end of the kinetic experiments (48 hours), lead concentrations increased regardless of temperature. These experiments had very little distinction regardless of temperature, which may mean that this system response was more pH-dependent than temperature-dependent.

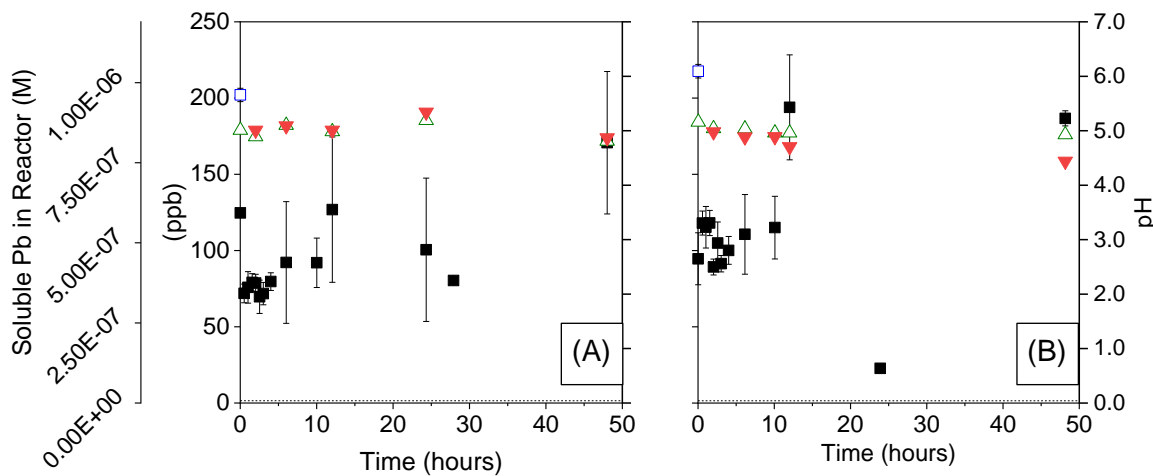


Figure 2.4. Changes in soluble lead (Pb) concentration (left axis, square) and pH reported (right axis, triangle) for pH 4.4-5.3 over 48 hours. Kinetic data compared against temperature at (A) 25°C, pH 4.8-5.3 and (B) 55°C, pH 4.4-5.2.

The kinetic experiments from pH 4.8-7.4 had more distinct overall trends in comparing the two temperatures. Starting at pH 6.8, higher temperature experiments ranged from pH 4.8-6.8 (Figure 2.5(A)) and showed immediately lower soluble lead at $t = 0$ hours than the corresponding 25°C experiments starting at pH 7.4 decreasing to pH 5.7 (Figure 2.5(B)). The lower temperature soluble lead measurements had an inconsistent trend and also had higher standard deviation per time point (Figure 2.5(B)). This initial soluble lead response at higher temperatures proved to be a pattern also extending above the neutral pH zone, shown in Figure 2.6(B) and Figure 2.7(B). Soluble lead in the 25°C experiment steadily decreased to 25% of original in kinetic test while the

55°C experiment consistently recovered around 25% soluble Pb²⁺. However, experiments at both 25°C and 55°C followed a similar recovery trend near the end of the kinetic experiment (past 24 hours). This trend could mean that temperature had an immediate effect on soluble lead concentrations, but pH eventually controlled the speciation of lead in this system.

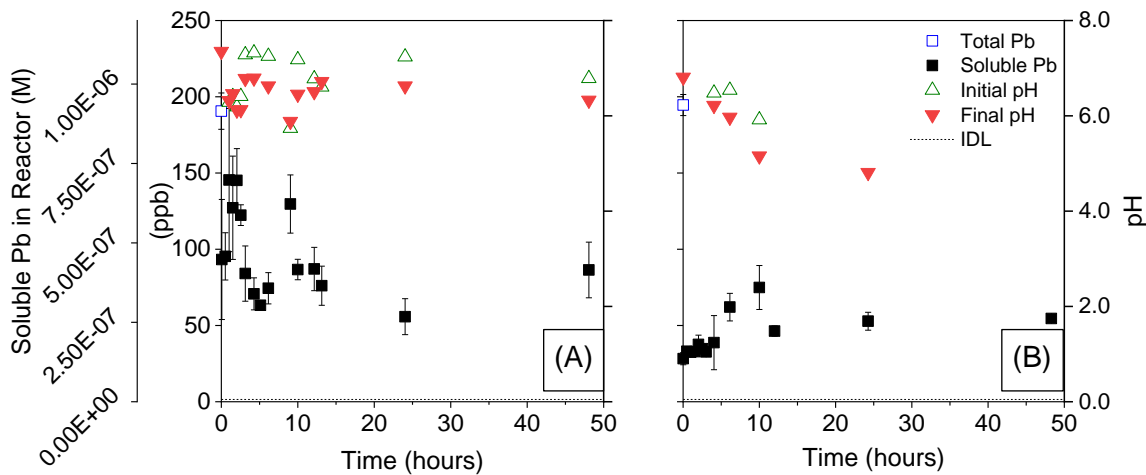


Figure 2.5. Changes in soluble lead (Pb) concentration (left axis, square) and pH reported (right axis, triangle) for pH 4.0-5.3 over 48 hours. Kinetic data compared against temperature at (A) 25°C, pH 5.7-7.4 and (B) 55°C, pH 4.8-6.8.

Immediately at $t = 0$ hours, lead precipitated in experiments pH 5.6-8.9 at both temperatures (Figure 2.6), similar to the trend previously noted at pH 4.8-6.8 experiment at 55°C (Figure 2.5(B)). The instantaneous low lead measurement that increased slightly around 25% recovery (2.5×10^{-7} M) by 48 hours was clearly tied to the higher temperature experiments. Soluble lead in 55°C decreased with several measurements below the IDL and LOQ, which was also mirrored in the higher pH (6.8-9.5) experiment (Figure 2.7(B)). Both experiments behaved similarly regardless of temperature differences, suggesting that the higher pH controlled the lead speciation in the system.

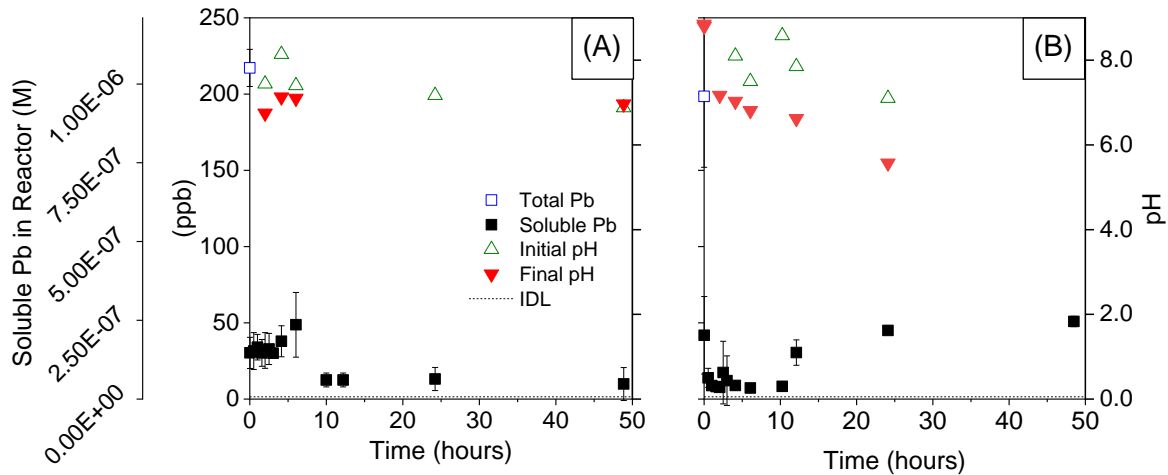


Figure 2.6. Changes in soluble lead (Pb) concentration (left axis, square) and pH reported (right axis, triangle) for pH 5.6-8.9 over 48 hours. Kinetic data compared against temperature at (A) 25°C, pH 6.8-8.1 and (B) 55°C, pH 5.6-8.9.

Neither the 25°C nor 55°C experiments from pH 7.3-9.8 confirmed the initial total added lead at 9.7×10^{-7} M, measuring at 90% and 81% of the total lead, respectively. The trend in the pH 7.3-9.8 experiment at 25°C in Figure 2.7(A) more closely followed that in the pH 5.7-7.4 experiment at 25°C than the immediate decrease in measured soluble lead seen in the neutral pH (6.8-8.1) experiment. The overall decrease to 22% of the originally added Pb in the pH 7.3-9.8 test could be a result of pH dropping near neutral, closely resembling the conditions outlined in Figure 2.5(A) by the end of 24 hours. Higher variability characterized the high-temperature-high-pH experiment, with many data measurements below the IDL and LOQ (Figure 2.7(B)). In comparison to other high temperature experiments, this experiment had a higher recovery of Pb^{2+} by 48 hours. Overall, the pH decreased at a relatively similar rate in these experiments, independent of temperature. In conjunction with the neutral pH experiment (Figure 2.5), this trend suggested that temperature immediately affected soluble lead concentrations, but the speciation of lead was controlled by pH.

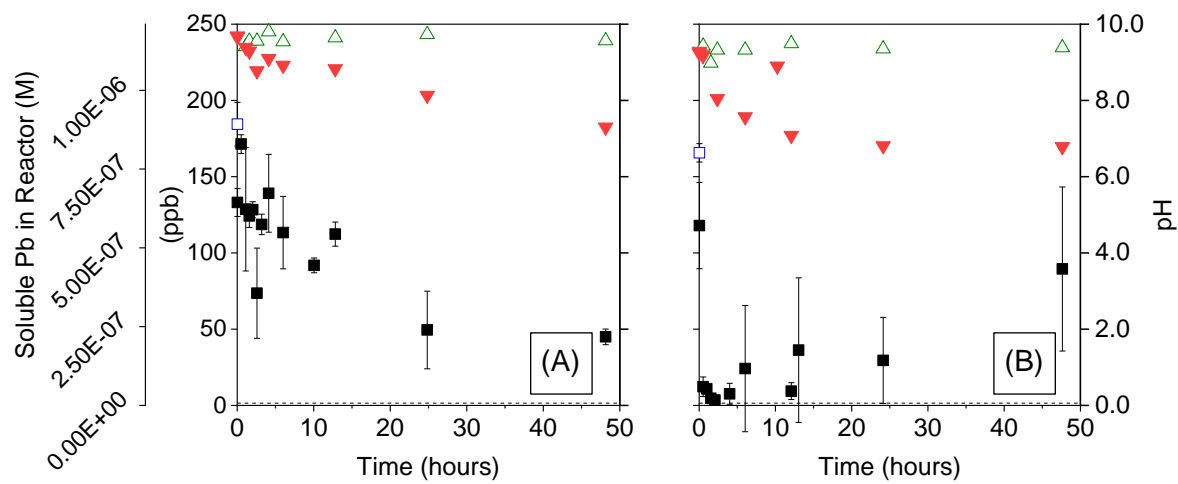


Figure 2.7. Changes in soluble lead (Pb) concentration (left axis, square) and pH reported (right axis, triangle) for pH 6.8-9.8 over 48 hours Kinetic data compared against temperature (A) 25°C, pH 7.3-9.8 and (B) 55°C, pH 6.8-9.5.

Changes in the soluble lead concentration was compared across pH, keeping temperature constant (Figure 2.8). Clearly, pH played a distinct role in the soluble Pb over time, which is consistent with previous studies' results. While not all trends are clearly defined for each experiment, results from 25°C tests at or above pH 6.5 resulted in higher lead precipitation early in the process. The complex kinetics in these experiments make it difficult to characterize the mechanisms that could be controlling the system.

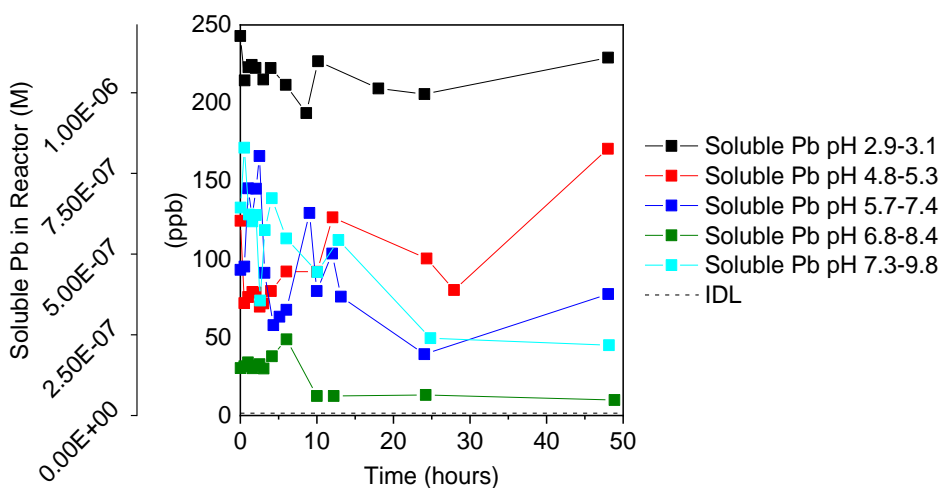


Figure 2.8. Soluble lead concentration over time. Comparison at $T = 25^\circ\text{C}$ from pH 2.9-9.8. Error bars removed for readability.

The 55°C experiments showed less variability in soluble lead concentrations across pH, while reaching a similar, lower final pH over time (Figure 2.9). In congruence with the data at 25°C, increasing pH led to a decrease in overall concentrations of soluble lead. All samples showed an initial drop in measured soluble lead concentrations at time = 0 hours, showing that increasing temperature caused a more dynamic rate of lead precipitation. None of the 55°C experiments recovered more than 58% of the original Pb added to the system until after 10 hours, suggesting the relationship that sustaining higher temperature for up to 10 hours could lead to higher precipitation of lead solids in a Pb-H₂O system. However, after 12 hours, samples at alkaline pH showed an increase in soluble lead, leading to the conclusion that both pH and temperature play integral roles in soluble lead concentrations.

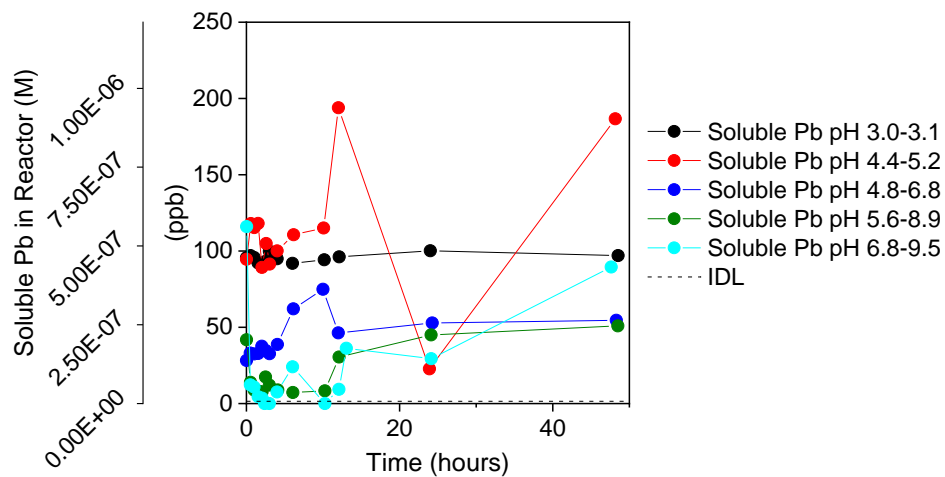


Figure 2.9. Soluble lead concentration over time. Comparison at T = 55°C from pH 3.0-9.5. Error bars removed for readability.

2.4.3 Effect of pH and temperature on soluble lead at equilibrium

Long-term points were taken approximately 6 weeks (1000 hours) after sample preparation and meant to simulate equilibrium conditions. In almost every case above pH 3.0, the final equilibrium pH was lower than the pH of the rest of the experiment, except one: there was an increase from average kinetic pH 5.06 to equilibrium pH 5.57 (compare to Figure 2.3). The higher temperature (55°C) experiments showed the greatest pH fluctuation, making it difficult to correlate pH to soluble lead concentrations in the long-term experiments.

The lead speciation model developed in this work included solubility of Pb to determine which lead complexes may be present in the Pb-H₂O system and which solid(s) may predominate

with a given set of conditions at equilibrium. For the Pb-H₂O system, potential solids include: Pb_(s), PbO_(s), Pb(OH)_{2(s)}, and PbO_{2(s)}. Due to the high unlikelihood of Pb_(s) and PbO_(s) forming (refer to Pourbaix diagram), only the oxide and hydroxide solids were included in this analysis [6].

Equilibrium constants are reported for infinite dilution conditions. With a constant ionic medium, it may be useful to apply a concentration-based equilibrium constant, ^cK. To account for the change due to ionic strength, equilibrium constant, K for a general reaction (aA + bB ⇌ cC + dD) is determined mathematically based on the relationship

$$K = \frac{\gamma_C[C]^c \gamma_D[D]^d}{\gamma_A[A]^a \gamma_B[B]^b} = {}^cK \times \frac{\gamma_C^c \gamma_D^d}{\gamma_A^a \gamma_B^b}$$

Eq. 2.9

where gamma (γ) is the activity coefficient, ($\gamma=1$) the system is. Activity, denoted with braces ({}), is the activity of a species. Ionic strength (I) of the system is calculated with the following equation:

$$I = \frac{1}{2} \sum_i m_i Z_i^2$$

Eq. 2.10

Ionic strength varied per experiment due to differences in the pH control but was estimated at 8.5×10⁻⁶ M for modeling purposes (Table 2.3).

Table 2.3. Ionic strength calculation for speciation model with Pb_{Total} = 9.7×10⁻⁷ at pH 7.0.

Species	Concentration M	Ionic Strength M
Pb ²⁺	9.7×10 ⁻⁷	1.9×10 ⁻⁶
H ⁺	1.0×10 ⁻⁷	5.0×10 ⁻⁸
NO ₃ ²⁻	3.2×10 ⁻⁶	6.5×10 ⁻⁶
Na ⁺	4.4×10 ⁻⁸	2.2×10 ⁻⁸
OH ⁻	1.6×10 ⁻⁷	8.0×10 ⁻⁸
I =		8.5×10⁻⁶

Activity coefficients (γ) were found using the ionic strength (I) and applying the Davies Equation (Eq. 2.11) for I < 0.5 M and reported in Table 2.4:

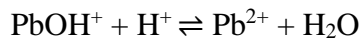
$$-\log \gamma_i = AZ_i^2 \left(\frac{\sqrt{I}}{1+\sqrt{I}} - 0.2I \right).$$

Eq. 2.11

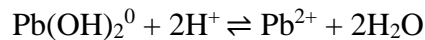
Table 2.4. Activity coefficients calculated for speciation model.

Charge	γ
1	0.997
2	0.986
3	0.970
4	0.947

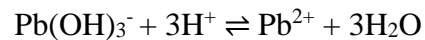
These relationships were used to recalculate the tabulated equilibrium °K values in relation to the ionic strength defined by the experiments laid out in Section 2.2.2. In the Pb-H₂O closed system, various species including lead ions (Pb²⁺), oxides and hydroxides could form. Aqueous complexes are included below.



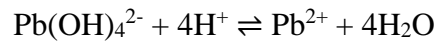
1.4



1.5



1.6

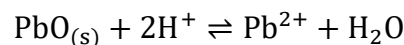


1.7

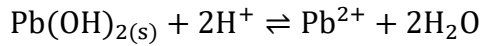
To characterize the system, total solubility of the Pb-H₂O system is given by the equation

$$\text{Pb}_{\text{TOT}}^{\text{II}} = [\text{Pb}^{2+}] + [\text{Pb(OH)}^+] + [\text{Pb(OH)}_2]_{(\text{aq})} + [\text{Pb(OH)}_3^-] + [\text{Pb(OH)}_4^{2-}] \quad \text{Eq. 2.12}$$

where a predominating solid (PbO_(s) or Pb(OH)_{2(s)}) controls the concentrations of each complex. Polynuclear lead species were not considered as a part of this system. Additionally, PbO_{2(s)} was excluded from the analysis due to the high unlikelihood of its formation under the experimental conditions.



1.18



1.20

Table 2.5 summarizes the model input values for the equilibrium constants of soluble lead complexes. Cumulative complexation constants, or beta (β) values, were calculated as a product of K_{eq} values for sequential ligands.

$$K_{\text{eq } 1} = \beta_1$$

Eq. 2.13

$$K_{\text{eq } 1} \times K_{\text{eq } 2} = \beta_2$$

Eq. 2.14

Hydrolysis complexation constants (${}^*\beta$) were calculated as a product of K_{eq} values in each reaction and K_w , based on ionic strength (Table 2.5). ${}^*\beta$ is a useful constant for sequential hydroxyl complexes, which simplifies these interdependent relationships and shows the pH-dependence of the equations:

$$K_w \times K_{\text{eq } 1, \text{PbOH}^+} = {}^*\beta_1 = \frac{\{\text{PbOH}^+\}\{\text{H}^+\}}{\{\text{Pb}^{2+}\}}$$

Eq. 2.15

$$K_w \times K_{\text{eq } 2, \text{Pb(OH)}_{2(\text{aq})}} \times {}^*\beta_1 = {}^*\beta_2 = \frac{\{\text{Pb(OH)}_{2(\text{aq})}\}\{\text{H}^+\}^2}{\{\text{Pb}^{2+}\}}$$

Eq. 2.16

$$K_w \times K_{\text{eq } 3, \text{Pb(OH)}_3^-} \times {}^*\beta_2 = {}^*\beta_3 = \frac{\{\text{Pb(OH)}_3^-\}\{\text{H}^+\}^3}{\{\text{Pb}^{2+}\}}$$

Eq. 2.17

$$K_w \times K_{\text{eq } 4, \text{Pb(OH)}_4^{2-}} \times {}^*\beta_3 = {}^*\beta_4 = \frac{\{\text{Pb(OH)}_4^{2-}\}\{\text{H}^+\}^4}{\{\text{Pb}^{2+}\}}$$

Eq. 2.18

Table 2.5. Equilibrium constants and β values for relevant complexes of Pb in a Pb-H₂O system.

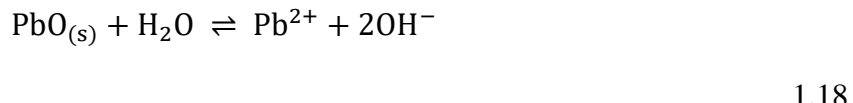
Complex	$\log cK$ at I=0 M [29]	$\log K_{eq}$ (Calc)	$\log \beta_i$ (Calc)	$\log * \beta_i$ at I=0 M [29]	$\log * \beta_i$ (Calc)	Name of Constant	β_i (Calc)
PbOH ⁺	6.40	6.40	6.40	-7.60	-7.60	* $\beta_{1, PbOH}$	2.5×10^{-8}
Pb(OH) _{2(aq)}	1.70	1.70	10.90	-19.99	-19.90	* $\beta_{2, Pb(OH)2}$	1.3×10^{-20}
Pb(OH) ₃ ⁻	1.28	1.27	13.90	-28.09	-32.63	* $\beta_{3, Pb(OH)3}$	2.3×10^{-33}
Pb(OH) ₄ ²⁻	0.14	0.14	2.00	-39.70	-46.49	* $\beta_{4, Pb(OH)4}$	3.3×10^{-47}

When $*\beta$ values are inserted into Eq. 2.12, the soluble lead concentration is calculated as follows, where all species are listed as a function of [Pb²⁺]:

$$Pb_{TOT}^{II} = [Pb^{2+}] \left(1 + \frac{*\beta_1}{[H^+]} + \frac{*\beta_2}{[H^+]^2} + \frac{*\beta_3}{[H^+]^3} + \frac{*\beta_4}{[H^+]^4} \right)$$

Eq. 2.19

Given Pb_{Total} = 9.7×10^{-7} M (200 ppb) to match the experimental maximum Pb concentration, {Pb²⁺} was determined as a function of pH and $*\beta$ values. Then, each hydroxyl complex concentration was calculated as a function of pH and {Pb²⁺}. Additionally, the ion activity product (IAP) is used to measure the solubility of solids. If the product of the complexes concentrations (IAP) in each reaction is equivalent to the solubility of a solid (K_{s0}) controlling the system, the system is in equilibrium. When IAP > K_{s0} , a solid will form; when IAP < K_{s0} , no precipitation occurs. The reactions between lead and water forming oxide or hydroxide solids all include water (K_w); therefore, the specific $*K_{s0}$ is used as the comparative value for IAP calculations.



$$K_{s0} = 10^{12.894} = \{Pb^{2+}\}\{OH^-\}^2$$

Eq. 2.20

$$*K_{s0} = \frac{\{Pb^{2+}\}\{OH^-\}^2}{\{H^+\}^2\{OH^-\}^2} = \frac{\{Pb^{2+}\}}{\{H^+\}^2}$$

Eq. 2.21(A)

If $IAP > K_{s0}$, the total soluble lead (Pb_{TOT}^{II}) decreases, as more Pb precipitates as a solid. The upper limit of $\{Pb^{2+}\}$ is therefore dependent on the solubility of the controlling solid ($*K_{s0}$).

$$\{Pb^{2+}\} = *K_{s0} \times \{H^+\}^2$$

Eq. 2.21(B)

Table 2.6. $*K_{s0}$ values for relevant solids used in the speciation model for the Pb-H₂O system.

Solid	$\log *K_{s0}$	Source
PbO _(s) (massicot)	12.894	[7]
Pb(OH) _{2(s)}	8.15	[7]

The new $\{Pb^{2+}\}$ was the basis to recalculate all other complex concentrations. This set of calculations was performed for each solid listed in Table 2.6, and graphical models for each predominating solid are included below. The graphic representation of the speciation model is presented as a pC-pH diagram to characterize the system, where pC is the negative log of lead concentration (-log $\{Pb\}$).

Pb_{TOT}^{II} is the sum of concentrations of all soluble lead complexes in the Pb-H₂O system, noted by C in subsequent diagrams. Figure 2.10 shows a pC-pH diagram where PbO_(s) and Pb(OH)_{2(s)} control the system individually. Because the relationship between their formation is the same (Eq. 2.21(B)), the models are identical regardless of the controlling solid. Neither solid is expected to precipitate at any point as they are not insoluble enough to control the system entirely. $\{Pb^{2+}\}$ and $\{PbOH^+\}$ have the highest predicted concentrations for most of the pH range. At pH 11.3, $\{PbOH^+\}$ is 10 times greater than that of $\{Pb(OH)_{2(aq)}\}$ but steadily decreases as pH increases past that point. Due to a lack of enthalpy data for several lead hydroxide complexes, the equilibrium model was unable to be adjusted to account for the effect of temperature on K.

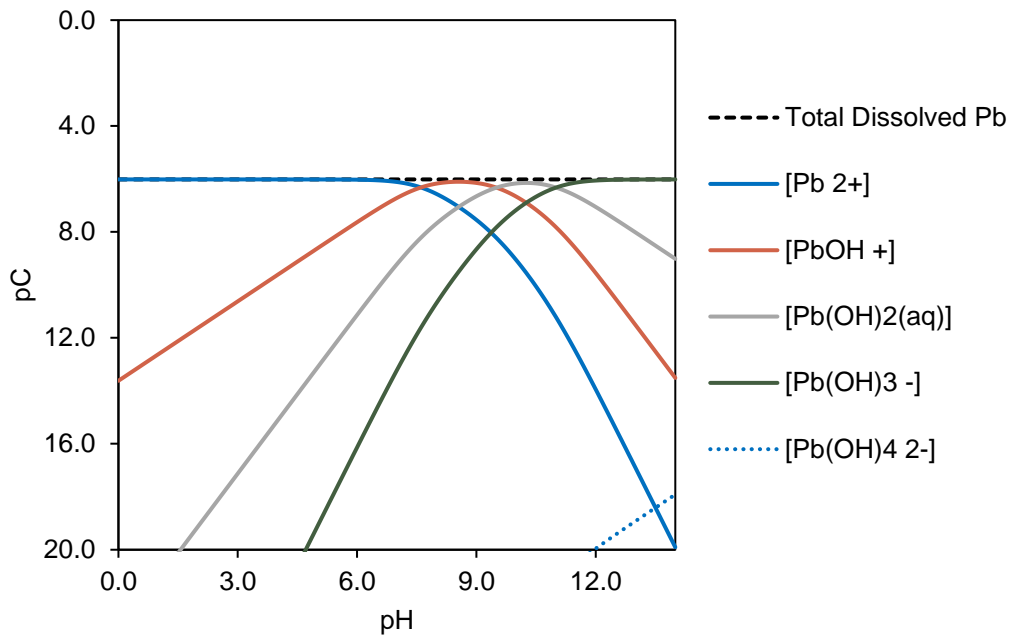


Figure 2.10. pC-pH diagram for the Pb-H₂O system at 25°C when either PbO_(s) or Pb(OH)_{2(s)} predominates. Pb_{Total} = 9.7×10⁻⁷ M and low I = 8.5×10⁻⁶ M.

Each long-term sample was prepared and analyzed in the same manner as the kinetic samples and was then combined with the solubility model shown in Figure 2.11. Experimental data values and other relevant information are recorded below in Table 2.7. The equilibrium point at pH 3.0 shows a distinct deviation from the model and the formation of solid at low pH is not supported in literature. A large variability characterized the equilibrium point at pH 5.45 (25°C) even after multiple attempts to accurately identify the data. In the neutral-pH experiments, the pH of the 25°C data (pH=6.8-8.4) decreased to 6.5 while the pH decreased to 4.9 at the final equilibrium point in the 55°C experiment (pH = 5.6-8.9). The drop in pH may have contributed to the soluble lead as concentrations slightly increased to 2.3×10⁻⁷ M (25°C) and 4.8×10⁻⁷ M (55°C). At a 0.7 pH-unit difference, the higher temperature experiment measured more than twice the value of lead at 25°C.

Table 2.7. Long-term equilibrium experiment recovery as a function of temperature and pH.

Initial pH	Final pH	Time (hours)	Measured $\{Pb^{2+}\}$ (M)	Measured $\{Pb^{2+}\}$ Error (M)	$\frac{Pb_{TOT}^{II}}{Pb_{Total}}$ (%)	$\frac{Pb_{TOT}^{II}}{Pb_{Total}}$ Error (%)
Temperature = 25°C						
3.0	2.96	1008.23	4.9×10^{-8}	1.0×10^{-8}	5%	1%
5.3	5.57	1010.22	8.9×10^{-7}	6.4×10^{-8}	92%	7%
6.7	5.45	1014.19	7.4×10^{-7}	3.3×10^{-7}	76%	35%
8.4	6.49	1016.82	2.3×10^{-7}	1.4×10^{-7}	24%	14%
9.7	7.02	1010.72	3.4×10^{-7}	5.4×10^{-8}	35%	6%
Temperature = 55°C						
3.0	3.15	1012.33	6.2×10^{-7}	1.1×10^{-7}	64%	12%
5.2	3.96	1009.36	1.0×10^{-6}	2.8×10^{-8}	103%	3%
6.8	4.12	1004.08	4.7×10^{-7}	3.8×10^{-8}	49%	4%
8.9	4.87	1011.24	4.8×10^{-7}	2.0×10^{-8}	50%	2%
9.4	4.38	1009.52	9.2×10^{-7}	1.3×10^{-7}	96%	13%

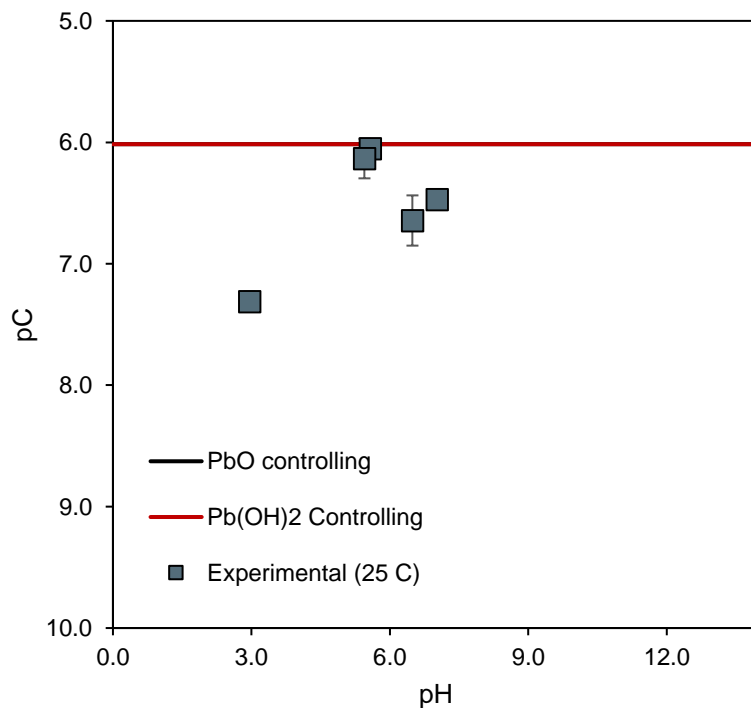


Figure 2.11. Comparison of experimental equilibrium solubility of Pb at various pH values with speciation model. Total dissolved Pb (Pb_{TOT}^{II} , M) over range of pH with $PbO_{(s)}$ and $Pb(OH)_{2(s)}$ predominating at 25°C with $Pb_{Total} = 9.7 \times 10^{-7}$ M and low $I = 8.5 \times 10^{-6}$ M.

Based on the inputs to the experimental samples, $\text{PbO}_{2(\text{s})}$ was unlikely to form. The non-chlorinated, nitrogen-sparged system would not have been oxidizing enough to form Pb(IV) species from Pb(II) [8]. $\text{PbO}_{(\text{s})}$ and $\text{Pb(OH)}_{2(\text{s})}$ were the only potential solids within the system, and neither were predicted to predominate.

The results indicate that both temperature and pH affect the speciation of lead in water. As pH increased, independent of temperature, generally concentrations of soluble lead decreased. Additionally, the long-term experiments could support the idea that higher temperature increased solubility of lead in a Pb-H₂O system. However, the final pH values of the 55°C experiments were generally lower than those of the 25°C experiments. The lack of correlation between model and experimental equilibrium points could be due to the experiment not yet being at equilibrium by six weeks. Further work is needed to characterize the higher temperature system at consistently higher pH values.

2.5 Conclusions

The kinetic experiments in this work verified that high temperatures (55°C) could be a factor in characterizing soluble lead concentrations over a range of environmentally relevant pH values (2.9-9.8). Formation of Pb solids was confirmed in most experimental scenarios at both 25°C and 55°C. The equilibrium thermodynamic model suggests that there would be minimal changes in lead speciation while maintaining all equilibrium conditions and solely increasing temperature to 55°C. Based on the equilibrium solubility model and how the experimental systems performed, the solid formation indicated that these experiments were not yet at equilibrium. Increases in temperature proved to decrease the concentrations of soluble lead in comparison to the identical pH 25°C experiment in both kinetic and equilibrium tests. However, final pH measurements for equilibrium points at 55°C showed significantly more variation than those taken at 25°C, which may mean that the combination of low pH and high temperature impacted the long-term soluble lead concentrations.

Application for these results could be tied to residential water heaters, which reach temperatures up to 60°C. Refer to Figure 1.1 and Section 1.4 for a fuller description of residential heaters. While these appliances are not a source of Pb themselves, lead can leach from materials used in municipal piping networks or residences when certain water quality parameters are present.

Previous research has shown that some solids take hours, days, or weeks for equilibrium conditions to stabilize, if at all [10],[11]. Practically, water entering a residential water heater has very little time to heat before the household requires it. The holding (stagnation) time within the heater could range depending on size and household usage for a short period up to 48 hours, which was the basis of the kinetic experiments.

2.6 Future Work

Integration of the speciation model with the thermodynamic model would allow for the interpretation of different solids forming at various temperatures. Further work on the speciation analysis of the experiments should be also performed. Solids analysis (such as x-ray diffraction) would help to accurately characterize the system. Follow-up experiments could include other water quality parameters, such as disinfectant residual (free chlorine or chloramines), comparing further kinetic and equilibrium data to the model discussed in this work.

2.7 References

- [1] S. Masters, G. J. Welter, and M. Edwards, “Seasonal Variations in Lead Release to Potable Water,” *Environ. Sci. Technol.*, vol. 50, no. 10, pp. 5269–5277, May 2016.
- [2] M. Lacroix, “Electric water heater designs for load shifting and control of bacterial contamination,” *Energy Convers. Manag.*, vol. 40, no. 12, pp. 1313–1340, 1999.
- [3] W. J. Rhoads, P. Ji, A. Pruden, and M. Edwards, “Water heater temperature set point and water use patterns influence Legionella pneumophila and associated microorganisms at the tap,” *Microbiome*, 2015.
- [4] J. O. Falkingham, E. D. Hilborn, M. J. Arduino, A. Pruden, and M. A. Edwards, “Epidemiology and Ecology of Opportunistic Premise Plumbing Pathogens: Legionella pneumophila, *Mycobacterium avium*, and *Pseudomonas aeruginosa*,” *Environ. Health Perspect.*, vol. 123, no. 8, pp. 749–758, 2015.
- [5] S. Chowdhury, F. Kabir, M. A. J. Mazumder, and M. H. Zahir, “Modeling lead concentration in drinking water of residential plumbing pipes and hot water tanks,” *Sci. Total Environ.*, 2018.

- [6] R. M. Harrison and D. P. H. Laxen, "Physicochemical speciation of lead in drinking water," *Nature*, 1980.
- [7] E. J. Kim, J. E. Herrera, D. Huggins, J. Braam, and S. Koshowski, "Effect of pH on the concentrations of lead and trace contaminants in drinking water: A combined batch, pipe loop and sentinel home study," *Water Res.*, 2011.
- [8] P. Delahay, M. Pourbaix, and P. Van Rysselberghe, "Potential-pH Diagram of Lead and its Applications to the Study of Lead Corrosion and to the Lead Storage Battery," *J. Electrochem. Soc.*, vol. 98, no. 2, pp. 57–64, 1951.
- [9] W. A. Brezonik, Patrick L.; Arnold, *Water Chemistry: An Introduction to the Chemistry of Natural and Engineered Aquatic Systems*, 1st ed. Oxford University Press, 2011.
- [10] D. E. Giammar, "Water Chemistry Effects on Dissolution Rates of Lead Corrosion Products Subject Area: Infrastructure."
- [11] Y. Wang, J. Wu, Z. Wang, A. Terenyi, and D. E. Giammar, "Kinetics of lead(IV) oxide (PbO₂) reductive dissolution: Role of lead(II) adsorption and surface speciation," *J. Colloid Interface Sci.*, vol. 389, no. 1, pp. 236–243, Jan. 2013.
- [12] D. W. Oxtoby, H. P. Gillis, and A. Campion, *Principles of Modern Chemistry*, 8th ed. Belmont, CA: Brooks Cole, 2011.
- [13] C. Muzny, "NIST Chemistry WebBook, NIST Standard Reference Database Number 69," in *Thermodynamics Source Database*, P. J. Linstrom and W. G. Mallard, Eds. Gaithersburg, MD: National Institute of Standards and Technology, 2018.
- [14] J. R. Rumble, Ed., *CRC Handbook of Chemistry and Physics [Web]*, 100th ed. 2019.
- [15] D. D. Wagman, W. H. Evans, V. B. Parker, I. Harlow, S. M. Bailey, and R. H. Schumm, "Selected Thermodynamic Values for Substances," in *Series 3*, Washington, D.C.: National Bureau of Standards, 1968, pp. 187–195.
- [16] A. J. Bard, R. Parsons, and J. Jordan, *Standard Potentials in Aqueous Solution*. New York, NY: Marcel Dekker, Inc., 1985.

- [17] W. D. Schecher and D. C. McAvoy, “MINEQL+: A Chemical Speciation Modeling for the Real World.” Environmental Research Software, 2015.
- [18] H. Bilinski and P. Schindler, “Solubility and equilibrium constants of lead in carbonate solutions (25°C, $I = 0.3 \text{ mol dm}^{-3}$),” *Geochim. Cosmochim. Acta*, vol. 46, no. 6, pp. 921–928, 1982.

3. IONIC STRENGTH DEPENDENCE OF SOLUBLE LEAD

3.1 Introduction

The main source of lead in U.S. drinking water systems and the ensuing health effects of lead poisoning is from preexisting service lines, solder, fittings, joints or the small percentage of Pb in pipes and components installed after 1986 [1]–[3]. The Safe Drinking Water Act (1974) and Lead and Copper Rule (1991) ensure that new construction does not include fully leaded components in distribution pipes or residential plumbing [2], [4], [5]. One aspect of residential plumbing that has received little research attention is water softeners. No part of the water softener is made with lead, but the changes in water chemistry due to use of a water softener may alter the speciation of incoming lead (Pb) from a distribution system. With residential water softening increasing in popularity, changes in ionic strength could be an important factor to consider when examining water quality effects within a potable water system.

Few publications have focused on the interactions of lead in a chemically softened water system. Research indicates that softeners could be effective mechanisms to remove metal contaminants, such as lead. Research in this area has been focused on resins, optimizing the ion-exchange process for heavy metal removal, or determining if a resin could assist in heavy metal removal [6]–[8]. Maliou, et al. researched zeolite mineral (clinoptilolite) resin in the early 1990s to determine its capability for Pb removal [6]. From several kinetic experiments, the authors determined that increased temperature (70°C) led to increased metal uptake due to resin selectivity placing lead higher than sodium. Another study measured the efficiency of particulate lead removal with seven anionic and cationic resins, with breakthrough values ranging from 4-75% of the original known value(s) [7]. Furthermore, a more recent study performed by Aydin, et al. used coal as a resin and determined that lower pH (0-3) resulted in lower Pb(II) removal [8]. The authors believed this was due to positive-positive ion repulsion with Pb(II) and H⁺. Above pH 5, there was also a noticeable decrease in Pb(II) sorption to the resin, which was likely due to Pb precipitation. Unlike the experiments with the zeolite resin, Pb uptake onto the coal resin was inversely proportional to the temperature, where the higher temperatures were less effective at Pb(II) removal.

While those works focused on resins and lead removal, previous research linking ionic strength and lead solubility is limited. Holm and Schock (1991) determined that lead solid chloropyromorphite ($\text{Pb}_5(\text{PO}_4)_3\text{Cl}_{(s)}$) solubility is dependent on ionic strength. The solubility of several lead solids (chloropyromorphite and hydrocerussite) were estimated to decrease in the presence of increased ionic strength (0.005 M versus 0.1 M) [9]. To close the gap on lead chemistry in water with high ionic strength, research in this work intends to focus on changes in ionic strength and the resulting speciation of lead in water.

3.2 Materials & Methods

3.2.1 Standards, Reagents, & Preparation of Stocks

Refer to Section 2.2.1 for reagents used. Ionic strength was controlled by addition of granular NaCl purchased from Aldrich.

Stock solutions for sample preparation in reactors were prepared by diluting the purchased 4.8×10^{-3} M (1000 ppm) Pb standard solution to 4.8×10^{-5} M (10 ppm) Pb in sparged DI water. Stock solutions for preparation of ICP-OES lead standards were prepared by diluting the original stock solution (4.8×10^{-3} M) to 4.8×10^{-5} M (10 ppm) and 4.8×10^{-7} M Pb (100 ppb) in 2% HNO₃, ranging from 2.4×10^{-8} M to 4.8×10^{-6} M (5-1000 ppb). Standards were periodically remade, and samples were calibrated to these standards when run on the ICP-OES. Stock solutions of 10^{-3} M and 10^{-2} M NaOH were used for pH control. Stock solutions for controlling ionic strength were prepared with granular NaCl in N₂ sparged DI water. A stock solution of 1.0 M NaCl was prepared and diluted in water to solutions of 0.02-0.14 M.

3.2.2 Experimental Procedure and Sample Analysis

The experimental procedure and sample analysis used in this chapter were identical to Section 2.2.2, although the reactors were additionally adjusted with NaCl to obtain a range of ionic strength values. Here, lead-containing synthetic waters were placed into 15 or 50 mL metal-free, non-sterile polypropylene (PP) centrifuge tubes. Depending on the ionic strength, the 15 mL plastic vials were filled to 7.35 mL with the corresponding NaCl stock solution and were adjusted to pH 7.0. An aliquot of the lead stock solution (4.8×10^{-5} M) was added to each solution to achieve a final reaction concentration of 9.7×10^{-7} M (200 ppb) Pb.

Ionic strength (I) was calculated for reactors with Eq. 2.11. An example of all the constituents in each sample reactor is shown below in Table 3.1, and these values of ionic strength were reflected in the developed equilibrium model. The ionic strength was primarily controlled by the addition of NaCl.

Table 3.1. Ionic strength calculations for speciation at $I = 0.02$ M, pH 7.0, T = 25°C.

Species	Concentration M	Ionic Strength M
Pb ²⁺	9.7×10^{-7}	1.9×10^{-6}
H ⁺	7.9×10^{-8}	4.0×10^{-8}
NO ₃ ²⁻	9.7×10^{-7}	1.9×10^{-6}
Na ⁺	1.8×10^{-2}	9.0×10^{-3}
Cl ⁻	1.8×10^{-2}	9.0×10^{-3}
OH ⁻	3.2×10^{-5}	1.6×10^{-5}
I =		1.8×10^{-2}

3.3 Results & Discussion

3.3.1 Effect of ionic strength on kinetic experiments

ICP-OES soluble lead concentrations and pH data from kinetic experiments can be found in Appendix C (Table C.6, Table C.12-C.14). The first set of experimental results were obtained when the ionic strength was varied from 0-0.15 M and the initial pH set at 7.0, as seen in Figure 3.1. In general, the pH remained relatively stable, fluctuating between pH 6.5-7.1 over the course of 48 hours. In addition, all the experiments were effectively able to exhibit 91-107% initial Pb recovery of the spiked Pb solution, which represented the initial time point at t = 0 hours. The only exception occurred when the ionic strength equaled 0.15 M where a low initial Pb recovery of 81% was obtained (Figure 3.1(D)).

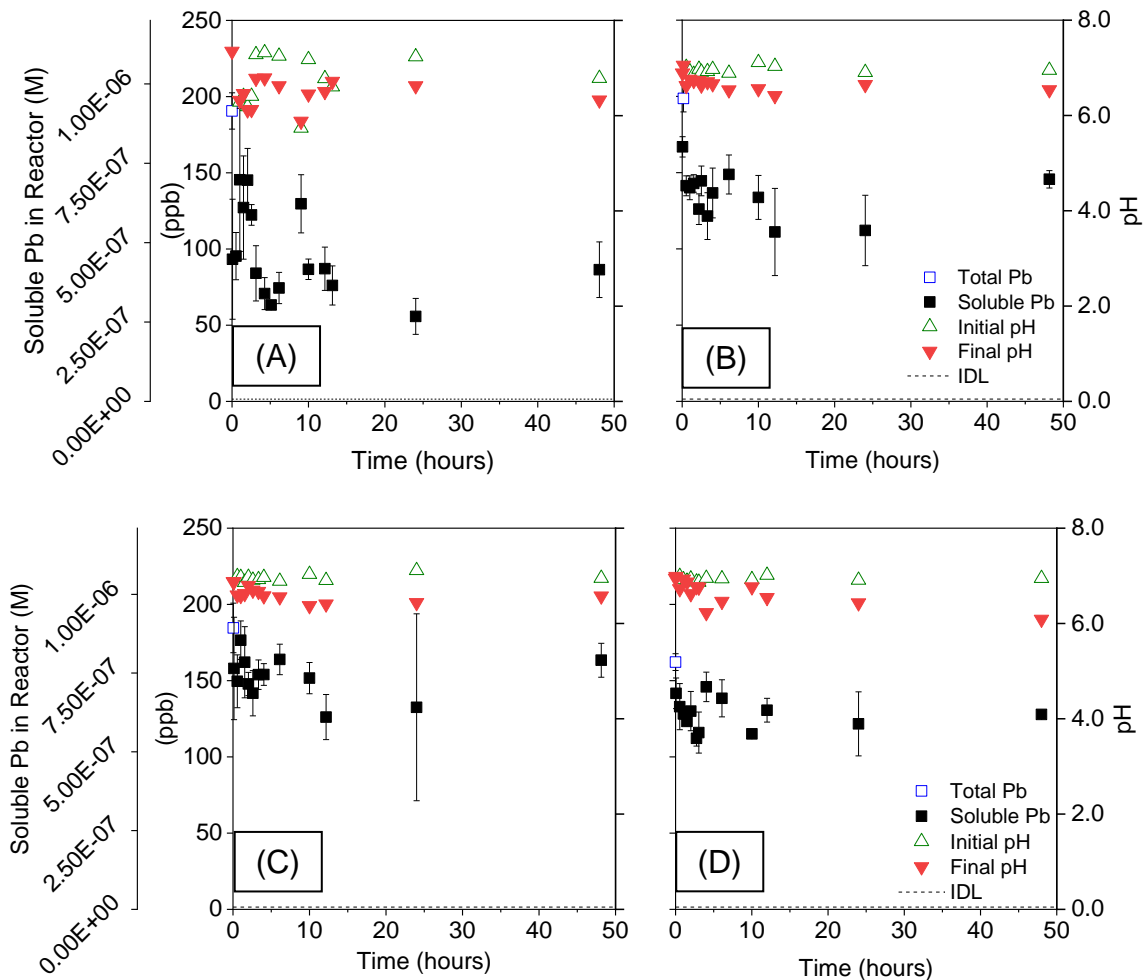


Figure 3.1. Measurement of soluble lead ($\text{Pb}_{\text{TOT}}^{\text{II}}$) over time at pH 7.0, 25°C with (A) $I = 8.5 \times 10^{-6}$ M, (B) $I = 0.02$ M, (C) $I = 0.07$ M, (D) $I = 0.15$ M.

All the experiments performed somewhat similarly and had a unified, steady trend. The kinetic experiments had a moderate recovery with consistency between triplicate points. The low ionic strength test ($I = 8.5 \times 10^{-6}$ M) showed the most unique response with an immediate drop to 44% of the original Pb added ($\text{Pb}_{\text{Total}} = 9.7 \times 10^{-7}$ M Pb). The soluble Pb concentration remained lower than Pb measured at higher ionic strengths for the duration of the experiment (<50% of Pb_{Total}). The higher ionic strength tests ($I = 0.02$ - 0.15 M) had higher measured concentrations of soluble lead, where no data was measured below 50% of the original Pb in the kinetic test.

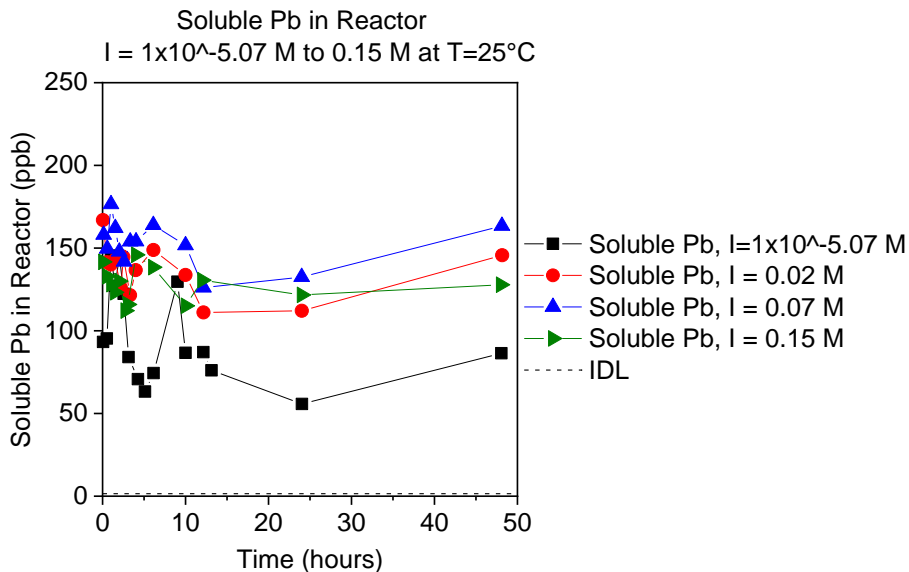


Figure 3.2. Comparison of soluble Pb measured in experimental reactors for 48 hours; $I = 8.5 \times 10^{-6}$ to 0.15 M at pH = 7.0, T = 25°C.

The kinetic data trend from each of the higher ionic strength tests was virtually indistinguishable between 0.02-0.15 M (Figure 3.2). This similarity could be due to the high overdose of NaCl to Pb in the system, resulting in a $1 \text{ Pb}^{2+} : 10^4 \text{ Cl}^-$ molar ratio at $I = 0.02 \text{ M}$ up to $1 \text{ Pb}^{2+} : 10^5 \text{ Cl}^-$ at $I = 0.15 \text{ M}$. With an increase in chloride ions from NaCl addition, soluble lead chloride complexes could form.

This difference between Pb_{Total} and measured soluble Pb in any of the experiments was most likely be due to the presence of $\text{Pb(OH)}_{2(s)}$ forming at neutral pH. Without an oxidizing agent, the experimental inputs did not provide enough ORP for the formation of $\text{PbO}_{2(s)}$, and $\text{PbO}_{(s)}$ is unlikely to form at neutral pH conditions. Additionally, all final concentration points at 48 hours increased from the trend leading up to it, indicating that the system was not yet at equilibrium by the end of the kinetic tests.

3.3.2 Effect of ionic strength on equilibrium experiments

Long-term points were taken approximately 6 weeks (1000 hours) after sample preparation and meant to simulate equilibrium conditions. Sample pH remained relatively constant throughout the experiment, with a maximum decrease of 0.8 pH units. To model the experiments, pH was held constant at 7.0, but ionic strength was varied at 0.02 M, 0.07 M, 0.15 M to address each of the

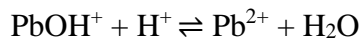
experimental conditions. Table 3.1 showed the ionic strength calculations for the $I = 0.02 \text{ M}$ condition, which were repeated for each condition. Activity coefficients (γ) were found using the ionic strength (I), applying the Davies Equation (Eq. 2.11), and are reported in Table 3.2.

$$-\log \gamma_i = AZ_i^2 \left(\frac{\sqrt{I}}{1 + \sqrt{I}} - 0.2I \right) \quad \text{Eq. 2.11}$$

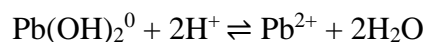
Table 3.2. Activity coefficients for Pb-H₂O-NaCl system at $I = 0.02\text{-}0.15 \text{ M}$, pH 7.0, T = 25°C.

Charge (z)	γ $I=0.02 \text{ M}$	γ $I=0.07 \text{ M}$	γ $I=0.15 \text{ M}$
1	0.875	0.794	0.749
2	0.585	0.397	0.315
3	0.300	0.125	0.074
4	0.117	0.025	0.010

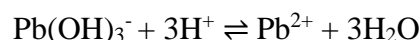
These relationships were used to recalculate the tabulated equilibrium °K values in relation to the ionic strength defined by the experiments laid out in 2.2.2 (values recorded in Appendix A). The lead speciation model discussed in Section 2.4.3 was also used to predict which lead complexes may be present in the Pb-H₂O-NaCl system and which solid(s) may predominate with a given set of conditions. For this system, potential solids included: Pb_(s), PbO_(s), Pb(OH)_{2(s)}, and PbO_{2(s)}. Due to the high unlikelihood of Pb_(s) or PbO_{2(s)} forming in this system (refer to Pourbaix diagram), only the oxide and hydroxide lead(II) solids were included in this analysis [23]. In the closed Pb-H₂O-NaCl closed system, various species including lead ions (Pb²⁺), oxides, hydroxides, and chlorides could form. Reactions of the soluble complexes are included below.



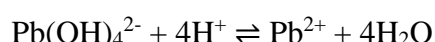
1.4



1.5



1.6



	1.7
$\text{PbCl}^+ \rightleftharpoons \text{Pb}^{2+} + \text{Cl}^-$	
	1.9
$\text{PbCl}_{2(\text{aq})} \rightleftharpoons \text{Pb}^{2+} + 2\text{Cl}^-$	
	1.10
$\text{PbCl}_3^- \rightleftharpoons \text{Pb}^{2+} + 3\text{Cl}^-$	
	1.11
$\text{PbCl}_4^{2-} \rightleftharpoons \text{Pb}^{2+} + 4\text{Cl}^-$	
	1.12

To characterize the system, total solubility of the Pb-H₂O-NaCl system is given by the equation

$$\begin{aligned} \text{Pb}_{\text{TOT}}^{\text{II}} = & [\text{Pb}^{2+}] + [\text{Pb}(\text{OH})^+] + [\text{Pb}(\text{OH})_{2(\text{aq})}] + [\text{Pb}(\text{OH})_3^-] + [\text{Pb}(\text{OH})_4^{2-}] + [\text{PbCl}^+] \\ & + [\text{PbCl}_{2(\text{aq})}] + [\text{PbCl}_3^-] + [\text{PbCl}_4^{2-}] \end{aligned} \quad \text{Eq. 3.1}$$

where a predominating solid ($\text{PbO}_{(\text{s})}$ or $\text{Pb}(\text{OH})_{2(\text{s})}$) controls the concentrations of each complex.

Table 3.3 summarizes the model input values for the equilibrium constants of soluble lead complexes at each ionic strength. Cumulative complexation constants, or beta (β) values, were calculated as a product of K_{eq} values for sequential ligands.

$$K_{\text{eq } 1, \text{PbCl}^-} = \beta_1 = \frac{\{\text{PbCl}^+\}}{\{\text{Pb}^{2+}\}\{\text{Cl}^-\}} \quad \text{Eq. 3.2}$$

$$\beta_1 \times K_{\text{eq } 2, \text{PbCl}_{2(\text{aq})}} = \beta_2 = \frac{\{\text{PbCl}_{2(\text{aq})}\}}{\{\text{Pb}^{2+}\}\{\text{Cl}^-\}^2} \quad \text{Eq. 3.3}$$

$$\beta_2 \times K_{eq\ 3,PbCl_3^-} = \beta_3 = \frac{\{PbCl_3^-\}}{\{Pb^{2+}\}\{Cl^-\}^3}$$

Eq. 3.4

$$\beta_3 \times K_{eq\ 4,PbCl_4^{2-}} = \beta_4 = \frac{\{PbCl_4^{2-}\}}{\{Pb^{2+}\}\{Cl^-\}^4}$$

Eq. 3.5

Hydrolysis complexation constants (${}^*\beta$) were calculated as a product of K_{eq} values in each reaction and K_w , based on ionic strength (Table 3.3).

$$K_w \times K_{eq\ 1,PbOH^+} = {}^*\beta_1 = \frac{\{PbOH^+\}\{H^+\}}{\{Pb^{2+}\}}$$

Eq. 3.6

$$K_w \times K_{eq\ 2,Pb(OH)_{2(aq)}} \times {}^*\beta_1 = {}^*\beta_2 = \frac{\{Pb(OH)_{2(aq)}\}\{H^+\}^2}{\{Pb^{2+}\}}$$

Eq. 3.7

$$K_w \times K_{eq\ 3,Pb(OH)_3^-} \times {}^*\beta_2 = {}^*\beta_3 = \frac{\{Pb(OH)_3^-\}\{H^+\}^3}{\{Pb^{2+}\}}$$

Eq. 3.8

$$K_w \times K_{eq\ 4,Pb(OH)_4^{2-}} \times {}^*\beta_3 = {}^*\beta_4 = \frac{\{Pb(OH)_4^{2-}\}\{H^+\}^4}{\{Pb^{2+}\}}$$

Eq. 3.9

Table 3.3. Equilibrium and complexation constants for relevant Pb species in Pb-H₂O-NaCl closed system.

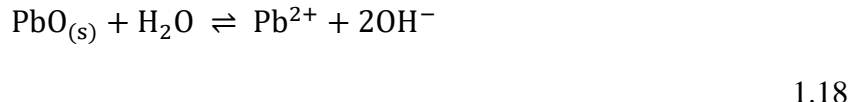
Species			log K				log *β _i			
	log β _i I=0 M	log cK I=0 M	I = 8.5x10 ⁻⁶ M	I = 0.02 M	I = 0.07 M	I = 0.15 M	I = 8.5x10 ⁻⁶ M	I = 0.02 M	I = 0.07 M	I = 0.15 M
PbOH ⁺	6.40	6.40	6.40	6.28	6.20	6.15	-7.60	-7.72	-7.80	-7.85
Pb(OH) _{2(aq)}	10.90	4.50	4.50	4.38	4.30	4.25	-17.11	-17.33	-17.50	-17.60
Pb(OH) ₃ ⁻	13.90	3.00	3.00	3.00	3.00	3.00	-28.09	-28.09	-28.09	-28.09
Pb(OH) ₄ ²⁻	2.00	-11.90	-11.89	-11.67	-11.50	-11.40	-53.99	-53.76	-53.59	-53.49
							log β _i			
PbCl ⁺	1.55	1.55	1.54	1.32	1.15	1.05	1.54	1.32	1.15	1.05
PbCl _{2(aq)}	2.20	0.65	0.64	0.30	0.05	-0.10	2.19	1.62	1.20	0.95
PbCl ₃ ⁻	1.80	-0.40	-0.41	-0.75	-1.00	-1.15	1.78	0.87	0.19	-0.21
PbCl ₄ ²⁻	1.46	-0.34	-0.35	-0.57	-0.74	-0.84	1.43	0.30	-0.55	-1.05

When the complexation constant relationships are inserted into Eq. 3.1, the soluble lead concentration is calculated as follows, where all species are listed as a function of $[Pb^{2+}]$:

$$Pb_{TOT}^{II} = [Pb^{2+}] \left(1 + \frac{*\beta_1}{[H^+]} + \frac{*\beta_2}{[H^+]^2} + \frac{*\beta_3}{[H^+]^3} + \frac{*\beta_4}{[H^+]^4} + \beta_1[Cl^-] + \beta_2[Cl^-]^2 + \beta_3[Cl^-]^3 + \beta_4[Cl^-]^4 \right)$$

Eq. 3.10

Given $Pb_{Total} = 9.7 \times 10^{-7}$ M (200 ppb) to match the experimental maximum Pb concentration, $\{Pb^{2+}\}$ was determined as a function of pH, β , and $*\beta$ values. Then, each complex concentration was calculated as a function of pH and $\{Pb^{2+}\}$. Additionally, the ion activity product (IAP) was used to measure the solubility of solids. If the product of the complexes' concentrations (IAP) in each reaction is equivalent to the solubility of a solid (K_{s0}) controlling the system, the system is in equilibrium. Eq. 3.12 shows the relationship for $PbO_{(s)}$ and $Pb(OH)_{2(s)}$. (This concept is further discussed in Section 2.4.3). For example, with $PbO_{(s)}$ as a solid:



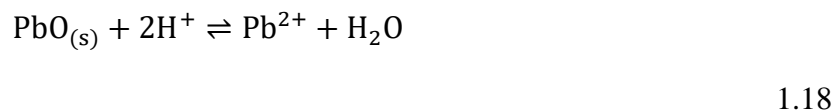
$$K_{s0} = 10^{12.894} = \{Pb^{2+}\}\{OH^-\}^2 \quad Eq. 3.11$$

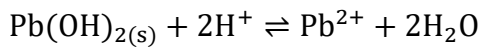
$$*K_{s0} = \frac{\{Pb^{2+}\}\{OH^-\}^2}{\{H^+\}^2\{OH^-\}^2} = \frac{\{Pb^{2+}\}}{\{H^+\}^2} \quad Eq. 3.12(A)$$

If IAP > K_{s0} , the total soluble lead (Pb_{TOT}^{II}) decreases, as more Pb precipitates as a solid. The upper limit of $\{Pb^{2+}\}$ is therefore dependent on the solubility of the controlling solid ($*K_{s0}$).

$$\{Pb^{2+}\} = *K_{s0} \times \{H^+\}^2 \quad Eq. 3.12(B)$$

Dissolution reactions are included below for each potential solid.





1.20

Table 3.4. Equilibrium solubility constants for relevant solids used in the speciation model.

Chemical Species	$\log *K_{s0}$		$\log *K_{s0}$			
	$I = 0 \text{ M}$	Source	$I = 8.5 \times 10^{-6} \text{ M}$	$I = 0.02 \text{ M}$	$I = 0.07 \text{ M}$	$I = 0.15 \text{ M}$
$\text{Pb(OH)}_{2(\text{s})}$	8.15	[29]	8.15	8.03	7.95	7.90
$\text{PbO}_{(\text{s})}$	12.894	[29]	12.89	12.78	12.69	12.67

The new $\{\text{Pb}^{2+}\}$ was the basis to recalculate all other complex concentrations. This set of calculations was performed for each solid listed in Table 3.4, and graphical models for each predominating solid are included below. $\text{Pb}_{\text{TOT}}^{\text{II}}$ is the sum of concentrations of all soluble lead complexes. The graphic representations of the speciation model are presented as a pC-pH diagram to characterize the system. Any dip of the total dissolved Pb (black dashed) line below $9.7 \times 10^{-7} \text{ M}$ ($-\log [\text{Pb}] = 6.0$) indicates the formation of the controlling solid.

In the lead oxide system, neither $\text{PbO}_{(\text{s})}$ nor $\text{Pb(OH)}_{2(\text{s})}$ were modeled to precipitate at any point and all dissolved species controlled the model (Figure 3.3). Because the relationship between their formation is the same (Eq. 3.12(B)), the models are identical regardless of the controlling solid. The low ionic strength model did not include NaCl; therefore, chloride complexes were not formed in the $I = 8.5 \times 10^{-6} \text{ M}$ models. Without the chloride complexes, most of the dissolved species until pH 10.7 were Pb^{2+} and PbOH^+ . Pb(OH)_3^- and Pb(OH)_4^{2-} were present in very small concentrations but dominated the system above pH 10.7. With ionic strength at 0.02 M in Figure 3.4, Pb^{2+} and PbOH^+ concentrations decreased by average factors of 1.2 and 1.6 (respectively) as the chloride complexes formed (Table 3.5). The model predicted that PbOH^+ concentration also declined sooner but at a slower rate at $I = 0.02 \text{ M}$ than at low ionic strength. Small but increased concentration of Pb(OH)_3^- formed as ionic strength increased to 0.02 M but decreased with the increase to $I = 0.15 \text{ M}$. Pb(OH)_4^{2-} concentration dropped off significantly as higher ionic strength was reached. In comparing $I = 0.02$ to 0.15 M , lead hydroxide complexes decreased in solubility by factors of 1.1 to 2.1, due to the presence of lead chlorides (Table 3.6). Lead ion (Pb^{2+}) was also modeled to decrease by a factor of 1.1, while chloride complexes increased by factors of 4.8 to

409. However, the dissolved lead concentration was expected to remain unchanged between the all ionic strength and controlling solid conditions (Figure 3.5).

Table 3.5. Average factors of change for each lead complex (right) with predominating solid (top) when comparing system at $I = 8.5 \times 10^{-6}$ M to 0.02 M. No chloride complexes included because NaCl present at low ionic strength.

Species	Predominating Solid
	$\text{PbO}_{(s)}$ & $\text{Pb(OH)}_{2(s)}$
Pb^{2+}	0.82
PbOH^+	0.66
Pb(OH)_2	411.74
Pb(OH)_3^-	0.81
Pb(OH)_4^{2-}	8.54×10^{-14}

Table 3.6. Average factors of change for each lead complex (right) with predominating solid (top) when comparing system at $I = 0.02$ M to 0.15 M.

Species	Predominating Solid
	$\text{PbO}_{(s)}$ & $\text{Pb(OH)}_{2(s)}$
Pb^{2+}	0.88
PbOH^+	0.65
Pb(OH)_2	0.48
Pb(OH)_3^-	0.88
Pb(OH)_4^{2-}	1.62
PbCl^+	4.76
PbCl_2	11.20
PbCl_3^-	75.55
PbCl_4^{2-}	409.19

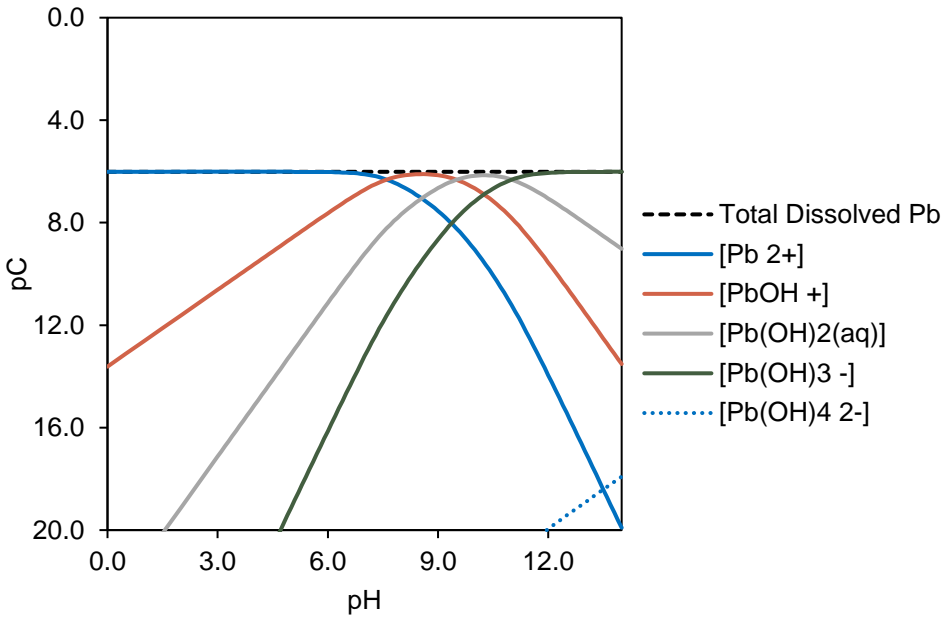


Figure 3.3. pC-pH diagram for the Pb-H₂O system at pH = 7.0, 25°C when either PbO_(s) or Pb(OH)_{2(s)} predominates. Pb_{Total} = 9.7×10⁻⁷ M and I = 8.5×10⁻⁶ M.

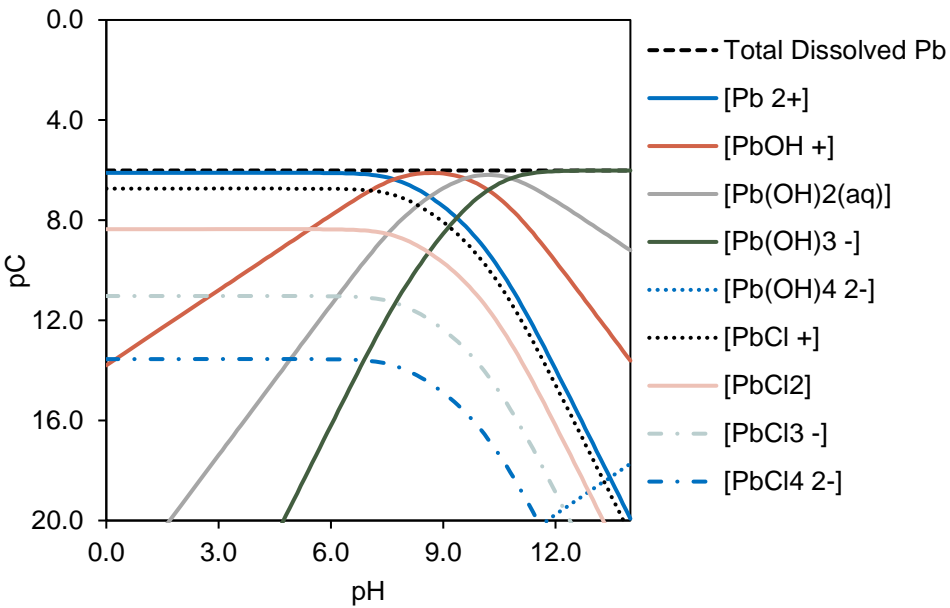


Figure 3.4. pC-pH diagram for the Pb-H₂O-NaCl system at pH = 7.0, 25°C when either PbO_(s) or Pb(OH)_{2(s)} predominates. Pb_{Total} = 9.7×10⁻⁷ M and I = 0.02 M.

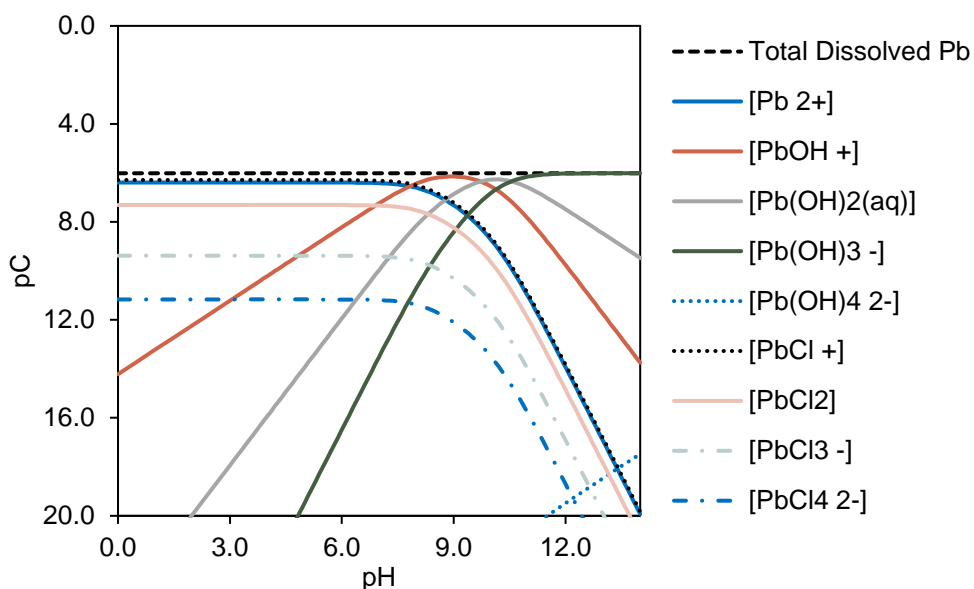


Figure 3.5. pC-pH diagram for the Pb-H₂O-NaCl system at pH = 7.0, 25°C when either PbO_(s) or Pb(OH)_{2(s)} predominates. Pb_{Total} = 9.7×10⁻⁷ M and I = 0.15 M.

Surprisingly, the I = 0.07 M experiment resulted in the lowest equilibrium soluble Pb concentration. With twice as much ionic strength (I = 0.15 M), soluble lead concentrations doubled. At negligible ionic strength (I = 8.5×10⁻⁶ M), soluble lead concentrations measured 4 times that in the ionic strength 0.07 M experiment. With 5 times less ionic strength (I = 0.02 M), soluble lead concentration increased 6-fold, which was consistent with the model prediction. There was no noticeable trend for the equilibrium lead measurements and variations in ionic strength. The condition at I = 0.02 M resulted in the highest measured soluble lead; however, the I = 0.15 M condition reported the second-highest lead precipitation which did not follow the model prediction. Measured soluble lead concentrations did not closely align with either solid-controlled system, as the experiments formed precipitates which were not expected according to the model. Less soluble lead was measured than the models predicted at all conditions tested. It is hypothesized that the system was not yet at equilibrium. Previous research verifies that many lead solid equilibrium points range on the orders of hours to months [11],[12].

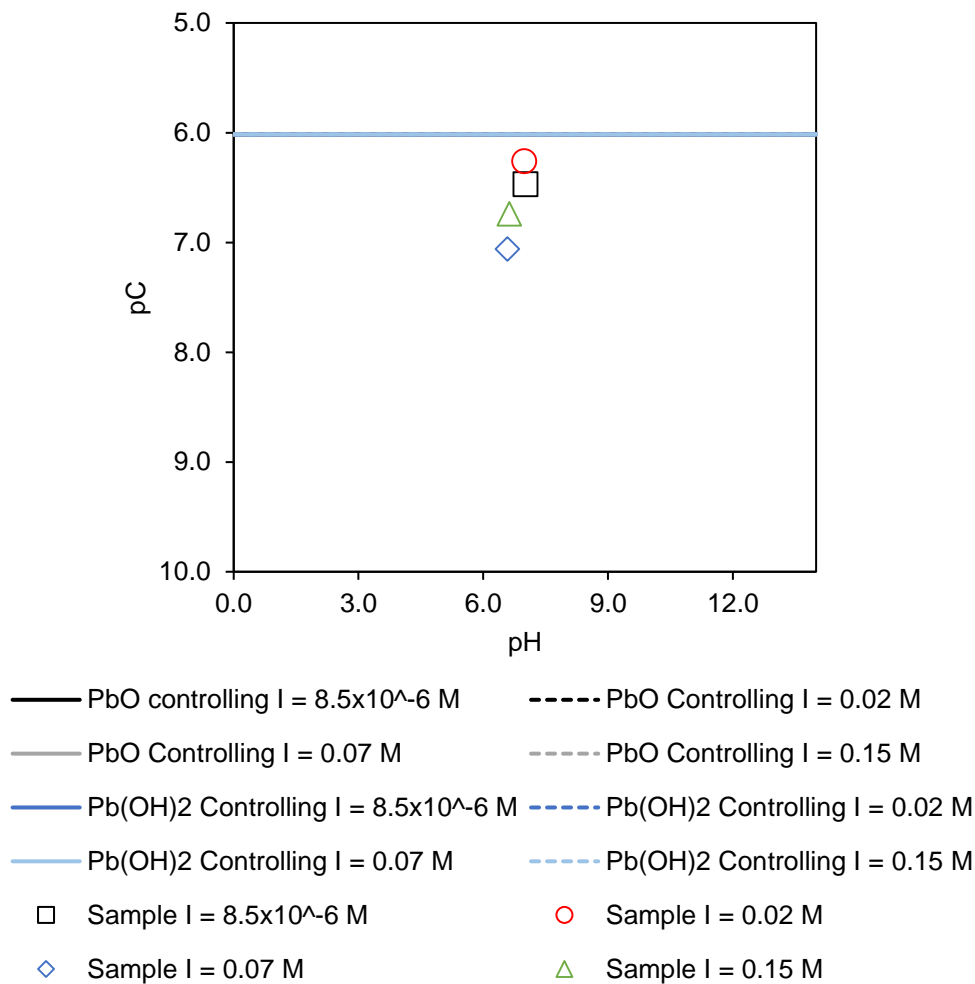


Figure 3.6. Long-term equilibrium model for all controlling solids in Pb-H₂O-NaCl system under different ionic strength conditions, ranging from 8.5×10⁻⁶ M to 0.15 M. Experimental points taken at 6 weeks are plotted on model lines.

Table 3.7. Long-term equilibrium Pb recovery as a function of ionic strength.

I (M)	Initial pH	Final pH	Time (hours)	Measured {Pb ²⁺ } (M)	Measured Error (M)	$\frac{Pb^{II}_{TOT}}{Pb_{Total}}$ (%)	$\frac{Pb^{II}_{TOT}}{Pb_{Total}}$ Error (%)
8.5×10 ⁻⁶	7.24	7.02	1010.72	3.39×10 ⁻⁷	5.40×10 ⁻⁸	35%	6%
0.02	6.95	6.99	983.56	5.49×10 ⁻⁷	1.04×10 ⁻⁷	57%	11%
0.07	6.95	6.58	995.14	8.72×10 ⁻⁸	1.00×10 ⁻⁷	9%	10%
0.15	7.11	6.63	994.53	1.83×10 ⁻⁷	6.52×10 ⁻⁹	19%	1%

3.4 Conclusions

From these results, speciation of lead was affected by the addition of ionic strength. Compared to low $I = 8.5 \times 10^{-6} M$, the increase of ionic strength due to addition of NaCl showed consistently higher dissolved concentration of Pb (around 50-65% of original value) in the kinetic experiments, while potentially facilitating greater lead precipitation in the long-term experiments. The long-term experimental data did not closely align with any of the models, which indicates that the systems were not yet at equilibrium. The specific impact of ionic strength on lead speciation in equilibrium conditions remains inconclusive. The authors hypothesize that model limitations or not attaining equilibrium conditions (at six weeks) inhibited a fuller interpretation of the lead speciation in the experiment.

The results of this work could have implications for water softening applications. Hard water continues to pose issues for plumbing and water softener usage in the U.S. has continued to rise [13]. Cation exchange technology allows the exchange of hardness cations(Ca^{2+} , Mg^{2+} , Fe^{2+}) for other cations like Na^+ or K^+ in salts. Since the softening process changes the ionic strength of the water, the results presented above could be used to interpret lead speciation with respect to softeners.

3.5 References

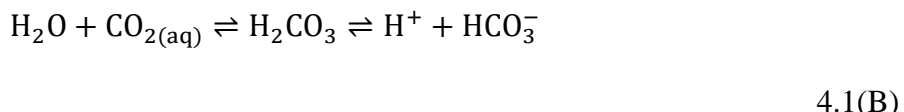
- [1] C. S. Wong and P. Berrang, “Contamination of tap water by lead pipe and solder,” *Bull. Environ. Contam. Toxicol.*, vol. 15, no. 5, pp. 530–534, May 1976.
- [2] United States Senate, *Safe Drinking Water Act, 1986 amendment*. U.S.A., 1986.
- [3] E. Deshommes, L. Laroche, S. Nour, C. Cartier, and M. Prévost, “Source and occurrence of particulate lead in tap water,” *Water Res.*, vol. 44, no. 12, pp. 3734–3744, Jun. 2010.
- [4] United States Senate, *Safe Water Drinking Act, 1974*. U.S.A., 1974.
- [5] United States EPA, *Lead and Copper Rule*. U.S.A., 1991.
- [6] E. Maliou, M. Malamis, and P. O. Sakellarides, “Lead and cadmium removal by ion exchange,” in *Water Science and Technology*, 1992, vol. 25, no. 1, pp. 133–138.
- [7] K. Vaaramaa and J. Lehto, “Removal of metals and anions from drinking water by ion exchange,” *Desalination*, vol. 155, pp. 157–170, 2003.

- [8] F. Aydin, F. Yasar, I. Aydin, and F. Guzel, “Determination of lead separated selectively with ion exchange method from solution onto BCW in Sırnak, East Anatolia of Turkey,” *Microchem. J.*, vol. 98, no. 2, pp. 246–253, Jul. 2011.
- [9] T. R. Holm and M. R. Schock, “Potential effects of polyphosphate products on lead solubility in plumbing systems,” *J. / Am. Water Work. Assoc.*, 1991.
- [10] P. Delahay, M. Pourbaix, and P. Van Rysselberghe, “Potential-pH Diagram of Lead and its Applications to the Study of Lead Corrosion and to the Lead Storage Battery,” *J. Electrochem. Soc.*, vol. 98, no. 2, pp. 57–64, 1951.
- [11] J. W. Patterson and J. E. O’Brien, “Water Technology Control of Lead Corrosion,” *J. Am. Water Work. Assoc.*, vol. 71, no. 5, pp. 264–271, 1979.
- [12] D. E. Giammar, “Water Chemistry Effects on Dissolution Rates of Lead Corrosion Products Subject Area: Infrastructure.”
- [13] S. Tanner, “Cation Exchange Water Softener Notification of Intent (NOI),” 2011.

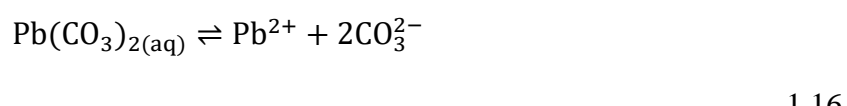
4. CARBONATE DEPENDENCE OF SOLUBLE LEAD

4.1 Introduction

Lead-containing materials within pipe networks and residences contribute substantially to lead in water and subsequent detrimental health effects [1]. Significant research has been dedicated to the intricacies of lead complexation in the presence of carbonate ($\text{HCO}_3^-/\text{CO}_3^{2-}$) in potable water systems [2]–[6]. Total carbonate (C_t) in water may be due to several sources. Many water systems have high alkalinity or hardness, whether a result of natural water chemistry or by chemical addition. Groundwater and surface water both have a range of alkalinity from 20–250 mg/L CaCO_3 . Another contributor to total carbonate is natural equilibration with atmospheric $\text{CO}_{2(g)}$. Because water treatment systems are open to the atmosphere, CO_2 sequestration is natural within potable water through the following mechanisms [7]:



Lead easily complexes with the carbonate and bicarbonate ions, as a function of pH. The following reactions show some of the aqueous lead species formed in the presence of carbonate.



Furthermore, solid lead carbonate (cerussite, $\text{PbCO}_{3(s)}$) and basic lead carbonate (hydrocerussite, $\text{Pb}_3(\text{CO}_3)_2(\text{OH})_{2(s)}$) are two common precipitates within distribution systems with leaded components. Studies have shown that Pb(II) solids like hydrocerussite and cerussite can be precursors that contribute to plumbosolvency control or promote the formation of other low-solubility solids within a distribution system, such as $\text{PbO}_{2(s)}$ [8],[9]. In response to the Washington, D.C. lead crisis of 2001-2004, Edwards and Dudi (2004) determined the effects of disinfectant on lead leaching from pipes as well as various solid formations, likely to be $\text{PbO}_{2(s)}$ [10]. Formation kinetics of carbonate solids at moderate total carbonate concentrations was investigated by Liu et al. (2008) with the intention of further characterizing lead(II) solids forming in the presence of chlorine [4]. Further research into the dissolution rate of carbonate solids was investigated as a function of various water quality parameters [11],[12]. This previous research has characterized traditional potable water systems with lower dissolved carbonate concentrations, generally at lower ionic strengths. Research in this work intends to prove the hypothesis that high total carbonate concentration can affect the speciation of lead without the effect of a disinfectant.

4.2 Methods & Materials

4.2.1 Standards, Reagents & Preparation of Stocks

Refer to Section 2.2.1 for reagents used. Total carbonate concentration was controlled by addition of granular $\text{NaHCO}_{3(s)}$ purchased from Aldrich.

Stock solutions for sample preparation were prepared by diluting the 4.8×10^{-3} M (1000 ppm) Pb standard solution to 4.8×10^{-5} M (10 ppm) Pb in sparged DI water. Stock solutions for ICP-OES standards preparation were prepared by diluting the stock solution to 4.8×10^{-5} M (10 ppm) and 4.8×10^{-7} M Pb (100 ppb) in 2% HNO_3 . ICP-OES lead standards were created in concentrations ranging from 2.4×10^{-8} M to 4.8×10^{-6} M (5-1000 ppb) from stock solutions. Standards were periodically remade, and samples were calibrated to these standards when run on the ICP-OES. Carbonate concentrations were added from initial stock solution of NaHCO_3 created at 1.0 M CO_3^{2-} . Dilutions of 0.014, 0.072 and 0.143 M total carbonate (C_t) were prepared at an initial pH = 7.0. Stock solutions of 4% HNO_3 were used for pH control and added in small volumes to avoid dilution of lead.

4.2.2 Experimental Procedure

All samples were contained in 15 or 50 mL metal-free, non-sterile polypropylene (PP) centrifuge tubes. Depending on C_t in each experiment, the 15 mL plastic vials were filled to 7.35 mL with the corresponding NaHCO_3 stock solution and were adjusted to pH 7.0 with 4% HNO_3 . Lead stock solution (4.8×10^{-5} M) was added to the solution for total volume of 7.50 mL as 9.7×10^{-7} M (200 ppb Pb). All experiments were conducted at 25°C on a benchtop. The remaining experimental procedure and analysis follow that which was discussed in Section 2.2.2.

4.3 Results & Discussion

4.3.1 Effect of carbonate concentration on kinetic experiments

The total carbonate concentrations (0.01, 0.07, 0.14 M) in each system resulted in high ionic strengths – 0.01, 0.09, 0.21 M, respectively. The experiment at $C_t = 0.01$ M consistently over recovered lead (above 9.7×10^{-7} M) and its data was excluded from the set. ICP-OES soluble lead concentrations and pH data can be found in Appendix C (Table C.6,

Table C.15-C.17).

At pH 5.0-6.0, CO_2 sequestration from the atmosphere did not affect soluble lead concentration significantly within the reactors. Refer to Section 2.4.1 for Figure 2.2. This relationship signified that lead behaved similarly under N_2 -sparged, open to atmosphere conditions as well as N_2 -sparged, closed conditions, suggesting that there could be an equivalent amount of carbonate complexes forming under both conditions. The measured concentrations of soluble lead were similar, which signified that no additional solid(s) formed from the potential carbonate from CO_2 in atmosphere.

At $C_t = 0$ M, ionic strength (I) remained low at 8.5×10^{-6} M. The soluble lead concentration decreased consistently to approximately 4.5×10^{-7} M (93 ppb), indicating solid formation early on, and the initial pH 7.0 decreased slightly to pH 6.33 at 48 hours (Figure 4.1(A)). However, the pH

did not remain steady for experiments with high C_t . Increased pH from 6.8-9.0 over time may have contributed to the speciation of lead during both tests, in addition to C_t addition (Figure 4.1(B), (C)). There was no significant trend noted by comparing experiments at $C_t = 0.07 \text{ M}$ or 0.14 M that were consistent with previous research. While lead remained highly soluble at $C_t = 0.07 \text{ M}$, the results indicate that doubling total carbonate to 0.14 M led to a decrease in soluble lead concentrations.

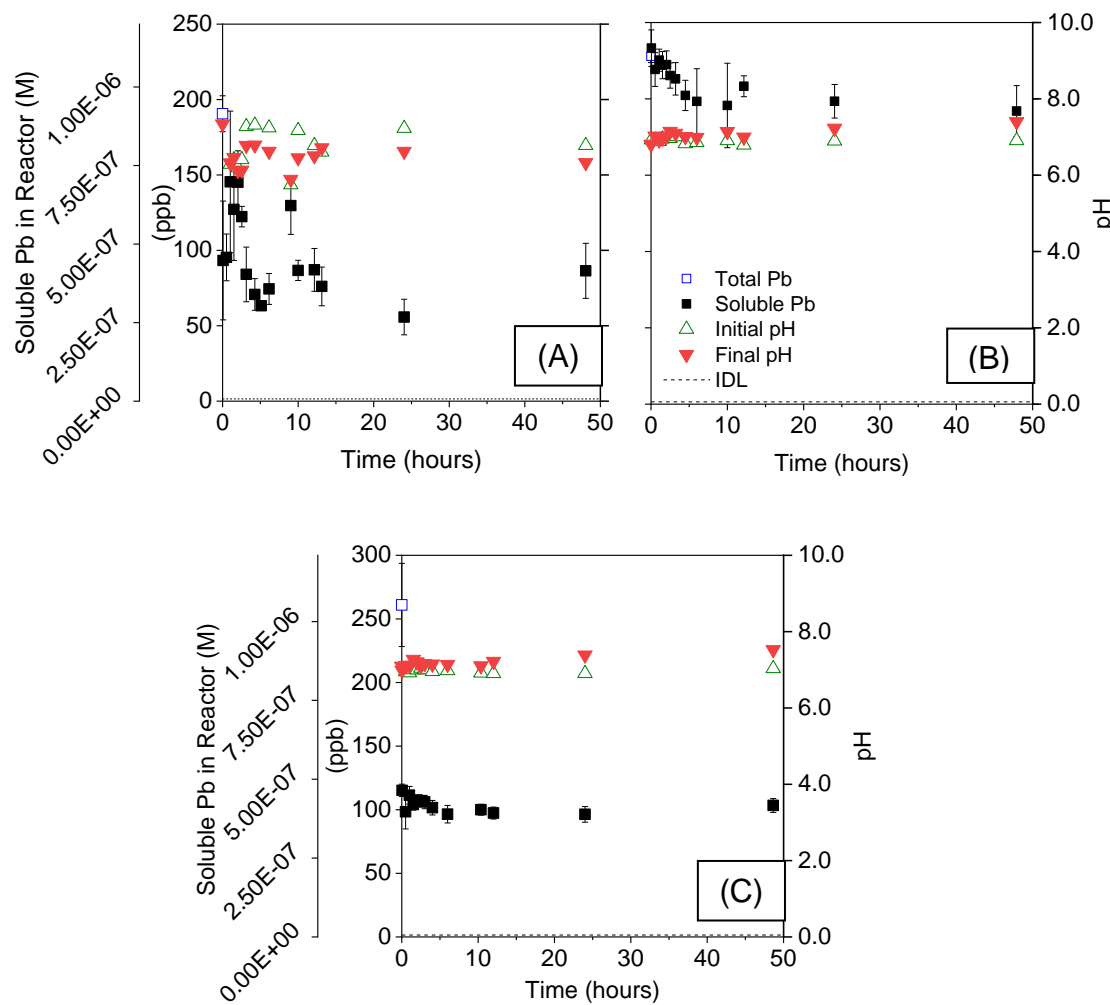


Figure 4.1. Measurement of soluble lead ($\text{Pb}_{\text{TOT}}^{\text{II}}$) over time at pH 7.0, 25°C with (A) $C_t = 0 \text{ M}$, $I = 8.5 \times 10^{-6} \text{ M}$, (B) $C_t = 0.07 \text{ M}$, $I = 0.09 \text{ M}$ (C) $C_t = 0.14 \text{ M}$, $I = 0.21 \text{ M}$.

When comparing all trends on Figure 4.2, the soluble lead concentrations at $C_t = 0 \text{ M}$ and 0.14 M responded very similarly over time, regardless of the differences in pH. The performance of the moderate $C_t = 0.07 \text{ M}$ experiment was starkly contrasted to the negligible (0 M) and high

(0.14 M) conditions, where some solid had been filtered out of the system. The trend reported in this work is not supported in previous literature and should be further investigated. The mechanisms changing lead speciation in this system were complex and interdependent. As C_t was adjusted, pH increased over time and ionic strength changed. Individually, these factors can change the speciation of lead, making it difficult to interpret their compounded effect(s).

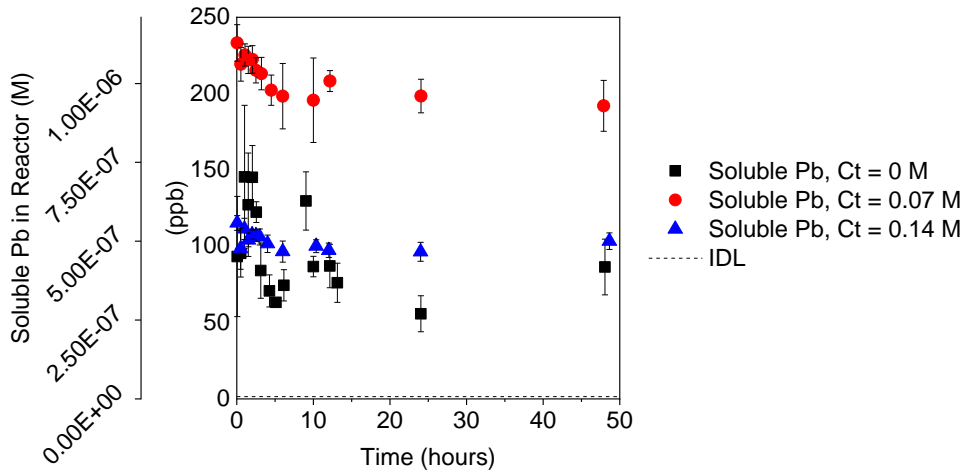
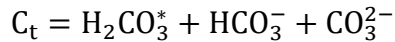


Figure 4.2. Soluble Pb in reactor with varying C_t from 8.5×10^{-6} M to 0.14 M. $Pb_{Total} = 9.7 \times 10^{-7}$ M at 25°C and pH = 7.0.

4.3.2 Effect of carbonate concentration on equilibrium experiments

Long-term points were taken approximately 6 weeks (1000 hours) after sample preparation and meant to simulate equilibrium conditions. Sample pH continued to increase throughout the experiment until the equilibrium point, 1.5-1.7 units above the originally measured pH. Using the same models from Chapter 2, the author determined the equilibrium chemical speciation for the Pb-H₂O-CO₂ system. In addition to PbO_(s) and Pb(OH)_{2(s)}, potential solids could include two additional solids: PbCO_{3(s)} (cerussite) and Pb₃(CO₃)₂(OH)_{2(s)} (hydrocerussite). One limitation of the model was that it did not consider formation of additional polynuclear solids, which could also affect the interpretation of the equilibrium data. PbO_{2(s)} was also intentionally omitted as the experimental conditions at low ORP were not suitable to form oxidized lead(IV) species.

To model the different experiments, the initial pH was set to 7.0 while total carbonate concentration (C_t) was varied at 0.01 M, 0.07 M, and 0.14 M to address each of the experimental conditions. Total carbonate was calculated as:



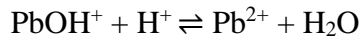
Eq. 4.1

Using the Davies equation (Eq. 2.11), the following activities were calculated in Table 4.1.

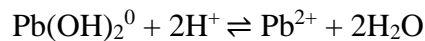
Table 4.1. Activity coefficients for Pb-H₂O-CO₂ system at C_t = 0.01-0.14 M (I = 0.01-0.21 M), pH° 7.0, T = 25°C.

Charge (z)	γ I=0.01 M	γ I=0.09 M	γ I=0.21 M
0	1.000	1.000	1.000
1	0.888	0.781	0.728
2	0.622	0.371	0.281
3	0.343	0.108	0.058
4	0.150	0.019	0.006

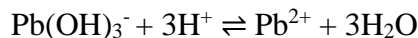
These relationships were used to recalculate the tabulated equilibrium °K values in relation to the adjusted ionic strength. In the Pb-H₂O-CO₂ closed system, various species including lead ions (Pb²⁺), oxides, hydroxides, and carbonates could form. Reactions of the soluble complexes are included below.



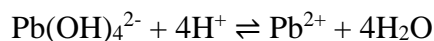
1.4



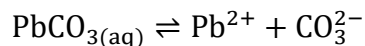
1.5



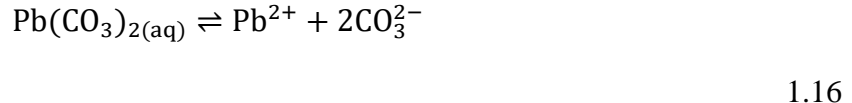
1.6



1.7



1.15



To characterize the system, total solubility of the Pb-H₂O-CO₂ system is given by the mass action equation

$$\begin{aligned} \text{Pb}_{\text{TOT}}^{\text{II}} = & [\text{Pb}^{2+}] + [\text{Pb}(\text{OH})^+] + [\text{Pb}(\text{OH})_{2(\text{aq})}] + [\text{Pb}(\text{OH})_3^-] + [\text{Pb}(\text{OH})_4^{2-}] + [\text{PbCO}_{3(\text{aq})}] \\ & + [\text{Pb}(\text{CO}_3)_2^{2-}] + [\text{PbHCO}_3^+] \end{aligned}$$

Eq. 4.2

where one of the solids controls the concentrations of each complex. Dissolution reactions are included below for each potential solid.

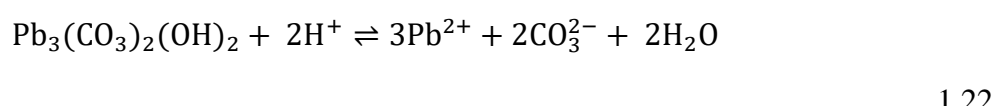
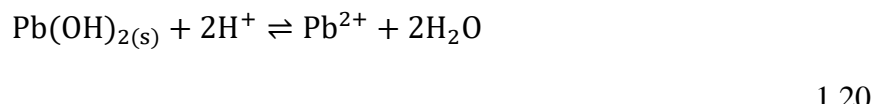
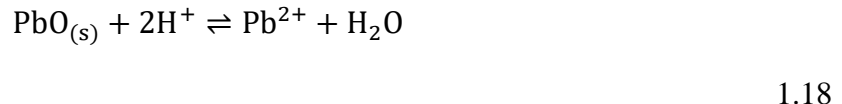


Table 4.2 summarizes the model input values for the equilibrium constants of soluble lead complexes. Cumulative complexation constants, or beta (β) values, were calculated as a product of K_{eq} values for sequential ligands (Eq. 4.3 to Eq. 4.5).

$$K_{\text{eq } 1, \text{PbCO}_{3(\text{aq})}} = \beta_{1, \text{PbCO}_{3(\text{aq})}} = \frac{\{\text{PbCO}_{3(\text{aq})}\}}{\{\text{Pb}^{2+}\}\{\text{CO}_3^{2-}\}}$$

Eq. 4.3

$$\beta_2 \times K_{eq\ 2,Pb(CO_3)_2^{2-}} = \beta_{2,\ (PbCO_3)_2^{2-}} = \frac{\{Pb(CO_3)_2^{2-}\}}{\{Pb^{2+}\}\{CO_3^{2-}\}^2}$$

Eq. 4.4

$$K_{eq,PbHCO_3^+} = \beta = \frac{\{PbHCO_3^-\}}{\{Pb^{2+}\}\{HCO_3^-\}}$$

Eq. 4.5

Hydrolysis complexation constants (β) were calculated as a product of K_{eq} values in each reaction and K_w , based on ionic strength (Table 4.2).

Table 4.2. Equilibrium and complexation constants for relevant Pb species in Pb-H₂O-CO₂ closed system with changes in I due to varying C_t.

Species	$\log \beta_i$	$\log K_{I=0\text{ M}}$	$\log ^cK$				$\log ^{*c}\beta$			
			$I = 10^{-5.07}$ M	$I = 0.01$ M	$I = 0.09$ M	$I = 0.21$ M	$I = 10^{-5.07}$ M	$I = 0.01$ M	$I = 0.09$ M	$I = 0.21$ M
PbOH ⁺	6.4	6.4	6.40	6.25	6.08	5.99	-7.60	-7.75	-7.92	-8.01
Pb(OH) _{2(aq)}	10.9	4.5	4.50	4.40	4.28	4.22	-17.11	-17.36	-17.64	-17.79
Pb(OH) ₃ ⁻	13.9	3.0	3.00	2.95	2.89	2.86	-28.11	-28.41	-28.75	-28.93
Pb(OH) ₄ ²⁻	2	-11.9	-11.90	-11.90	-11.90	-11.90	-54.01	-54.31	-54.65	-54.83
$\log \beta$										
PbCO ₃	6.478	6.478	6.47	6.03	6.07	5.38	6.47	6.07	5.62	5.38
Pb(CO ₃) ₂ ²⁻	9.938	3.46	3.47	3.69	3.67	4.01	9.93	9.73	9.51	9.39
PbHCO ₃ ⁻	13.2	13.2	13.19	12.75	12.79	12.10	13.19	12.79	12.34	12.10

When the complexation constant relationships are inserted into the mass action Eq. 4.2, the soluble lead concentration is calculated as follows, where all species are listed as a function of $[Pb^{2+}]$:

$$Pb_{TOT}^{II} = [Pb^{2+}] \left(1 + \frac{^*\beta_1}{[H^+]} + \frac{^*\beta_2}{[H^+]^2} + \frac{^*\beta_3}{[H^+]^3} + \frac{^*\beta_4}{[H^+]^4} + \beta_1[CO_3^{2-}] + \beta_2[CO_3^{2-}]^2 + \beta[HCO_3^-] \right).$$

Eq. 4.6

Given $Pb_{Total} = 9.7 \times 10^{-7}$ M (200 ppb) to match the experimental maximum Pb concentration, $\{Pb^{2+}\}$ was determined as a function of pH, β and $^*\beta$ values. Then, each complex concentration was calculated as a function of pH and $\{Pb^{2+}\}$. Additionally, the ion activity product (IAP) was used to measure the solubility of solids. If the product of the complexes' concentrations (IAP) in each reaction is equivalent to the solubility of a solid (K_{s0}) controlling the system, the system is in equilibrium. If $IAP > K_{s0}$, the total soluble lead (Pb_{TOT}^{II}) decreases, as more Pb precipitates as a solid. The upper limit of $\{Pb^{2+}\}$ is therefore dependent on the solubility of the controlling solid ($^*K_{s0}$). Eq. 4.7 shows the relationship for $PbO_{(s)}$ and $Pb(OH)_{2(s)}$. (Further discussed in Section 2.4.3).

$$\{Pb^{2+}\} = ^*K_{s0}\{H^+\}^2$$

Eq. 4.7

Dissolved lead(II) under control of cerussite and hydrocerussite is calculated using Eq. 4.8 and Eq. 4.9, respectively. These relationships as a function of ionic strength are recorded in Table 4.3.

$$\{Pb^{2+}\} = \frac{^*K_{s0}}{\{CO_3^{2-}\}}$$

Eq. 4.8

$$\{Pb^{2+}\} = \left(\frac{^*K_{s0} \times \{H^+\}^2}{\{CO_3^{2-}\}^2} \right)^{1/3}$$

Eq. 4.9

Table 4.3. Equilibrium solubility constants for relevant solids used in the speciation model.

Chemical Species	$\log *K_{s0}$	Source	$\log *cK_{s0}$			
	$I = 0 \text{ M}$		$I = 10^{-5.07} \text{ M}$	$I = 0.01 \text{ M}$	$I = 0.09 \text{ M}$	$I = 0.21 \text{ M}$
$\text{PbO}_{(s)}$	12.894	[7]	12.891	12.732	12.611	12.576
$\text{Pb(OH)}_{2(s)}$	8.15	[7]	8.147	7.988	7.867	7.832
$\log K_{s0}$		$\log cK_{s0}$				
$\text{PbCO}_{3(s)}$	-13.13	[7]	-13.142	-13.780	-14.263	-14.403
$\text{Pb}_3(\text{CO}_3)_2(\text{OH})_{2(s)}$	-18.77	[13]	-18.802	-20.557	-21.884	-22.272

Due to irregularities with the experiment at $C_t = 0.01 \text{ M}$, the data was excluded from the reported data. The following model descriptions compare low ionic strength ($8.5 \times 10^{-6} \text{ M}$) with no carbonate present to higher ionic strength experiments at $C_t = 0.07 \text{ M}$ and 0.14 M . At the low ionic strength condition, carbon dioxide was assumed to be fully removed through nitrogen sparging, resulting in $C_t = 0 \text{ M}$. Any dip of the total dissolved Pb (black dashed) line below $9.7 \times 10^{-7} \text{ M}$ (-log [Pb] = 6.0) indicates the formation of the controlling solid.

Because the relationship between their formation is the same (Eq. 4.7), the models controlled by either $\text{PbO}_{(s)}$ or $\text{Pb(OH)}_{2(s)}$ are identical regardless of the individual controlling solid. When $\text{PbO}_{(s)}$ or $\text{Pb(OH)}_{2(s)}$ were set as the predominating solid in the model, all conditions resulted in the dissolved species controlling the model. With low ionic strength ($I = 8.5 \times 10^{-6} \text{ M}$), lead(II) ion controls the system until pH 6.0, and then consistently decreases. Following this trend, consecutive lead(II) hydroxide complexes control the system as a function of pH. As pH increases, multiligand complexes dominate more fully.

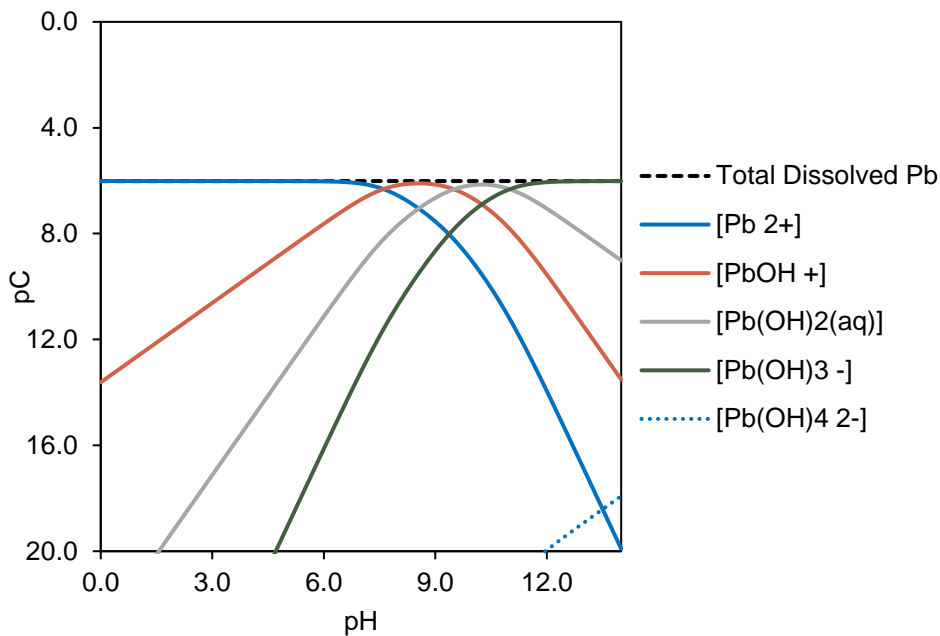


Figure 4.3. pC-pH diagram for the Pb-H₂O-CO₂ system at pH = 7.0, 25°C when either PbO_(s) or Pb(OH)_{2(s)} predominates at C_t = 0 M. Pb_{Total} = 9.7×10⁻⁷ M and I = 8.5×10⁻⁶ M.

At C_t = 0.07 M, all lead complex concentrations decrease dramatically, by factors of 10⁵-10¹³, as lead bicarbonate dominates the system from pH 0-12.7 (Table 4.4 and Figure 4.4). Doubling C_t to 0.1 M in Figure 4.5 shows a decrease in hydroxide complexes and lead ion concentrations by more than a factor of two. Concentrations of carbonate ligand complexes double with increasing ionic strength (as bicarbonate is added) (Table 4.6). Lead bicarbonate controls the dissolved lead concentration of the system up to pH 12.9 in all cases with carbonate. In the high pH ranges at both C_t = 0.09 M and 0.14 M, Pb(OH)₃⁻ is modeled to predominate as the dissolved species above pH 12.9.

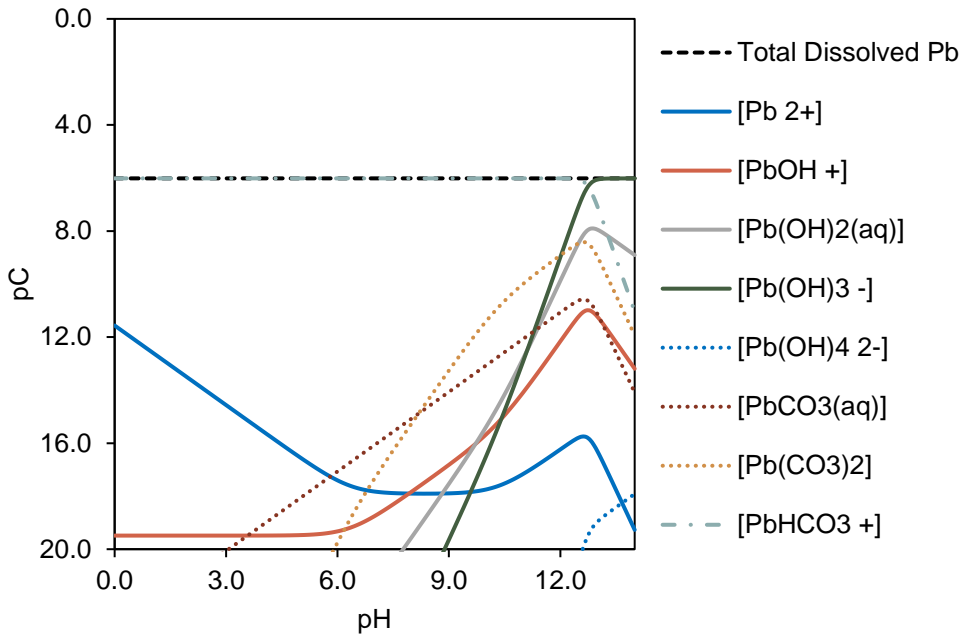


Figure 4.4. pC-pH diagram for the Pb-H₂O-CO₂ system at pH = 7.0, 25°C when either PbO_(s) or Pb(OH)_{2(s)} predominates at C_t = 0.07 M. Pb_{Total} = 9.7×10⁻⁷ M and I = 0.09 M.

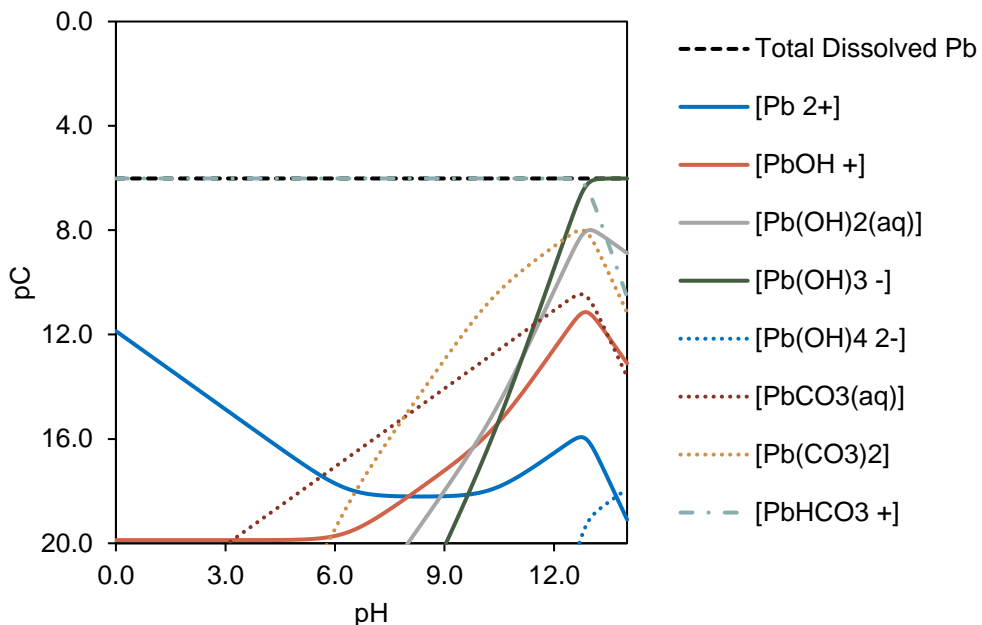


Figure 4.5. pC-pH diagram for the Pb-H₂O-CO₂ system at pH = 7.0, 25°C when either PbO_(s) or Pb(OH)_{2(s)} predominates at C_t = 0.14 M. Pb_{Total} = 9.7×10⁻⁷ M and I = 0.21 M.

Table 4.4. Average factors of change for each lead complex (right) with predominating solid (top) when comparing system at $C_t = 0$ M to 0.07 M ($I = 8.5 \times 10^{-6}$ M to 0.09 M). No carbonate complexes included because no carbonate was present at low ionic strength.

Species	Predominating Solid
	$\text{PbO}_{(s)}$ & $\text{Pb(OH)}_{2(s)}$
Pb^{2+}	10^{-5} to 10^{-12}
PbOH^+	10^{-5} to 10^{-13}
Pb(OH)_2	10^{-6} to 10^{-13}
Pb(OH)_3^-	10^{-6} to 10^{-13}
Pb(OH)_4^{2-}	10^{-6} to 10^{-13}

Table 4.5. Average factors of change for each lead complex (right) with predominating solid (top) when comparing system at $C_t = 0.07$ M to 0.14 M ($I = 0.09$ M to 0.21 M).

Species	Predominating Solid			
	$\text{PbO}_{(s)}$	$\text{Pb(OH)}_{2(s)}$	$\text{PbCO}_{3(s)}$	$\text{Pb}_3(\text{CO}_3)_2(\text{OH})_{2(s)}$
Pb^{2+}	0.56	0.56	0.56	0.56
PbOH^+	0.50	0.49	0.50	0.50
$\text{Pb(OH)}_{2(aq)}$	0.46	0.46	0.46	0.46
Pb(OH)_3^-	0.44	0.44	0.44	0.44
Pb(OH)_4^{2-}	0.44	0.44	0.44	0.44
$\text{PbCO}_{3(aq)}$	1.13	1.12	1.13	1.13
$\text{Pb}(\text{CO}_3)_2^{2-}$	2.25	2.24	2.25	2.25
PbHCO_3^+	1.13	1.12	1.13	1.13

No carbonate-based lead solids (cerussite or hydrocerussite) could form without the addition of carbonate; therefore, there is no instance at low ionic strength with carbonate solids predominating. At $C_t = 0.07$ M, most other complexes reach (relative) maximums at pH = 12.7-12.9 (Figure 4.6). Lead bicarbonate controls the system until pH 12.8. Pb(OH)_3^- controls the system in the extremely high pH ranges. When carbonate concentration is doubled ($C_t = 0.14$ M) in Figure 4.7, the trends under $C_t = 0.07$ M conditions are echoed but generally at lower concentrations. Only lead carbonate complexes increase in concentration with an increase in ionic strength. Pb^{2+} and hydroxide complexes decrease by a factor of 1.7-2.3 (Table 4.6).

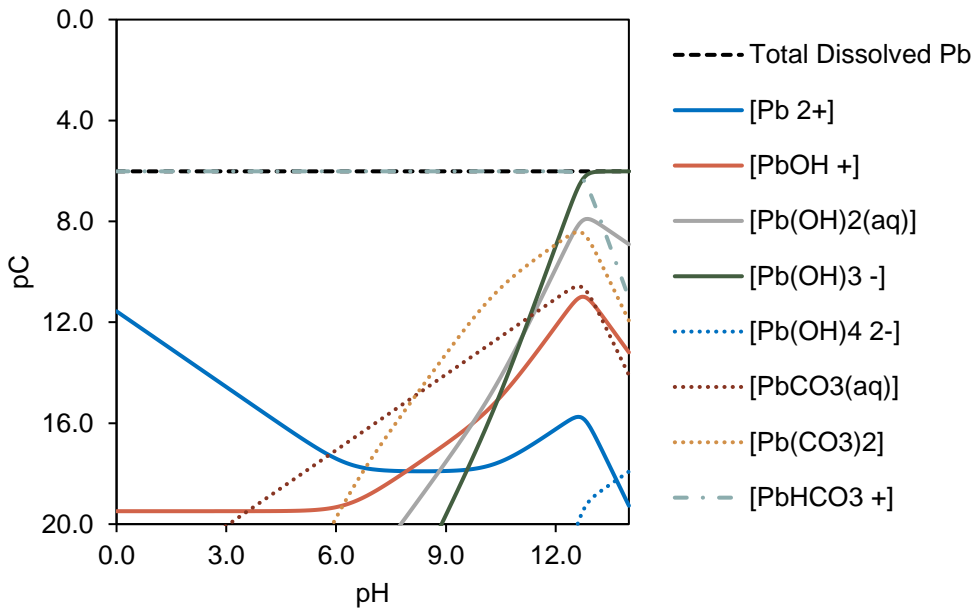


Figure 4.6. pC-pH diagram for the Pb-H₂O-CO₂ system at pH = 7.0, 25°C when PbCO_{3(s)} predominates at C_t = 0.07 M. Pb_{Total} = 9.7×10⁻⁷ M and I = 0.09 M.

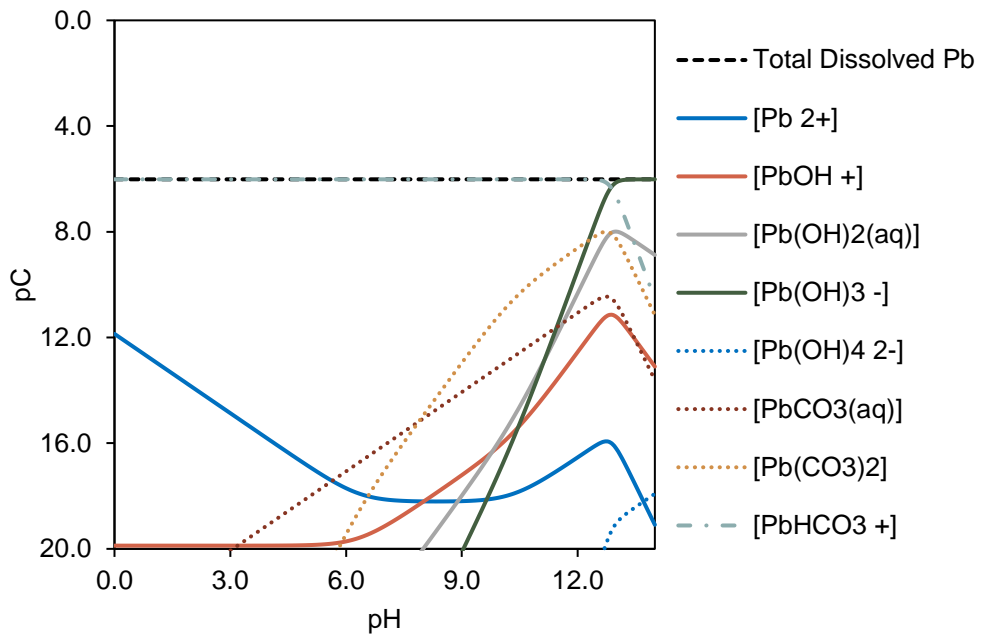


Figure 4.7. pC-pH diagram for the Pb-H₂O-CO₂ system at pH = 7.0, 25°C when PbCO_{3(s)} predominates at C_t = 0.14 M. Pb_{Total} = 9.7×10⁻⁷ M and I = 0.21 M.

Hydrocerussite, Pb₃(CO₃)₂(OH)_{2(s)}, is not predicted to form under any tested conditions, closely mirroring the PbCO_{3(s)} model at all points. Lead bicarbonate is the only significant

dissolved species until pH 12.7-12.9 under each modeled C_t condition. Above pH 12.8, $\text{Pb}(\text{OH})_3^-$ has the greatest soluble complex concentration (Figure 4.8). Only lead carbonate complexes increase in concentration with an increase in C_t , shown in Figure 4.9. With the increase to high total carbonate, Pb^{2+} and hydroxide complexes decrease by a factor of 1.7-2.3 (Table 4.6).

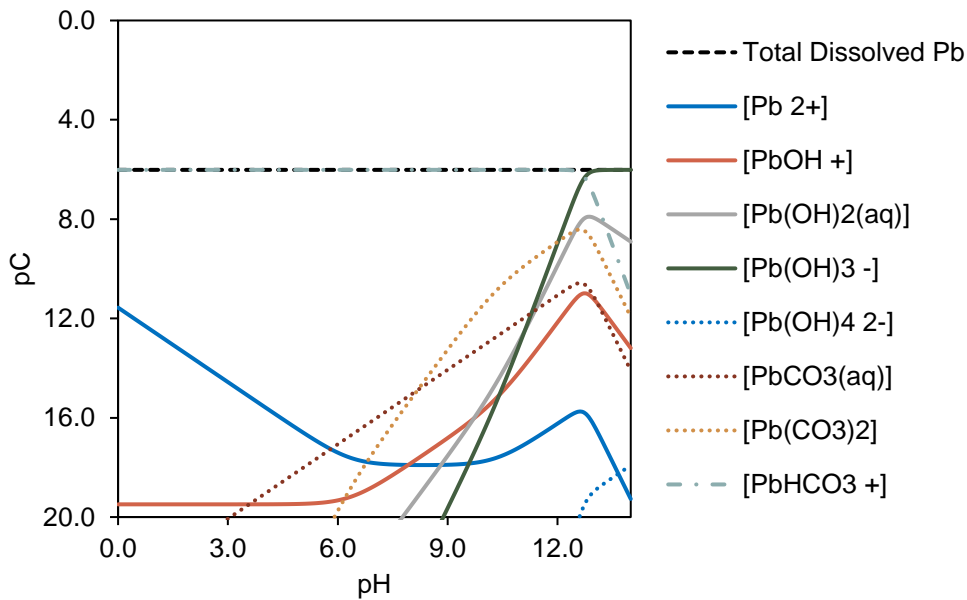


Figure 4.8. pC-pH diagram for the $\text{Pb}-\text{H}_2\text{O}-\text{CO}_2$ system at $\text{pH} = 7.0$, 25°C when $\text{Pb}_3(\text{CO}_3)_2(\text{OH})_{2(s)}$ predominates at $C_t = 0.07 \text{ M}$. $\text{Pb}_{\text{Total}} = 9.7 \times 10^{-7} \text{ M}$ and $I = 0.09 \text{ M}$.

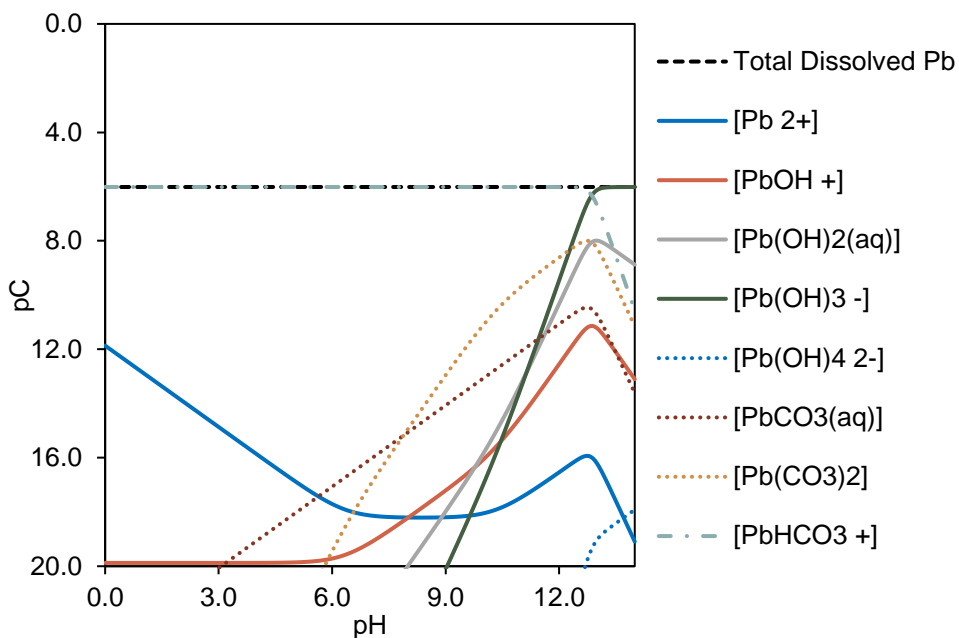


Figure 4.9. pC-pH diagram for the Pb-H₂O-CO₂ system at pH = 7.0, 25°C when Pb₃(CO₃)₂(OH)_{2(s)} predominates at C_t = 014 M. Pb_{Total} = 9.7×10⁻⁷ M and I = 0.21 M.

Figure 4.10 combines the solubility of total dissolved Pb with each controlling solid modeled at the various ionic strength conditions. The recorded data from each equilibrium experiment at varying carbonate concentrations and ionic strengths are compared to the model and shown on the graph as points. Data for each experiment is listed in Table 4.6.

Table 4.6. Long-term equilibrium Pb recovery as a function of carbonate concentration.

C _t (M)	I (M)	Initial pH	Final pH	Time (hours)	Measured {Pb ²⁺ } (M)	Measured {Pb ²⁺ } Error (M)	Pb ^{II} _{TOT} Pb _{Total} (%)	Pb ^{II} _{TOT} Pb _{Total} Error (%)
0	8.5×10 ⁻⁶	-	5.45	1014.19	7.4×10 ⁻⁷	3.3×10 ⁻⁷	65%	30%
0.01	0.01	7.28	8.82	997.44	1.1×10 ⁻⁶	8.0×10 ⁻⁸	110%	8%
0.07	0.07	7.20	8.96	984.00	8.7×10 ⁻⁷	7.3×10 ⁻⁸	87%	8%
0.14	0.14	7.34	8.82	984.00	4.5×10 ⁻⁷	3.8×10 ⁻⁸	46%	4%

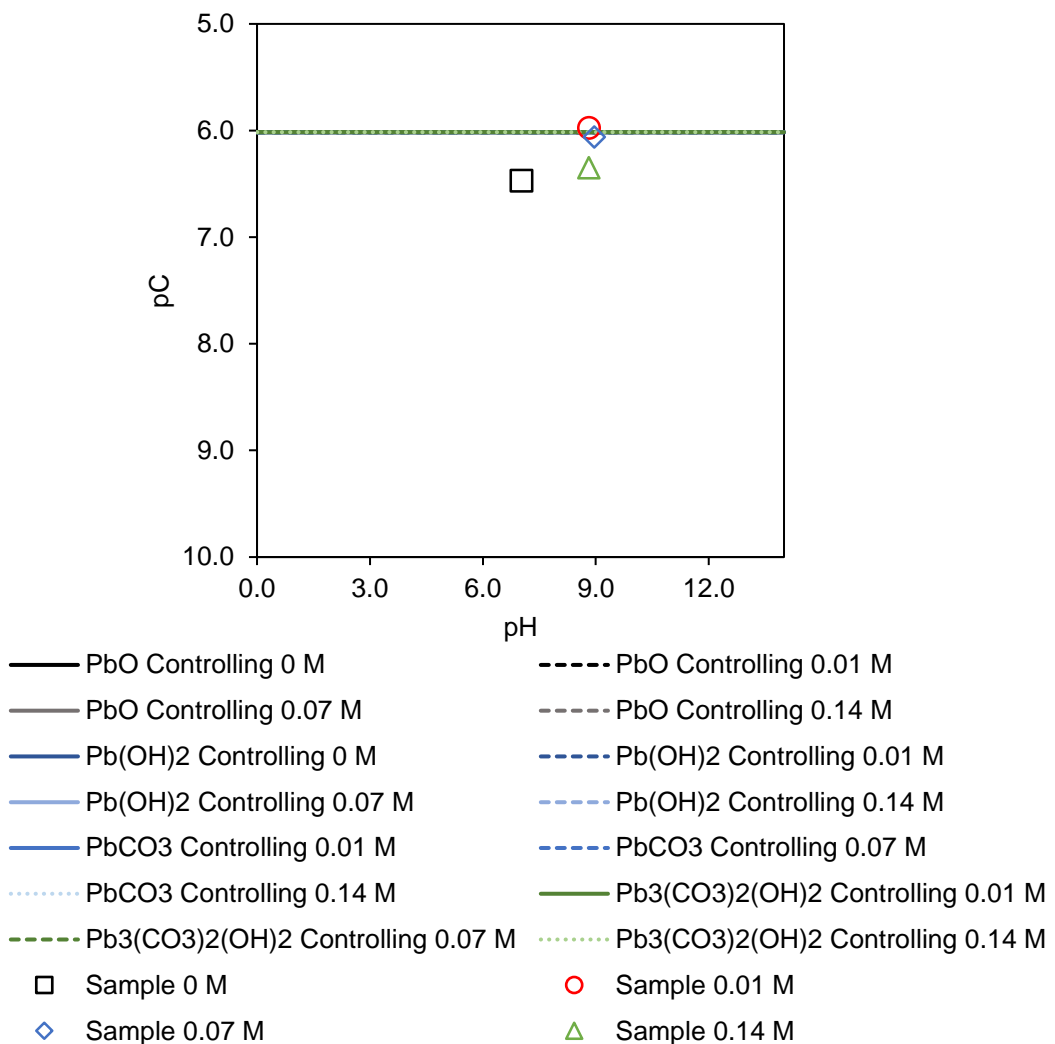


Figure 4.10. Long-term equilibrium model plotted as pC-pH diagram for all solids in Pb-H₂O-CO₂ system under various C_t conditions (listed in legend). Experiments measured at 6 weeks plotted as points on model lines. Pb_{Total} = 9.7×10⁻⁷ M, C_t = 0-0.14 M with corresponding I = 8.5×10⁻⁶-0.21 M.

Dissolved lead concentration in this system could have been a combination of several compounds but, based on the model, are likely to be Pb²⁺ or Pb(OH)⁺ at neutral pH, or small amounts of Pb(OH)_{2(aq)} at higher pH without carbonate. In the presence of carbonate, the model solely predicts the formation of aqueous PbHCO₃⁺. No solid was modeled to precipitate at any point and only the moderately high carbonate condition (C_t = 0.07 M) followed the model predictions. Data from the C_t = 0.01 M experiment over-recovered lead consistently, even at the long-term equilibrium point (shown in red). The experiments at C_t = 0 M and 0.14 M measured lower soluble lead than predicted, indicating that experiments were not at equilibrium by six weeks.

4.4 Conclusion

Lead speciation was determined at 25°C over a variety of total carbonate concentrations with a set of kinetic and equilibrium experiments. The addition of total carbonate did not follow a specific trend during the 48-hour kinetic experiments, but the moderately high values ($C_t = 0.07\text{ M}$) showed a 2-fold increase in measured soluble lead concentrations over low (0 M) and high (0.14 M) carbonate concentrations. Only one of the equilibria results moderately aligned with the model, suggesting that the system was not yet at equilibrium. The specific trends concerning lead speciation while increasing carbonate concentration in a Pb-H₂O-CO₂ system at equilibrium conditions remains inconclusive. The deviation of equilibrium experimental points from the model could be due to a combination of factors including the varied carbonate concentration, intrinsic change in ionic strength, or changing pH over time. The complexity of the system made it difficult to characterize the mechanism that affected lead speciation. The authors hypothesize that model limitations inhibited a fuller interpretation of the lead speciation in the experiment. Further work could be performed on the mathematical model to include less common lead solids.

This work could have further applications to the residential water softener. Through ion exchange, Na⁺ ions that coat a resin inside the softener tank. These ions are exchanged for incoming Ca²⁺/Mg²⁺ hardness ions, softening the water. The action could lead to a higher concentration of carbonate or bicarbonate ions in the water as the hardness ions are sequestered onto the resin without the carbonate ligands, resulting in higher C_t concentrations in water.

4.5 References

- [1] E. Deshommes, L. Laroche, S. Nour, C. Cartier, and M. Prévost, “Source and occurrence of particulate lead in tap water,” *Water Res.*, vol. 44, no. 12, pp. 3734–3744, Jun. 2010.
- [2] M. R. Schock, “Response of lead solubility to dissolved carbonate in drinking water,” *Am. Water Work. Assoc.*, vol. 72, no. 12, pp. 695–704, 1980.
- [3] D. W. Shoesmith, M. G. Bailey, and P. Taylor, “Anodic oxidation of lead in aqueous carbonate solutions. II. Film formation and dissolution in the pH range 9 to 14,” *Can. J. Chem.*, vol. 66, no. 11, pp. 2941–2946, May 2006.

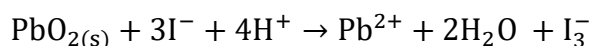
- [4] H. Liu, G. V. Korshin, and J. F. Ferguson, “Investigation of the kinetics and mechanisms of the oxidation of cerussite and hydrocerussite by chlorine,” *Environ. Sci. Technol.*, vol. 42, no. 9, pp. 3241–3247, 2008.
- [5] Y. Xie, Y. Wang, V. Singhal, and D. E. Giammar, “Effects of pH and carbonate concentration on dissolution rates of the lead corrosion product PbO₂,” *Environ. Sci. Technol.*, 2010.
- [6] Y. Xie, “Dissolution, Formation, and Transformation of the Lead Corrosion Product PbO₂: Rates and Mechanisms of Reactions that Control Lead Release in Drinking Water Distribution Systems (Doctoral dissertation),” University of Washington, St. Louis, 2010.
- [7] W. A. Brezonik, Patrick L.; Arnold, *Water Chemistry: An Introduction to the Chemistry of Natural and Engineered Aquatic Systems*, 1st ed. Oxford University Press, 2011.
- [8] D. A. Lytle and M. R. Schock, “Formation of Pb(IV) oxides in chlorinated water,” *Journal /American Water Works Association*, vol. 97, no. 11. Nov-2005.
- [9] M. R. Schock and R. Giani, “Oxidant/Disinfectant Chemistry and Impacts on Lead Corrosion,” in *In Proceedings, Sunday Workshop Getting the Lead Out: Analysis and Treatment of Elevated Lead Levels in DC’s Drinking Water*, 2004.
- [10] M. Edwards and D. Abhijeetdudi, “Role of chlorine and chloramine in corrosion of lead-bearing plumbing materials,” 2004.
- [11] D. E. Giammar, J. D. Noel, Y. Xie, K. Nelson, Y. Wang, and V. Singhal, “Influence of water chemistry on the dissolution rates of lead corrosion products,” in *Water Quality Technology Conference and Exposition 2009*, 2009.
- [12] J. D. Noel, Y. Wang, and D. E. Giammar, “Effect of water chemistry on the dissolution rate of the lead corrosion product hydrocerussite,” *Water Res.*, vol. 54, pp. 237–246, May 2014.
- [13] W. D. . Schecher and D. C. McAvoy, “MINEQL+: A Chemical Speciation Modeling for the Real World.” Environmental Research Software, 2015.

5. METHOD TO DETERMINE LEAD DIOXIDE CONCENTRATION

5.1 Introduction

Lead concentrations in distribution systems are generally limited by solid species and their dissolution rates. Solids like hydrocerussite ($\text{Pb}_3(\text{CO}_3)_2(\text{OH})_{2(s)}$) and lead(IV) dioxide ($\text{PbO}_{2(s)}$) can result in very low total dissolved lead by controlling the lead release into water in pipe networks. Therefore, measurement of these controlling solids could be beneficial in determining the stability of pipe scale in addition to lead speciation in a system. If higher ORP is maintained with the addition of free chlorine, lead(IV) solids can dominate a system. However, lead(IV) is reduced to the +2 oxidation state at moderate ORP or in neutral or acidic pH because its reduction potential is greater than the $\text{O}_2/\text{H}_2\text{O}$ boundary under these conditions [1]. Direct Pb(IV) measurement experiments remain a challenge because of this relationship.

The standard method (EPA 200.8) for total Pb quantification requires acidification of any lead sample to 0.15% v/v HNO_3 for at least 16 hours prior to analysis [2]. This method has proven to drastically underestimate the concentration of total Pb when solid lead – especially PbO_2 – is present because of its incomplete dissolution [3], [4]. Additionally, ICP-OES analysis requires acidification to 2% v/v HNO_3 for metals analysis. Acidification of Pb(IV) reducing lead to Pb(II) makes it difficult to measure original concentrations of Pb(IV) solids. However, lead(IV) dioxide can easily oxidize iodide (I^-) to triiodide (I_3^-) through the following reaction.



5.1

Closely following the iodometric method detailed in Lin et al. (2008) and follow-up work of Zhang et al. (2010), the method and results presented in this work aim to quantify Pb(IV) with a disinfectant residual in aqueous samples. Analysis is performed by colorimetry, measuring the product formed from reaction 5.1, triiodide (I_3^-), with a UV-vis spectrophotometer [5], [6]. The aim of this work is to replicate the results of the original method developers.

5.2 Methods & Materials

5.2.1 Standards, Reagents, & Preparation of Stocks

All experiments used reagent grade chemicals. PbO_2 was purchased from Alfa Aesar as solid particles and was 99.995% (metals basis) pure. Concentrated hydrochloric acid, HCl, was purchased from Aldrich, but was diluted to 1.0 F for the experiments. Sodium hypochlorite (NaOCl) was purchased as a ~5% NaOCl stock from ACROS Organics. Free chlorine stock solutions of 0.015 M were diluted from the 5% NaOCl stock with DI water. The source of iodide was potassium iodide purchased from ACROS Organics at a purity of 99+% for analysis and nitrogen flushed. All solutions were prepared with ultrapure deionized water from a THERMO Barnstead GenPure Pro water system with a resistivity of 18.0-18.2 $\text{M}\Omega\text{-cm}$.

5.2.2 Experimental Procedure

For each experiment, a 1000 mL glass screw cap bottle was filled with 1000 mL of DI water as the stock solution. NaOCl stock solution (0.015 M) was added to the DI water to achieve 0.5 mg/L Cl_2 in each experimental sample. After chlorination, the capped bottle was inverted several times to ensure the sample was homogenous. The uncapped reactor was continuously mixed on a stir plate for the remainder of the experiment. Solid lead as $\text{PbO}_{2(s)}$ was measured with a Sartorius CP2P microbalance. Experiments ranged in lead concentration from 0.06-15.0 mg/L Pb, and corresponding amounts of lead were added per experiment.

Refer to the original and follow-up work for additional details in the iodometric process [5],[6]. Zhang et al. (2010) used a range of KI concentrations (2-4 g/L) to optimize lead recovery [6]. Based on that investigation, the research team in this work decided that the data associated with 2.0 g/L KI in the original work yielded adequate and precise recovery. This dosage was used in this work, which still overdosed the system with iodide by factors of 1.9×10^2 to 5.4×10^4 (molar comparison) to the lead concentration at any point. Because KI and free chlorine react quickly at ambient pH, the original authors determined that the absorbance due to this reaction could easily be subtracted at the beginning of the experiment [5]. Additionally, based on reaction 5.1, the dissolution of $\text{PbO}_{2(s)}$ to Pb^{2+} by triiodide is most effective at low pH and is slower at neutral to alkaline pH. Therefore, solid KI was measured on the analytical balance to 2.0 g/L within each sample and was added to the reactor while at ambient pH and continuing to mix on the stir plate.

Within 30 seconds of KI addition, the sample had a color change due to the reaction between KI and free chlorine. An aliquot of the mixture was taken 30 seconds after KI addition to calculate the contribution of the non-lead reaction. Absorbance was measured via UV-spectrophotometer at 351 nm.

The sample was then quickly acidified to pH 2.0 ± 0.05 with 1.0 F HCl while continuing to stir, activating the fast reaction between KI and $\text{PbO}_{2(s)}$. Sample aliquots were removed and analyzed via colorimetry every 3-5 minutes until 20 minutes elapsed. Absorbance of each aliquot was recorded as a function of time. All experiments were run for at least 20 minutes. The original authors determined a pattern of diminishing return past 20 minutes, which was replicated for several samples (to 60 minutes) in this work to verify this phenomenon [5]. Because colorimetry is not a destructive process, all aliquots were returned to the reactor after analysis. Additionally, pH was recorded when every aliquot was taken to ensure the sample maintained a low pH.

Overall, the concentration of I_3^- was measured by colorimetry with a UV-vis spectrophotometer (UV2700, Shimadzu), corresponding to the concentration of PbO_2 added originally based on reaction 5.1. Using the Beer-Lambert law, all absorbance values were correlated to concentration. Initial experiments were used to determine and verify the molar absorption coefficient (ϵ) of I_3^- at 351 nm, which was found to equal $23,325 \text{ M}^{-1}\text{cm}^{-1}$, verifying the previous work's value [7]. Previous literature also cited a value of $25,700 \text{ M}^{-1}\text{cm}^{-1}$ at 351 nm [5], [8]. While a peak also exists at 288 nm, this wavelength was not used due to interferences. The initial absorbance measured from the immediate reaction between KI and free chlorine was subtracted from all subsequent measurements to differentiate the reactions of KI and free chlorine from KI and $\text{PbO}_{2(s)}$. This action was performed for each individual experiment. Recovery of lead was calculated for each aliquot that was measured. The recovery was calculated as the measured absorbance, converted to concentration of Pb (mg/L) compared to the total concentration, originally determined as a fraction of mass $\text{PbO}_{2(s)}$ added in the total volume of water. This value is converted to a percentage of the total and reported in Table 5.1.

5.3 Results & Discussion

This work verified the accuracy of the original method to measure $\text{PbO}_{2(s)}$ in reactors with 0.05 mg/L Cl_2 and 2 g/L KI. Figure 5.1 shows a recovery curve that had an added lead concentration of 7.05 mg/L Pb. Triiodide was measured as a function of time and the absorbance readings of I_3^-

corresponded to both $\text{Pb}^{2+}/\text{PbO}_{2(s)}$ concentration, according to the 1:1 molar comparison (triiodide to lead) in reaction 5.1. As shown in the figure below, the recovery of lead followed a somewhat logarithmic trend over time during each experiment, increasing to a maximum around 20 minutes. This experiment continued to 40 minutes and was an example of the diminished recovery of lead over time after 20 minutes.

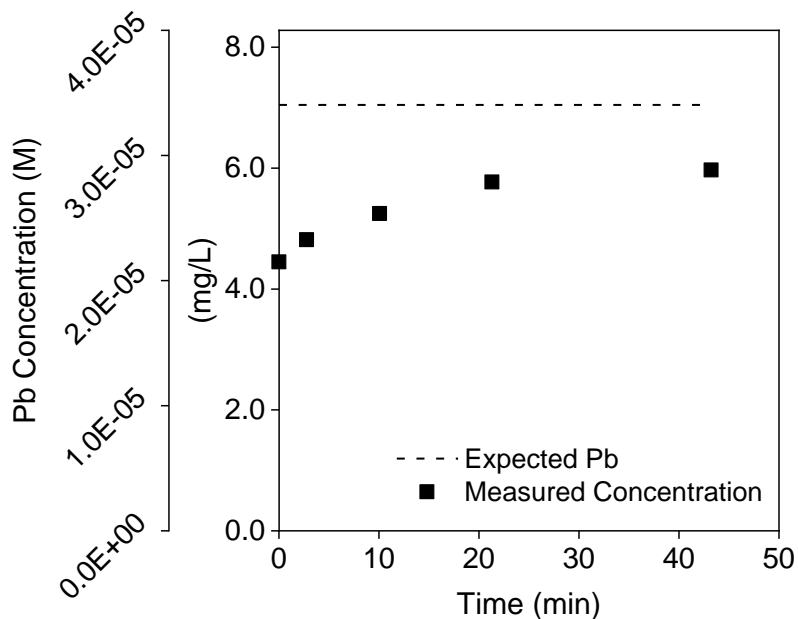


Figure 5.1. Results of iodometric experiment with 7.05 mg/L (3.4×10^{-5} M) Pb shown as the dashed line with 0.5 mg/L Cl_2 . Recovery over time shown as points. Maximum recovery of 85% original Pb at 20 minutes.

Overall results of the experiments in this work and Zhang et al. (2010) are shown in Table 5.1, reporting high recovery of lead over variable parameters. Recovery of each experiment is reported as individual points in Figure 5.2. Each data point shown is a comparison of the added Pb in one experiment and the corresponding measured value of Pb at 20 minutes. Recovery varied per experiment and ranged from 53-103% of original Pb added to the system. The average recovery in this work was $81 \pm 10.8\%$ with the bulk of readings falling between 81-88%. Further details concerning recovery experiments are reported in Table D.1 in Appendix D.

Table 5.1. Summary of experimental input parameters and results comparing Zhang et al. (2010) and this work [6].

PbO ₂ (mg/L as Pb)	Chlorine (mg/L as Cl ₂)	pH	KI in Original Work (g/L)	Pb Recovery in Original Work	KI in This Work (g/L)	Pb Recovery in This Work
0.01-19.7	0	2.0	2-4	90-111%	2	N/A
0.01-20	0.9-4.3	2.0	2-4	92-103%	2	53-103%

These results are significantly lower than the original work (92-103%) but remained consistent throughout experimentation, with lead concentrations above 1 mg/L (Figure 5.2) [6]. Despite this variation, the research team determined this to be a usable method of PbO₂ quantification due to consistent recovery. Still, the consistent recovery did not explain the failure to match the previous work's values. Some of the lack of recovery may have been due to the use of glassware instead of plasticware for experimentation. Previous literature has shown that lead may adhere to holding materials, thus resulting in lower overall recovery of lead in samples [4], [9], [10], [11]. Lead may also have adhered to the plastic stir bar during the experiment. Another possibility exists that while KI was in excess compared to lead, some percentage of the lead may have remained solid due to lack of interaction with iodide.

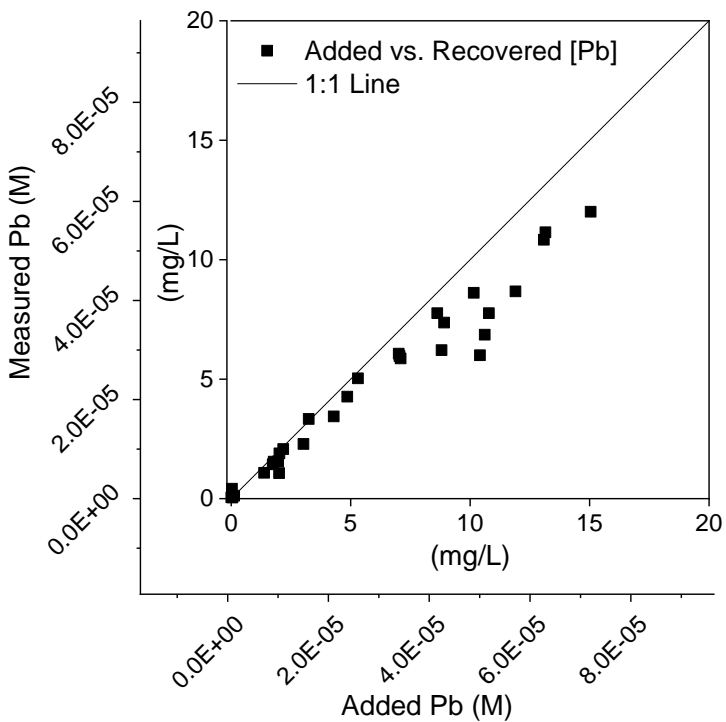


Figure 5.2. Plot showing the recovery of PbO_2 from 0.06-15.0 mg/L Pb with free chlorine = 0.5 mg/L as Cl_2 , $\text{KI} = 2.0 \text{ g/L}$, temp = 25°C , pH = 2.0. Specific experiment recoveries are reported in Table D.1 in Appendix D.

Experiments with lower concentrations of lead (0 to $9.7 \times 10^{-6} \text{ M}$, 0-2 mg/L) over-recovered Pb, shown in the lower left-hand corner of Figure 5.2. This variability could have been due to reaching the lower limits of the microbalance that was used to measure small $\text{PbO}_{2(\text{s})}$ masses. Though it would have been relevant to prepare lower-range concentrations (less than $2.4 \times 10^{-7} \text{ M}$ or 0.05 mg/L Pb) of lead, those values could not be reached due to inaccuracy of multiple dilutions with solid Pb. The team was limited by available resources (larger volumetric containers) and a dissolution analysis would have been skewed with dilutions into several smaller containers.

5.4 Conclusions & Future Work

This work was able to replicate the results of the original work, but with less accuracy. This precise quantitative method of PbO_2 measurement could be used to aid in future speciation studies. Further work could include performing both the iodometric method and ICP-OES analysis on duplicate samples to determine both what concentration of Pb(II) was present in the system as well as the

concentration $\text{PbO}_{2(s)}$, if present at all. This analysis could be performed on laboratory samples or real system draws of tap water.

Future work is also required to compare the levels of PbO_2 in samples that have passed through a water heater, water softener, or a combination. This experimentation could be performed with synthetic water samples or tap water draws from sample residences. The integrated system would give insight into the speciation of Pb(II) and Pb(IV) (iodometric analysis), as well as the solid-dissolved fractions of Pb (ICP-OES analysis) with respect to temperature and ionic strength variation.

5.5 References

- [1] P. Delahay, M. Pourbaix, and P. Van Rysselberghe, “Potential-pH Diagram of Lead and its Applications to the Study of Lead Corrosion and to the Lead Storage Battery,” *J. Electrochem. Soc.*, vol. 98, no. 2, pp. 57–64, 1951.
- [2] United States EPA, *EPA Method 200.8: Determination of Trace Elements in Waters and Wastes by Inductively Coupled Plasma-Mass Spectrometry*. U.S.A., 1994.
- [3] M. Edwards and D. Abhijeetdudi, “Role of chlorine and chloramine in corrosion of lead-bearing plumbing materials,” 2004.
- [4] S. Triantafyllidou, J. Parks, and M. Edwards, “Lead particles in potable water,” *J. / Am. Water Work. Assoc.*, 2007.
- [5] Y. P. Lin, M. P. Washburn, and R. L. Valentine, “Reduction of lead oxide (PbO_2) by iodide and formation of iodoform in the $\text{PbO}_2/\text{I-}/\text{NOM}$ system,” *Environ. Sci. Technol.*, 2008.
- [6] Y. Zhang, Y. Zhang, and Y. P. Lin, “Fast detection of lead dioxide (PbO_2) in chlorinated drinking water by a two-stage iodometric method,” *Environ. Sci. Technol.*, 2010.
- [7] Y. P. Lin and R. L. Valentine, “Release of Pb(II) from monochloramine-mediated reduction of lead oxide (PbO_2),” *Environ. Sci. Technol.*, vol. 42, no. 24, pp. 9137–9143, Dec. 2008.
- [8] Y. Bichsel and U. Von Gunten, “Determination of iodide and iodate by ion chromatography with postcolumn reaction and UV/visible detection,” *Anal. Chem.*, 1999.
- [9] J. L. Parks *et al.*, “Determination of total chromium in environmental water samples,” *Water Res.*, vol. 38, pp. 2827–2838, 2004.

- [10] N. D. Kim and S. J. Hill, “Sorption of lead and thallium on borosilicate glass and polypropylene: Implications for analytical chemistry and soil science,” *Environ. Technol. (United Kingdom)*, 1993.
- [11] W. Liang, L. Zhan, L. Piao, and C. Rüssel, “Lead and copper removal from aqueous solutions by porous glass derived calcium hydroxyapatite,” *Mater. Sci. Eng. B Solid-State Mater. Adv. Technol.*, 2011.

6. CONCLUSIONS

Lead has been used as a building material in water distribution systems for centuries. However, the quality of water passing through pipes controls lead contamination and the subsequent health effects. Several water quality parameters were assessed in this work to determine the effect of these fundamental characteristics on the speciation of lead within water systems. Kinetic (0-48 hours) and long-term (6 weeks) experiments were developed to determine the effect of temperature, ionic strength, and carbonate concentrations on soluble lead concentrations over environmentally relevant pH ranges. Equilibrium modeling calculations were performed to predict changes in soluble lead and the potential solid(s) that could predominate under the experimental conditions. Finally, a recently developed experimental method for $\text{PbO}_{2(\text{s})}$ measurement in water was verified.

Across a pH range of 3.0-9.8, experiments with increased water temperature (55°C) proved to decrease the measured soluble lead concentrations (i.e. increased lead precipitation) in comparison to the identical pH 25°C experiment in all experiments. The equilibrium thermodynamic model suggested that very little change in lead speciation would occur while maintaining all equilibrium conditions and solely increasing temperature to 55°C . Interestingly enough, final pH measurements for equilibrium points at 6 weeks at 55°C showed significantly more variation than those taken at 25°C , which may mean that the combination of low pH and high temperature impacted the long-term measurements of soluble lead.

Increasing both ionic strength (NaCl) and total carbonate (C_t) concentrations in solutions for 48 hours at 25°C resulted in higher measured soluble lead at pH 7.0 than the equivalent experiments without the added variables. Experiments with high ionic strength showed higher amounts of soluble lead during the first 48 hours than low ionic strength samples. The corresponding equilibrium experiments proved that higher ionic strength tended to promote more solid formation. Also, lead speciation at 25°C over a variety of total carbonate concentrations was tested with a set of kinetic and equilibrium experiments but failed to follow a specific trend.

In the non-carbonate systems at the tested pH range, dissolved lead concentration was likely a combination of several compounds: Pb^{2+} or $\text{Pb}(\text{OH})^+$ at neutral pH, or small amounts of $\text{Pb}(\text{OH})_{2(\text{aq})}$ at higher pH. In the presence of carbonate, the model solely predicts the formation of aqueous PbHCO_3^+ at relevant pH ranges. Under all tested conditions of temperature change, ionic strength, and total carbonate, the equilibrium chemical speciation model did not predict any solid

formation. Experiments that measured low dissolved lead concentrations contribute to the hypothesis that the systems were not yet at equilibrium by six weeks.

Additional experiments were also performed to verify how effectively $\text{PbO}_{2(\text{s})}$, a lead(IV) solid, could be measured using a colorimetric method. The previously developed iodometric method proved to be a feasible method of quantifying $\text{PbO}_{2(\text{s})}$ in chlorinated water with 80-88% accuracy. Results of this work were significantly lower than the original work but remained consistent throughout experimentation when testing lead concentrations above 1 mg/L.

6.1 Future work & application

Application for these results could be tied to usage of residential water appliances. Water heaters, which reach temperatures up to 60°C, are a universal convenience in developed countries. (Refer to Section 1.4 and Figure 1.1 for a fuller description of residential heaters.) While these appliances are not a source of Pb themselves, lead can leach from materials used in municipal piping networks or residences when certain water quality parameters are present, and this process can be affected by temperature fluctuations. Additionally, the experiments and modeling work concerning ionic strength and carbonate concentration changes could have applications to the residential water softener. Through ion exchange, Na^+ ions coat a resin inside the softener tank. These ions are released upon exchange for incoming $\text{Ca}^{2+}/\text{Mg}^{2+}$ hardness ions, resulting in softened water. The action leads to higher sodium concentrations and could also lead to a higher concentration of carbonate or bicarbonate ligands in the water. As the hardness ions are bound to the softener resin, without the carbonate ligands, higher C_t concentrations may be found in water.

Future work could be performed that compares the levels of $\text{PbO}_{2(\text{s})}$ in samples that have passed through a water heater, water softener, or a combination. This experimentation could be performed with synthetic water samples or tap water draws from sample residences. The integrated system would give insight into the speciation of Pb(II) and Pb(IV) (iodometric analysis), as well as the solid-dissolved fractions of Pb (ICP-OES analysis) with respect to temperature and ionic strength variation.

APPENDIX A: TABULATED THERMODYNAMIC & EQUILIBRIUM VALUES

Table A.1. Thermodynamic data for relevant Pb species: standard enthalpy of formation.

Species	ΔH°_f at 25°C (kJ mol ⁻¹)	Source
Pb(0)		
Pb (s)	0	[12]
Pb(II)		
Pb ²⁺	-1.02	[12],[9]
PbO (s) - Massicot/yellow	-219.09	[12]
PbO (s) - Litharge/red	-217.83	[12],[9],[13]
PbOH ⁺	-	
Pb(OH) ₂ (aq)	-	
Pb(OH) ₂ (s)	-515.46	[15],[16]
Pb(OH) ₃ ⁻	-	
Pb(OH) ₄ ²⁻	-	
PbHCO ₃ ⁺	-	
PbCO ₃ (s)	-662.51	[15], [16]
PbCO ₃ (aq)	-699.40	[14],[9]
Pb(CO ₃) ₂ (aq)	-	
PbCl ⁺ (aq)	-180.20	[14]
PbCl ₂ (s)	-359.35	[14], [15], [16]
PbCl ₂ (aq)	-335.98	[15]
PbCl ₃ ⁻ (aq)	-179.20	[14]
PbCl ₄ ²⁻ (aq)	-329.20	[14]
PbNO ₃ ⁺	-	
Pb(NO ₃) ₂ (s)	-226.63	[14], [15]
Pb ₃ (CO ₃) ₂ (OH) ₂ (s)	-1711.70	[15]

Table A.2. Thermodynamic data for relevant Pb species: standard Gibbs free energy of formation.

Species	ΔG°_f at 25°C (kJ mol ⁻¹)	Source
Pb(0)		
Pb (s)	0	[13], [12]
Pb(II)		
Pb ²⁺	-24.384	[12],[9]
PbO (s) - Massicot/yellow	-188.563	[12]
PbO (s) - Litharge/red	-187.903	[12],[9]
PbOH ⁺	-226.325	[9]
Pb(OH) ₂ (aq)	-400.83	[9],[16]
Pb(OH) ₂ (s)	-436.573	[9]
Pb(OH) ₃ ⁻	-575.71	[9]
Pb(OH) ₄ ²⁻	-	
PbHCO ₃ ⁺	-	
PbCO ₃ (s)	-625.51	[15]
PbCO ₃ (aq)	-625.767	[9],[14]
Pb(CO ₃) ₂ (aq)		
PbCl ⁺ (aq)	-239.955	[14],[15]
PbCl ₂ (s)	-314.075	[14], [15]
PbCl ₂ (aq)	-286.9	[15]
PbCl ₃ ⁻ (aq)	-369.725	[14], [15]
PbCl ₄ ²⁻ (aq)	-259	[15]
PbNO ₃ ⁺	-	
Pb(NO ₃) ₂ (s)	-251.65	[16]
Pb ₃ (CO ₃) ₂ (OH) ₂ (s)	-	[13], [12]

APPENDIX B: DETERMINATION OF ICP-OES ANALYSIS WAVELENGTH

Table B.1. ICP-OES output data at various wavelengths. Sixteen (16) replicates of eight (8) standards ranging from 1.0-20 ppb Pb were analyzed to determine the most accurate wavelength for Pb analysis. Standard deviation (STD Dev), relative standard deviation (RSD), limit of quantitation (LOQ), and instrument detection limit (IDL) were determined from the output data.

Wavelength (182.205 nm)	Average Pb Concentration	1	2	3	4	5	6	7	8	9	10	11	12	13	14	15	16	STD Dev	RSD	Recovery of STD	Accuracy Difference	LOQ	IDL (99% confidence)
		ppb	%	%	%	ppb	ppb																
STD 0.6 ppb	1.295	4.469	-1.008	0.446	1.901	1.930	1.141	-0.157	2.562	3.789	1.889	4.187	-1.920	-0.196	0.525	1.061	0.095	1.771	137%				
STD 1 ppb	1.720	0.380	4.845	2.374	1.094	2.182	2.803	-0.067	2.244	0.756	2.142	0.410	0.752	2.488	-0.142	2.217	3.035	1.300	76%				
STD 2 ppb	2.440	3.091	4.037	1.812	2.490	1.717	2.384	4.392	3.009	4.272	5.108	0.784	1.746	1.379	1.256	1.837	-0.271	1.414	58%				
STD 3 ppb	3.303	4.088	3.680	5.960	2.883	2.850	2.301	1.922	4.275	2.200	2.484	3.531	2.472	1.804	5.484	3.964	2.947	1.179	36%				
STD 5 ppb	5.982	6.201	6.220	3.804	6.659	5.128	4.184	6.035	5.307	3.792	11.040	6.375	3.822	6.634	6.752	6.387	7.373	1.733	29%				
STD 6 ppb	6.725	8.312	7.592	5.179	7.615	4.417	5.064	5.645	10.031	6.760	5.913	7.359	7.392	6.460	6.933	7.486	5.444	1.380	21%				
STD 10 ppb	10.665	12.104	11.008	10.652	10.253	10.605	13.037	9.556	9.825	11.565	9.644	7.774	11.695	10.485	11.341	11.767	9.332	1.242	12%				
STD 20 ppb	19.775	20.469	17.839	20.316	18.217	22.137	18.251	20.197	19.926	19.714	21.162	18.190	20.786	18.362	20.841	20.591	19.409	1.236	6%	97%	-3%	12.362	3.643
Wavelength (220.353 nm)	Average Pb Concentration	1	2	3	4	5	6	7	8	9	10	11	12	13	14	15	16	STD Dev	RSD	Recovery of STD	Accuracy Difference	LOQ	IDL (99% confidence)
		ppb	%	%	%	ppb	ppb																
STD 0.6 PPB	0.476	0.244	0.314	-0.505	-0.227	0.258	2.015	0.178	0.899	0.472	0.608	0.308	-0.052	1.491	-0.069	0.485	1.194	0.632	133%				
STD 1 ppb	0.787	0.622	1.273	0.523	1.583	0.727	1.030	0.908	0.667	1.102	0.795	0.677	1.548	0.897	0.534	0.273	-0.563	0.494	63%				
STD 2 ppb	1.728	1.875	0.983	2.572	1.727	1.148	1.403	1.997	1.449	1.796	1.306	1.621	1.296	3.087	1.889	1.568	1.929	0.512	30%				
STD 3 ppb	2.997	3.838	3.204	2.403	2.687	2.797	2.248	3.988	2.110	2.126	2.750	4.259	2.715	3.076	2.576	3.316	3.857	0.665	22%				
STD 5 ppb	4.682	4.235	4.679	4.118	4.831	4.518	3.025	4.373	6.266	5.229	4.478	4.496	4.104	6.009	5.379	5.283	3.880	0.786	17%				
STD 6 ppb	5.979	5.485	6.445	5.242	6.262	6.160	5.357	6.927	5.814	4.668	6.950	6.000	5.181	5.987	6.524	6.990	5.669	0.668	11%				
STD 10 ppb	10.626	9.988	10.353	10.448	10.835	10.686	10.959	11.020	10.639	9.805	10.084	10.272	10.730	10.008	11.071	11.636	11.476	0.516	5%	105%	5%	5.156004	1.519
STD 20 ppb	20.548	22.418	20.911	20.191	20.168	20.442	22.170	20.275	20.049	19.984	19.969	20.222	19.716	20.737	20.675	20.527	20.319	0.726	4%	100%	0%	7.256	2.138
Wavelength (216.999 nm)	Average Pb Concentration	1	2	3	4	5	6	7	8	9	10	11	12	13	14	15	16	STD Dev	RSD	Recovery of STD	Accuracy Difference	LOQ	IDL (99% confidence)
		ppb	%	%	%	ppb	ppb																
STD 0.6 PPB	0.244	7.475	-4.197	2.533	2.829	0.016	-8.599	-6.114	-5.197	3.262	0.320	3.210	4.091	8.404	-8.800	2.163	2.500	5.136	2109%				
STD 1 ppb	2.473	6.672	6.948	-4.510	-0.800	3.249	8.841	2.311	4.430	-3.861	1.751	3.038	0.858	4.094	-4.010	6.703	3.860	3.954	160%				
STD 2 ppb	1.251	0.152	1.735	4.897	-1.970	-4.138	4.736	-0.950	3.556	0.951	2.381	2.802	1.092	3.327	0.469	-2.064	3.036	2.492	199%				
STD 3 ppb	2.681	0.512	2.735	1.355	5.357	1.955	0.880	6.336	3.066	-5.004	6.980	4.134	3.349	0.631	8.932	-0.376	2.054	3.202	119%				
STD 5 ppb	6.631	7.035	2.226	3.682	10.481	13.187	4.273	7.199	6.906	2.545	5.430	4.752	8.491	5.383	5.365	10.707	8.437	2.960	45%				
STD 6 ppb	7.431	9.767	4.177	4.928	8.755	4.728	9.340	9.925	9.480	8.001	9.718	8.473	7.603	7.884	5.484	8.443	2.193	2.299	31%				
STD 10 ppb	10.785	9.476	10.263	9.227	12.421	9.540	5.045	8.169	15.778	15.315	9.140	8.456	9.791	9.811	12.708	12.634	14.786	2.818	26%				
STD 20 ppb	19.529	22.070	18.258	21.654	17.966	21.850	16.269	17.301	22.892	15.551	20.474	16.101	16.690	26.831	18.933	16.498	23.122	3.158	16%				

Wavelength (168.215 nm)	Average Pb Concentration	1	2	3	4	5	6	7	8	9	10	11	12	13	14	15	16	STD Dev	RSD	Recovery of STD	Accuracy Difference	LOQ	IDL (99% confidence)
		ppb	%	%	%	ppb	ppb																
STD 0.6 PPB	2.120	2.262	12.205	2.392	-2.483	3.573	2.104	-0.500	-0.687	-3.896	5.330	-3.133	2.601	5.030	3.381	1.793	3.940	3.772	178%				
STD 1 ppb	2.795	7.443	0.720	3.279	3.692	-0.478	2.189	1.059	2.426	4.494	2.748	3.319	5.341	0.590	-2.314	4.313	5.906	2.421	87%				
STD 2 ppb	2.808	-0.082	-3.596	0.969	8.742	4.273	0.121	1.533	9.138	0.449	7.720	-4.059	4.290	-4.235	1.488	6.595	11.584	4.748	169%				
STD 3 ppb	4.211	2.799	4.189	2.624	3.211	9.239	3.629	-0.031	7.251	4.432	7.629	4.714	2.454	3.223	5.053	3.409	3.556	2.182	52%				
STD 5 ppb	4.867	4.115	6.528	5.533	4.584	6.013	3.059	-0.297	5.465	2.720	4.867	10.352	5.539	4.200	3.319	5.426	6.454	2.183	45%				
STD 6 ppb	5.846	11.928	4.607	1.737	2.584	4.884	7.725	5.273	7.511	9.595	9.539	4.494	4.053	0.370	8.505	7.053	3.680	3.057	52%				
STD 10 ppb	11.393	8.414	6.883	18.832	9.477	12.764	5.895	10.623	9.420	9.640	15.826	11.623	18.318	10.087	14.674	9.742	10.070	3.644	32%				
STD 20 ppb	19.698	22.182	22.888	22.877	19.781	16.606	13.369	25.589	19.758	18.058	22.527	15.437	22.527	20.781	26.764	12.719	13.301	4.245	22%				

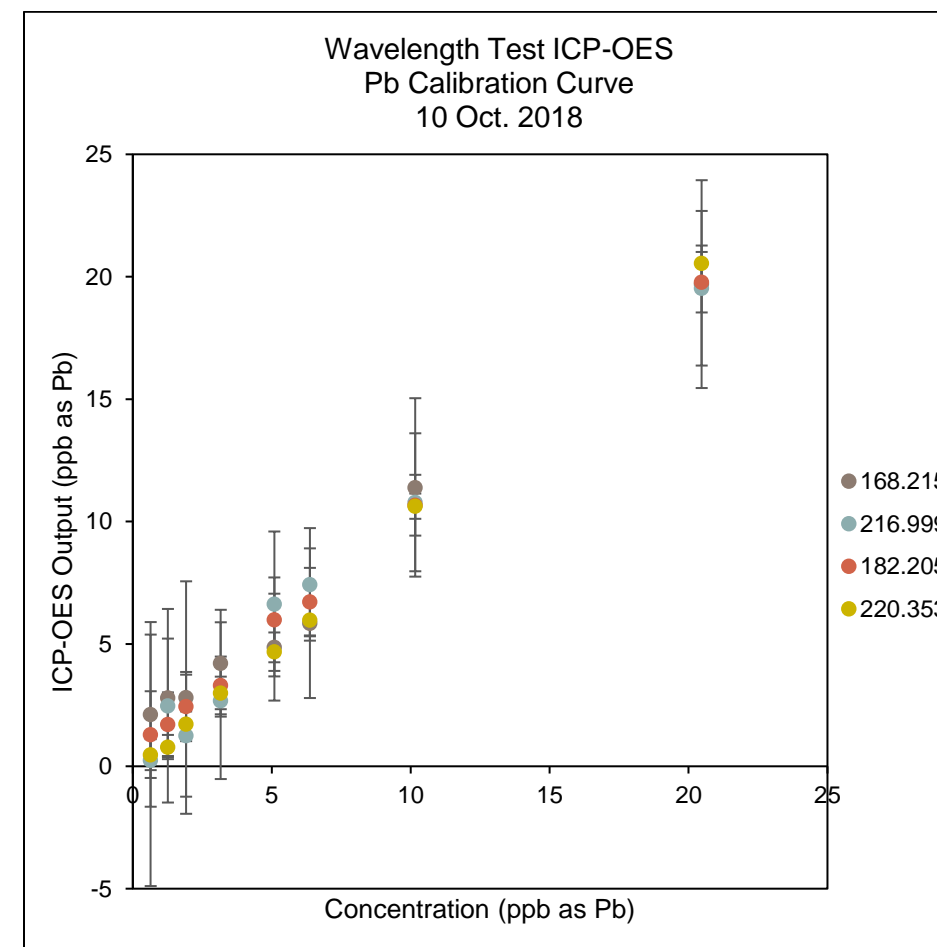


Figure B. 1. Experimental set to determine accurate wavelength for ICP-OES analysis of Pb. Due to consistency and accuracy of measurement, the author chose 220.353 nm.

APPENDIX C: EXPERIMENTAL KINETIC & EQUILIBRIUM DATA

For Pb-H₂O System

Table C.1. Kinetic data output from ICP-OES at pH 5.0, T = 25°C within glovebox.

Time (hours)	[Pb ²⁺] (ppb)	Std Dev. (ppb)	[Pb ²⁺] (M)	Standard Dev. (M)	[Pb ²⁺] Recovery (%)	Standard Dev. (%)
0.11	210.00	8.95	1.01X10 ⁻⁶	4.32X10 ⁻⁸	109%	5%
0.07	91.86	6.06	4.43X10 ⁻⁷	2.92X10 ⁻⁸	49%	3%
1.08	105.59	8.24	5.10X10 ⁻⁷	3.98X10 ⁻⁸	54%	5%
2.20	124.60	6.66	6.01X10 ⁻⁷	3.21X10 ⁻⁸	62%	3%
6.09	86.25	20.88	4.16X10 ⁻⁷	1.01X10 ⁻⁷	44%	11%

Table C.2. Kinetic and equilibrium data output from ICP-OES at pH 2.9-3.1, T = 25°C.

Time (hours)	pH initial	pH final	[Pb ²⁺] (ppb)	Std Dev. (ppb)	[Pb ²⁺] (M)	Std Dev. (M)	[Pb ²⁺] Recovery (%)	Std Dev. (%)
0.00	-	3.01	227.87	1.11	1.10X10 ⁻⁶	5.34X10 ⁻⁹	128%	0%
0.00	2.90	-	242.91	2.66	1.17X10 ⁻⁶	1.28X10 ⁻⁸	117%	1%
0.57	3.06	-	214.54	3.92	1.04X10 ⁻⁶	1.89X10 ⁻⁸	110%	2%
1.04	3.16	2.99	222.95	2.57	1.08X10 ⁻⁶	1.24X10 ⁻⁸	109%	1%
1.50	2.92	-	224.38	3.57	1.08X10 ⁻⁶	1.72X10 ⁻⁸	108%	2%
2.00	2.97	3.05	222.47	1.99	1.07X10 ⁻⁶	9.59X10 ⁻⁹	111%	1%
2.30	3.04	3.10	-	-	-	-	-	-
3.00	-	-	215.08	6.03	1.04X10 ⁻⁶	2.91X10 ⁻⁸	111%	3%
3.97	3.03	3.08	222.40	1.10	1.07X10 ⁻⁶	5.32X10 ⁻⁹	108%	0%
5.93	3.00	2.94	211.63	2.99	1.02X10 ⁻⁶	1.44X10 ⁻⁸	110%	1%
8.62	-	-	193.56	3.45	9.34X10 ⁻⁷	1.67X10 ⁻⁸	94%	2%
10.14	3.00	-	226.77	2.40	1.09X10 ⁻⁶	1.16X10 ⁻⁸	111%	1%
18.03	-	-	209.32	3.02	1.01X10 ⁻⁶	1.46X10 ⁻⁸	102%	1%
24.05	2.95	-	205.76	1.74	9.93X10 ⁻⁷	8.39X10 ⁻⁹	106%	1%
48.03	-	-	229.07	0.92	1.11X10 ⁻⁶	4.44X10 ⁻⁹	110%	0%
72.02	-	-	218.68	2.44	1.06X10 ⁻⁶	1.18X10 ⁻⁸	108%	1%
140.58	-	-	218.27	3.47	1.05X10 ⁻⁶	1.67X10 ⁻⁸	106%	2%
1008.23	2.85	2.96	10.12	2.11	4.88X10 ⁻⁸	1.02X10 ⁻⁸	5%	21%

Table C.3. Kinetic and equilibrium data output from ICP-OES at pH 3.0-3.1, T = 55°C.

Time (hours)	pH initial	pH final	[Pb ²⁺] (ppb)	Std Dev. (ppb)	[Pb ²⁺] (M)	Std Dev. (M)	[Pb ²⁺] Recovery (%)	Std Dev. (%)
0.00	-	-	210.33	16.02	1.02X10 ⁻⁶	7.73X10 ⁻⁸	105%	4%
0.02	-	-	95.55	4.05	4.61X10 ⁻⁷	1.96X10 ⁻⁸	47%	2%
0.54	-	-	97.03	3.45	4.68X10 ⁻⁷	1.66X10 ⁻⁸	48%	2%
1.01	3.13	3.11	95.74	3.41	4.62X10 ⁻⁷	1.65X10 ⁻⁸	47%	2%
1.52	-	-	92.22	4.72	4.45X10 ⁻⁷	2.28X10 ⁻⁸	48%	3%
2.02	3.00	3.00	90.08	9.01	4.35X10 ⁻⁷	4.35X10 ⁻⁸	44%	4%
2.52	-	-	93.21	3.91	4.50X10 ⁻⁷	1.89X10 ⁻⁸	48%	2%
3.01	-	-	99.87	4.13	4.82X10 ⁻⁷	1.99X10 ⁻⁸	49%	2%
4.01	3.03	3.03	94.88	7.33	4.58X10 ⁻⁷	3.54X10 ⁻⁸	47%	4%
6.02	3.07	3.05	91.91	12.76	4.44X10 ⁻⁷	6.16X10 ⁻⁸	45%	5%
10.17	2.97	2.97	94.26	8.91	4.55X10 ⁻⁷	4.30X10 ⁻⁸	46%	4%
12.12	-	-	96.20	4.42	4.64X10 ⁻⁷	2.13X10 ⁻⁸	48%	2%
24.01	-	-	100.13	5.42	4.83X10 ⁻⁷	2.62X10 ⁻⁸	49%	2%
48.53	-	-	96.99	2.36	4.68X10 ⁻⁷	1.14X10 ⁻⁸	47%	1%
1012.33	-	3.15	128.11	23.06	6.18X10 ⁻⁷	1.11X10 ⁻⁷	62%	11%

Table C.4. Kinetic and equilibrium data output from ICP-OES at pH 4.8-5.6, T = 25°C.

Time (hours)	pH initial	pH final	[Pb ²⁺] (ppb)	Std Dev. (ppb)	[Pb ²⁺] (M)	Std Dev. (M)	[Pb ²⁺] Recovery (%)	Std Dev. (%)
0.02	-	5.01	202.04	4.39	9.75X10 ⁻⁷	2.12X10 ⁻⁸	100%	2%
0.02	-	-	124.68	2.25	6.02X10 ⁻⁷	1.09X10 ⁻⁸	61%	1%
0.52	-	-	71.90	6.14	3.47X10 ⁻⁷	2.96X10 ⁻⁸	35%	3%
1.01	-	-	75.81	10.34	3.66X10 ⁻⁷	4.99X10 ⁻⁸	37%	5%
1.56	-	-	79.11	5.70	3.82X10 ⁻⁷	2.75X10 ⁻⁸	39%	3%
2.01	4.89	5.01	78.70	5.73	3.80X10 ⁻⁷	2.76X10 ⁻⁸	39%	3%
2.54	-	-	69.65	10.93	3.36X10 ⁻⁷	5.28X10 ⁻⁸	34%	5%
3.01	-	-	71.73	7.31	3.46X10 ⁻⁷	3.53X10 ⁻⁸	35%	3%
4.00	-	-	79.63	5.76	3.84X10 ⁻⁷	2.78X10 ⁻⁸	39%	3%
6.01	5.10	5.09	92.16	39.91	4.45X10 ⁻⁷	1.93X10 ⁻⁷	45%	19%
10.02	-	-	91.99	16.22	4.44X10 ⁻⁷	7.83X10 ⁻⁸	46%	7%
12.05	4.98	5.01	126.84	47.67	6.12X10 ⁻⁷	2.30X10 ⁻⁷	63%	24%
24.33	5.19	5.34	100.49	46.99	4.85X10 ⁻⁷	2.27X10 ⁻⁷	49%	24%
27.92	-	-	80.31	0.86	3.88X10 ⁻⁷	4.17X10 ⁻⁹	39%	0%
48.02	4.81	4.87	170.73	46.70	8.24X10 ⁻⁷	2.25X10 ⁻⁷	84%	22%
72.18	-	-	118.00	5.08	5.69X10 ⁻⁷	2.45X10 ⁻⁸	59%	3%
168.43	-	-	72.93	1.66	3.52X10 ⁻⁷	7.99X10 ⁻⁹	37%	1%
1010.22	-	5.57	184.52	13.19	8.91X10 ⁻⁷	6.37X10 ⁻⁸	92%	7%

Table C.5. Kinetic and equilibrium data output from ICP-OES at pH 4.0-5.2, T = 55°C.

Time (hours)	pH initial	pH final	[Pb ²⁺] (ppb)	Std Dev. (ppb)	[Pb ²⁺] (M)	Std Dev. (M)	[Pb ²⁺] Recovery (%)	Std Dev. (%)
0.03	-	5.16	217.60	4.45	1.05X10 ⁻⁶	2.15X10 ⁻⁸	109%	3%
0.02	-	-	94.62	17.03	4.57X10 ⁻⁷	8.22X10 ⁻⁸	53%	4%
0.58	-	-	118.03	7.88	5.70X10 ⁻⁷	3.80X10 ⁻⁸	62%	3%
1.04	-	-	115.29	13.65	5.56X10 ⁻⁷	6.59X10 ⁻⁸	60%	5%
1.53	-	-	118.10	8.25	5.70X10 ⁻⁷	3.98X10 ⁻⁸	59%	4%
2.03	5.04	4.98	89.22	5.22	4.31X10 ⁻⁷	2.52X10 ⁻⁸	46%	3%
2.58	-	-	104.94	13.78	5.06X10 ⁻⁷	6.65X10 ⁻⁸	55%	7%
3.03	-	-	91.38	5.38	4.41X10 ⁻⁷	2.60X10 ⁻⁸	46%	2%
4.01	-	-	100.11	9.13	4.83X10 ⁻⁷	4.41X10 ⁻⁸	50%	4%
6.16	5.04	4.89	110.65	26.12	5.34X10 ⁻⁷	1.26X10 ⁻⁷	55%	13%
10.08	4.96	4.89	115.05	20.55	5.55X10 ⁻⁷	9.92X10 ⁻⁸	58%	11%
12.02	4.96	4.71	193.91	34.42	9.36X10 ⁻⁷	1.66X10 ⁻⁷	96%	17%
23.89	-	-	22.79	2.74	1.10X10 ⁻⁷	1.32X10 ⁻⁸	11%	1%
48.17	4.93	4.44	186.68	4.94	9.01X10 ⁻⁷	2.39X10 ⁻⁸	93%	2%
96.92	-	4.40	148.19	15.35	7.15X10 ⁻⁷	7.41X10 ⁻⁸	72%	5%
1009.36	-	3.96	206.55	5.86	9.97X10 ⁻⁷	2.83X10 ⁻⁸	103%	3%

Table C.6. Kinetic and equilibrium data output from ICP-OES at pH 5.5-7.4, T = 25°C.

Time (hours)	pH initial	pH final	[Pb ²⁺] (ppb)	Std Dev. (ppb)	[Pb ²⁺] (M)	Std Dev. (M)	[Pb ²⁺] Recovery (%)	Std Dev. (%)
0.00	-	7.35	190.55	11.91	9.20X10 ⁻⁷	5.75X10 ⁻⁸	107%	20%
0.06	-	-	93.26	39.38	4.50X10 ⁻⁷	1.90X10 ⁻⁷	45%	19%
0.51	-	-	95.33	15.47	4.60X10 ⁻⁷	7.47X10 ⁻⁸	48%	8%
1.01	6.29	6.32	145.38	46.93	7.02X10 ⁻⁷	2.27X10 ⁻⁷	72%	24%
1.51	6.41	6.47	127.20	33.86	6.14X10 ⁻⁷	1.63X10 ⁻⁷	64%	18%
2.03	6.19	6.12	145.20	20.78	7.01X10 ⁻⁷	1.00X10 ⁻⁷	73%	11%
2.54	6.41	6.13	122.37	6.79	5.91X10 ⁻⁷	3.28X10 ⁻⁸	62%	3%
3.13	7.28	6.78	84.07	18.12	4.06X10 ⁻⁷	8.75X10 ⁻⁸	43%	11%
4.27	7.32	6.79	70.74	10.50	3.41X10 ⁻⁷	5.07X10 ⁻⁸	35%	5%
5.12	-	-	63.26	0.21	3.05X10 ⁻⁷	1.04X10 ⁻⁹	31%	0%
6.16	7.25	6.63	74.42	10.25	3.59X10 ⁻⁷	4.95X10 ⁻⁸	29%	11%
9.03	5.74	5.88	129.66	19.12	6.26X10 ⁻⁷	9.23X10 ⁻⁸	65%	9%
10.00	7.18	6.45	86.69	6.71	4.18X10 ⁻⁷	3.24X10 ⁻⁸	43%	4%
12.14	6.78	6.51	87.07	14.20	4.20X10 ⁻⁷	6.85X10 ⁻⁸	44%	7%
13.13	6.61	6.72	76.10	12.83	3.67X10 ⁻⁷	6.19X10 ⁻⁸	40%	6%
24.03	7.24	6.63	55.78	11.81	2.69X10 ⁻⁷	5.70X10 ⁻⁸	28%	6%

Table C.6. Kinetic and equilibrium data output from ICP-OES at pH 5.5-7.4, T = 25°C.
(Continued from previous.)

Time (hours)	pH initial	pH final	[Pb ²⁺] (ppb)	Std Dev. (ppb)	[Pb ²⁺] (M)	Std Dev. (M)	[Pb ²⁺] Recovery (%)	Std Dev. (%)
48.07	6.79	6.33	86.40	18.25	4.17X10 ⁻⁷	8.81X10 ⁻⁸	42%	9%
72.16	-	-	62.33	3.98	3.01X10 ⁻⁷	1.92X10 ⁻⁸	31%	2%
169.25	-	-	59.77	1.16	2.88X10 ⁻⁷	5.58X10 ⁻⁹	29%	1%
193.83	-	-	55.75	1.96	2.69X10 ⁻⁷	9.47X10 ⁻⁹	28%	1%
1014.19	-	5.45	152.26	69.28	7.35X10 ⁻⁷	3.34X10 ⁻⁷	65%	30%

Table C.7. Kinetic and equilibrium data output from ICP-OES at pH 4.1-6.8, T = 55°C.

Time (hours)	pH initial	pH final	[Pb ²⁺] (ppb)	Std Dev. (ppb)	[Pb ²⁺] (M)	Std Dev. (M)	[Pb ²⁺] Recovery (%)	Std Dev. (%)
0.02	-	6.81	194.60	6.93	9.39X10 ⁻⁷	3.34X10 ⁻⁸	96%	3%
0.01	-	-	28.24	3.98	1.36X10 ⁻⁷	1.92X10 ⁻⁸	15%	2%
0.50	-	-	33.10	1.98	1.60X10 ⁻⁷	9.56X10 ⁻⁹	17%	1%
1.00	-	-	32.46	1.79	1.57X10 ⁻⁷	8.63X10 ⁻⁹	16%	1%
1.55	-	-	32.81	2.82	1.58X10 ⁻⁷	1.36X10 ⁻⁸	17%	1%
2.02	-	-	37.56	6.07	1.81X10 ⁻⁷	2.93X10 ⁻⁸	19%	3%
2.54	-	-	34.76	2.82	1.68X10 ⁻⁷	1.36X10 ⁻⁸	18%	2%
3.01	-	-	32.69	2.82	1.58X10 ⁻⁷	1.36X10 ⁻⁸	16%	1%
4.05	6.48	6.22	38.76	17.78	1.87X10 ⁻⁷	8.58X10 ⁻⁸	20%	9%
6.14	6.54	5.97	62.08	9.04	3.00X10 ⁻⁷	4.36X10 ⁻⁸	30%	4%
10.00	5.92	5.16	74.90	14.44	3.62X10 ⁻⁷	6.97X10 ⁻⁸	36%	7%
12.00	-	-	46.37	3.41	2.24X10 ⁻⁷	1.64X10 ⁻⁸	23%	2%
24.27	-	4.81	52.81	5.85	2.55X10 ⁻⁷	2.83X10 ⁻⁸	26%	3%
48.30	-	-	54.62	2.52	2.64X10 ⁻⁷	1.22X10 ⁻⁸	27%	1%
1004.08	-	4.12	97.65	7.86	4.71X10 ⁻⁷	3.79X10 ⁻⁸	48%	4%

Table C.8. Kinetic and equilibrium data output from ICP-OES at pH 6.5-8.4, T = 25°C.

Time (hours)	pH initial	pH final	[Pb ²⁺] (ppb)	Std Dev. (ppb)	[Pb ²⁺] (M)	Std Dev. (M)	[Pb ²⁺] Recovery (%)	Std Dev. (%)
0.00	-	-	217.16	12.20	1.05X10 ⁻⁶	5.89X10 ⁻⁸	107%	4%
0.03	-	-	30.30	10.24	1.46X10 ⁻⁷	4.94X10 ⁻⁸	15%	5%
0.52	-	-	31.49	12.10	1.52X10 ⁻⁷	5.84X10 ⁻⁸	16%	5%
0.99	-	-	34.02	8.39	1.64X10 ⁻⁷	4.05X10 ⁻⁸	17%	4%
1.58	-	-	30.29	8.80	1.46X10 ⁻⁷	4.25X10 ⁻⁸	15%	4%
2.00	7.44	6.75	31.90	11.72	1.54X10 ⁻⁷	5.65X10 ⁻⁸	16%	5%
2.52	-	-	32.87	10.21	1.59X10 ⁻⁷	4.93X10 ⁻⁸	16%	5%
3.04	-	-	30.08	3.43	1.45X10 ⁻⁷	1.65X10 ⁻⁸	16%	2%
4.13	8.14	7.13	37.94	10.15	1.83X10 ⁻⁷	4.90X10 ⁻⁸	19%	5%
6.03	7.40	7.10	48.71	21.18	2.35X10 ⁻⁷	1.02X10 ⁻⁷	23%	11%
10.00	-	-	12.53	4.55	6.05X10 ⁻⁸	2.20X10 ⁻⁸	6%	2%
12.20	-	-	12.53	4.55	6.05X10 ⁻⁸	2.20X10 ⁻⁸	6%	2%
24.22	7.17	-	13.16	7.61	6.35X10 ⁻⁸	3.67X10 ⁻⁸	7%	4%
48.87	6.88	6.97	9.89	10.78	4.77X10 ⁻⁸	5.20X10 ⁻⁸	5%	5%
1016.82	8.35	6.49	47.05	28.71	2.27X10 ⁻⁷	1.39X10 ⁻⁷	23%	13%

Table C.9. Kinetic and equilibrium data output from ICP-OES at pH 4.9-8.9, T = 55°C.

Time (hours)	pH initial	pH final	[Pb ²⁺] (ppb)	Std Dev. (ppb)	[Pb ²⁺] (M)	Std Dev. (M)	[Pb ²⁺] Recovery (%)	Std Dev. (%)
0.00	-	8.85	198.54	46.55	9.58X10 ⁻⁷	2.25X10 ⁻⁷	102%	24%
0.02	-	8.80	41.80	25.42	2.02X10 ⁻⁷	1.23X10 ⁻⁷	22%	13%
0.54	-	-	13.91	6.25	6.71X10 ⁻⁸	3.02X10 ⁻⁸	7%	3%
1.01	-	-	8.85	1.30	4.27X10 ⁻⁸	6.27X10 ⁻⁹	5%	1%
1.58	-	-	8.18	0.93	3.95X10 ⁻⁸	4.49X10 ⁻⁹	4%	0%
2.05	-	7.17	7.69	1.07	3.71X10 ⁻⁸	5.18X10 ⁻⁹	4%	1%
2.50	-	-	17.39	20.52	8.39X10 ⁻⁸	9.91X10 ⁻⁸	9%	11%
3.00	-	-	12.07	16.26	5.82X10 ⁻⁸	7.85X10 ⁻⁸	6%	8%
4.10	8.10	7.03	8.89	1.29	4.29X10 ⁻⁸	6.25X10 ⁻⁹	5%	1%
6.06	7.50	6.81	7.24	1.81	3.49X10 ⁻⁸	8.73X10 ⁻⁹	4%	1%
10.24	8.58	-	8.32	2.95	4.02X10 ⁻⁸	1.42X10 ⁻⁸	4%	2%
12.10	7.85	6.62	30.52	8.33	1.47X10 ⁻⁷	4.02X10 ⁻⁸	16%	4%
24.12	7.10	5.57	44.99	2.31	2.17X10 ⁻⁷	1.11X10 ⁻⁸	23%	1%
48.49	-	-	50.89	3.35	2.46X10 ⁻⁷	1.61X10 ⁻⁸	26%	2%
1011.24	-	4.87	99.84	4.15	4.82X10 ⁻⁷	2.00X10 ⁻⁸	51%	2%

Table C.10. Kinetic and equilibrium data output from ICP-OES at pH 7.0-9.8, T = 25°C.

Time (hours)	pH initial	pH final	[Pb ²⁺] (ppb)	Std Dev. (ppb)	[Pb ²⁺] (M)	Std Dev. (M)	[Pb ²⁺] Recovery (%)	Std Dev. (%)
0.04	-	9.69	184.42	14.36	8.90X10 ⁻⁷	6.93X10 ⁻⁸	90%	7%
0.04	-	9.67	133.04	9.15	6.42X10 ⁻⁷	4.41X10 ⁻⁸	65%	4%
0.52	-	-	171.39	6.15	8.27X10 ⁻⁷	2.97X10 ⁻⁸	83%	3%
1.11	9.41	9.39	128.68	40.49	6.21X10 ⁻⁷	1.95X10 ⁻⁷	63%	19%
1.58	9.56	9.29	124.27	7.55	6.00X10 ⁻⁷	3.64X10 ⁻⁸	60%	4%
2.04	-	-	128.34	5.26	6.19X10 ⁻⁷	2.54X10 ⁻⁸	63%	2%
2.58	9.56	8.78	73.55	29.59	3.55X10 ⁻⁷	1.43X10 ⁻⁷	37%	14%
3.19	-	-	118.71	6.72	5.73X10 ⁻⁷	3.24X10 ⁻⁸	58%	3%
4.12	9.80	9.10	139.11	25.56	6.71X10 ⁻⁷	1.23X10 ⁻⁷	69%	13%
6.01	9.54	8.92	113.35	23.74	5.47X10 ⁻⁷	1.15X10 ⁻⁷	55%	11%
10.04	-	-	91.81	4.85	4.43X10 ⁻⁷	2.34X10 ⁻⁸	45%	2%
12.82	9.64	8.83	112.32	7.94	5.42X10 ⁻⁷	3.83X10 ⁻⁸	55%	4%
24.83	9.73	8.13	49.47	25.44	2.39X10 ⁻⁷	1.23X10 ⁻⁷	24%	12%
48.14	9.57	7.30	44.96	5.13	2.17X10 ⁻⁷	2.48X10 ⁻⁸	22%	2%
1010.72	9.50	7.02	70.31	11.19	3.39X10 ⁻⁷	5.40X10 ⁻⁸	34%	5%

Table C.11. Kinetic and equilibrium data output from ICP-OES at pH 4.4-9.5, T = 55°C.

Time (hours)	pH initial	pH final	[Pb ²⁺] (ppb)	Std Dev. (ppb)	[Pb ²⁺] (M)	Std Dev. (M)	[Pb ²⁺] Recovery (%)	Std Dev. (%)
0.04	-	9.24	165.63	6.01	7.99X10 ⁻⁷	2.90X10 ⁻⁸	81%	4%
0.03	-	9.29	116.01	26.02	5.60X10 ⁻⁷	1.26X10 ⁻⁷	57%	13%
0.52	9.43	9.18	12.21	6.53	5.89X10 ⁻⁸	3.15X10 ⁻⁸	6%	3%
1.01	-	-	10.80	3.22	5.21X10 ⁻⁸	1.56X10 ⁻⁸	5%	2%
1.54	8.98	-	4.50	3.31	2.17X10 ⁻⁸	1.60X10 ⁻⁸	2%	2%
2.07	-	-	3.49	2.53	1.68X10 ⁻⁸	1.22X10 ⁻⁸	2%	1%
2.38	9.32	8.05	-	-	-	-	-	-
3.01	-	-	-	-	-	-	-	-
4.00	-	-	7.59	6.93	3.66X10 ⁻⁸	3.34X10 ⁻⁸	4%	3%
6.04	9.33	7.57	24.08	41.42	1.16X10 ⁻⁷	2.00X10 ⁻⁷	12%	20%
10.24	-	8.90	-	-	-	-	-	-
12.08	9.49	7.08	9.35	5.54	4.51X10 ⁻⁸	2.67X10 ⁻⁸	5%	3%
13.06	-	-	36.27	47.40	1.75X10 ⁻⁷	2.29X10 ⁻⁷	18%	23%
24.14	9.36	6.81	29.44	28.33	1.42X10 ⁻⁷	1.37X10 ⁻⁷	15%	14%
47.64	9.38	6.79	89.48	53.80	4.32X10 ⁻⁷	2.60X10 ⁻⁷	47%	27%
1009.52	9.22	4.38	191.26	26.64	9.23X10 ⁻⁷	1.29X10 ⁻⁷	93%	13%

For Pb-H₂O-NaCl System at 25°C

Table C.6. Kinetic data output from ICP-OES at I = 8.5x10⁻⁶ M, pH 7.0, T = 25°C. (Graph repeated from Pb-H₂O system.)

Time (hours)	pH initial	pH final	[Pb ²⁺] (ppb)	Std Dev. (ppb)	[Pb ²⁺] (M)	Std Dev. (M)	[Pb ²⁺] Recovery (%)	Std Dev. (%)
0.00	-	7.35	190.55	11.91	9.20X10 ⁻⁷	5.75X10 ⁻⁸	107%	20%
0.06	-	-	93.26	39.38	4.50X10 ⁻⁷	1.90X10 ⁻⁷	45%	19%
0.51	-	-	95.33	15.47	4.60X10 ⁻⁷	7.47X10 ⁻⁸	48%	8%
1.01	6.29	6.32	145.38	46.93	7.02X10 ⁻⁷	2.27X10 ⁻⁷	72%	24%
1.51	6.41	6.47	127.20	33.86	6.14X10 ⁻⁷	1.63X10 ⁻⁷	64%	18%
2.03	6.19	6.12	145.20	20.78	7.01X10 ⁻⁷	1.00X10 ⁻⁷	73%	11%
2.54	6.41	6.13	122.37	6.79	5.91X10 ⁻⁷	3.28X10 ⁻⁸	62%	3%
3.13	7.28	6.78	84.07	18.12	4.06X10 ⁻⁷	8.75X10 ⁻⁸	43%	11%
4.27	7.32	6.79	70.74	10.50	3.41X10 ⁻⁷	5.07X10 ⁻⁸	35%	5%
5.12	-	-	63.26	0.21	3.05X10 ⁻⁷	1.04X10 ⁻⁹	31%	0%
6.16	7.25	6.63	74.42	10.25	3.59X10 ⁻⁷	4.95X10 ⁻⁸	29%	11%
9.03	5.74	5.88	129.66	19.12	6.26X10 ⁻⁷	9.23X10 ⁻⁸	65%	9%
10.00	7.18	6.45	86.69	6.71	4.18X10 ⁻⁷	3.24X10 ⁻⁸	43%	4%
12.14	6.78	6.51	87.07	14.20	4.20X10 ⁻⁷	6.85X10 ⁻⁸	44%	7%
13.13	6.61	6.72	76.10	12.83	3.67X10 ⁻⁷	6.19X10 ⁻⁸	40%	6%
24.03	7.24	6.63	55.78	11.81	2.69X10 ⁻⁷	5.70X10 ⁻⁸	28%	6%
48.07	6.79	6.33	86.40	18.25	4.17X10 ⁻⁷	8.81X10 ⁻⁸	42%	9%
72.16	-	-	62.33	3.98	3.01X10 ⁻⁷	1.92X10 ⁻⁸	31%	2%
169.25	-	-	59.77	1.16	2.88X10 ⁻⁷	5.58X10 ⁻⁹	29%	1%
193.83	-	-	55.75	1.96	2.69X10 ⁻⁷	9.47X10 ⁻⁹	28%	1%
1014.19	-	5.45	152.26	69.28	7.35X10 ⁻⁷	3.34X10 ⁻⁷	65%	30%

Table C.12. Kinetic and equilibrium data output from ICP-OES at I = 0.02 M, pH 7.0, T = 25°C.

Time (hours)	pH initial	pH final	[Pb ²⁺] (ppb)	Std Dev. (ppb)	[Pb ²⁺] (M)	Std Dev. (M)	[Pb ²⁺] Recovery (%)	Std Dev. (%)
0.17	-	7.05	198.67	8.84	9.59X10 ⁻⁷	4.27X10 ⁻⁸	100%	3%
0.06	-	6.89	166.91	6.63	8.06X10 ⁻⁷	3.20X10 ⁻⁸	83%	3%
0.53	7.01	6.63	141.39	6.54	6.82X10 ⁻⁷	3.16X10 ⁻⁸	71%	4%
1.01	6.92	6.76	140.06	7.84	6.76X10 ⁻⁷	3.78X10 ⁻⁸	69%	3%
1.52	6.86	6.73	142.91	5.73	6.90X10 ⁻⁷	2.77X10 ⁻⁸	72%	3%
2.21	6.97	6.73	126.05	10.06	6.08X10 ⁻⁷	4.86X10 ⁻⁸	60%	2%
2.51	6.91	6.64	144.57	9.75	6.98X10 ⁻⁷	4.70X10 ⁻⁸	72%	5%
3.32	6.92	6.71	121.53	15.33	5.87X10 ⁻⁷	7.40X10 ⁻⁸	62%	8%
3.99	6.97	6.66	136.65	16.31	6.60X10 ⁻⁷	7.87X10 ⁻⁸	69%	8%
6.13	6.89	6.54	148.81	12.78	7.18X10 ⁻⁷	6.17X10 ⁻⁸	74%	6%
10.01	7.11	6.56	133.72	14.41	6.45X10 ⁻⁷	6.96X10 ⁻⁸	67%	7%
12.16	7.03	6.42	111.12	28.58	5.36X10 ⁻⁷	1.38X10 ⁻⁷	56%	14%
24.02	6.90	6.65	112.08	23.08	5.41X10 ⁻⁷	1.11X10 ⁻⁷	56%	12%
48.17	6.95	6.54	145.64	5.72	7.03X10 ⁻⁷	2.76X10 ⁻⁸	74%	3%
983.56	6.95	6.99	113.77	21.52	5.49X10 ⁻⁷	1.04X10 ⁻⁷	52%	13%

Table C.13. Kinetic and equilibrium data output from ICP-OES at I = 0.07 M, pH 7.0, T = 25°C.

Time (hours)	pH initial	pH final	[Pb ²⁺] (ppb)	Std Dev. (ppb)	[Pb ²⁺] (M)	Std Dev. (M)	[Pb ²⁺] Recovery (%)	Std Dev. (%)
0.05	-	6.88	184.59	16.24	8.91X10 ⁻⁷	7.84X10 ⁻⁸	91%	8%
0.14	-	6.88	157.99	33.58	7.62X10 ⁻⁷	1.62X10 ⁻⁷	79%	16%
0.57	6.99	6.60	149.61	17.34	7.22X10 ⁻⁷	8.37X10 ⁻⁸	75%	8%
1.01	6.97	6.59	176.54	12.60	8.52X10 ⁻⁷	6.08X10 ⁻⁸	88%	6%
1.53	6.86	6.63	162.10	23.34	7.82X10 ⁻⁷	1.13X10 ⁻⁷	81%	11%
2.02	6.97	6.80	147.81	7.62	7.13X10 ⁻⁷	3.68X10 ⁻⁸	75%	5%
2.61	6.91	6.70	141.73	14.84	6.84X10 ⁻⁷	7.16X10 ⁻⁸	71%	8%
3.33	6.92	6.67	153.91	9.64	7.43X10 ⁻⁷	4.65X10 ⁻⁸	78%	5%
4.04	6.97	6.58	154.03	7.13	7.43X10 ⁻⁷	3.44X10 ⁻⁸	78%	4%
6.11	6.89	6.56	163.91	10.02	7.91X10 ⁻⁷	4.84X10 ⁻⁸	83%	5%
10.00	7.03	6.37	151.66	10.28	7.32X10 ⁻⁷	4.96X10 ⁻⁸	76%	5%
12.16	6.90	6.41	126.11	14.79	6.09X10 ⁻⁷	7.14X10 ⁻⁸	62%	7%
24.01	7.11	6.44	132.53	61.29	6.40X10 ⁻⁷	2.96X10 ⁻⁷	66%	30%
48.13	6.95	6.58	163.38	11.10	7.89X10 ⁻⁷	5.36X10 ⁻⁸	84%	5%
995.14	6.95	6.58	18.07	20.75	8.72X10 ⁻⁸	1.00X10 ⁻⁷	9%	10%

Table C.14. Kinetic and equilibrium data output from ICP-OES at I = 0.15 M, pH 7.0, T = 25°C

Time (hours)	pH initial	pH final	[Pb ²⁺] (ppb)	Std Dev. (ppb)	[Pb ²⁺] (M)	Std Dev. (M)	[Pb ²⁺] Recovery (%)	Std Dev. (%)
0.00	-	6.95	162.15	5.48	7.83X10 ⁻⁷	2.65X10 ⁻⁸	81%	3%
0.07	-	6.99	141.69	10.02	6.84X10 ⁻⁷	4.84X10 ⁻⁸	72%	4%
0.55	6.99	6.73	132.96	15.09	6.42X10 ⁻⁷	7.28X10 ⁻⁸	65%	7%
1.03	6.92	6.93	128.14	3.55	6.18X10 ⁻⁷	1.72X10 ⁻⁸	64%	2%
1.51	6.89	6.87	123.23	3.02	5.95X10 ⁻⁷	1.46X10 ⁻⁸	62%	2%
2.01	6.94	6.62	130.04	12.88	6.28X10 ⁻⁷	6.22X10 ⁻⁸	65%	6%
2.76	6.87	6.77	112.20	5.12	5.42X10 ⁻⁷	2.47X10 ⁻⁸	57%	2%
3.05	6.87	6.76	115.92	13.46	5.59X10 ⁻⁷	6.50X10 ⁻⁸	58%	7%
4.03	6.95	6.23	145.95	9.67	7.04X10 ⁻⁷	4.67X10 ⁻⁸	73%	5%
6.08	6.94	6.46	138.42	12.16	6.68X10 ⁻⁷	5.87X10 ⁻⁸	69%	6%
10.02	6.92	6.77	115.06	1.84	5.55X10 ⁻⁷	8.88X10 ⁻⁹	57%	1%
12.00	7.01	6.54	130.62	7.80	6.30X10 ⁻⁷	3.77X10 ⁻⁸	64%	4%
24.00	6.91	6.43	121.64	21.01	5.87X10 ⁻⁷	1.01X10 ⁻⁷	60%	11%
48.00	6.95	6.09	127.82	0.01	6.17X10 ⁻⁷	4.97X10 ⁻¹¹	65%	10%
994.53	7.11	6.63	37.84	1.35	1.83X10 ⁻⁷	6.50X10 ⁻⁹	19%	29%

Pb-H₂O-CO₂ System at 25°C

Table C.6. Kinetic data output from ICP-OES at C_t = 0 M, I = 8.5x10⁻⁶ M, pH 7.0, T = 25°C. No carbonate within this system. (Graph repeated from Pb-H₂O system.)

Time (hours)	pH initial	pH final	[Pb ²⁺] (ppb)	Std Dev. (ppb)	[Pb ²⁺] (M)	Std Dev. (M)	[Pb ²⁺] Recovery (%)	Std Dev. (%)
0.00	-	7.35	190.55	11.91	9.20X10 ⁻⁷	5.75X10 ⁻⁸	107%	20%
0.06	-	-	93.26	39.38	4.50X10 ⁻⁷	1.90X10 ⁻⁷	45%	19%
0.51	-	-	95.33	15.47	4.60X10 ⁻⁷	7.47X10 ⁻⁸	48%	8%
1.01	6.29	6.32	145.38	46.93	7.02X10 ⁻⁷	2.27X10 ⁻⁷	72%	24%
1.51	6.41	6.47	127.20	33.86	6.14X10 ⁻⁷	1.63X10 ⁻⁷	64%	18%
2.03	6.19	6.12	145.20	20.78	7.01X10 ⁻⁷	1.00X10 ⁻⁷	73%	11%
2.54	6.41	6.13	122.37	6.79	5.91X10 ⁻⁷	3.28X10 ⁻⁸	62%	3%
3.13	7.28	6.78	84.07	18.12	4.06X10 ⁻⁷	8.75X10 ⁻⁸	43%	11%
4.27	7.32	6.79	70.74	10.50	3.41X10 ⁻⁷	5.07X10 ⁻⁸	35%	5%
5.12	-	-	63.26	0.21	3.05X10 ⁻⁷	1.04X10 ⁻⁹	31%	0%
6.16	7.25	6.63	74.42	10.25	3.59X10 ⁻⁷	4.95X10 ⁻⁸	29%	11%
9.03	5.74	5.88	129.66	19.12	6.26X10 ⁻⁷	9.23X10 ⁻⁸	65%	9%
10.00	7.18	6.45	86.69	6.71	4.18X10 ⁻⁷	3.24X10 ⁻⁸	43%	4%
12.14	6.78	6.51	87.07	14.20	4.20X10 ⁻⁷	6.85X10 ⁻⁸	44%	7%
13.13	6.61	6.72	76.10	12.83	3.67X10 ⁻⁷	6.19X10 ⁻⁸	40%	6%
24.03	7.24	6.63	55.78	11.81	2.69X10 ⁻⁷	5.70X10 ⁻⁸	28%	6%
48.07	6.79	6.33	86.40	18.25	4.17X10 ⁻⁷	8.81X10 ⁻⁸	42%	9%
72.16	-	-	62.33	3.98	3.01X10 ⁻⁷	1.92X10 ⁻⁸	31%	2%
169.25	-	-	59.77	1.16	2.88X10 ⁻⁷	5.58X10 ⁻⁹	29%	1%
193.83	-	-	55.75	1.96	2.69X10 ⁻⁷	9.47X10 ⁻⁹	28%	1%
1014.19	-	5.45	152.26	69.28	7.35X10 ⁻⁷	3.34X10 ⁻⁷	65%	30%

Table C.15. Kinetic and equilibrium data output from ICP-OES at $C_t = 0.01$ M, $I = 0.01$ M, $pH^{\circ} = 7.0$, $T = 25^{\circ}\text{C}$. Not included in final data set.

Time (hours)	pH initial	pH final	[Pb ²⁺] (ppb)	Std Dev. (ppb)	[Pb ²⁺] (M)	Std Dev. M)	[Pb ²⁺] Recovery (%)	Std Dev. (%)
0.00	-	7.06	219.95	48.80	1.06×10^{-6}	2.36×10^{-7}	106%	26%
0.08	-	7.05	196.73	7.05	9.49×10^{-7}	3.40×10^{-8}	96%	4%
0.57	6.96	7.08	180.96	6.81	8.73×10^{-7}	3.29×10^{-8}	88%	3%
0.98	7.01	7.24	185.25	6.49	8.94×10^{-7}	3.13×10^{-8}	89%	5%
1.52	7.00	7.15	332.96	103.19	1.61×10^{-6}	4.98×10^{-7}	164%	51%
2.16	6.94	7.04	279.65	10.93	1.35×10^{-6}	5.28×10^{-8}	136%	5%
2.62	7.01	7.25	274.00	13.25	1.32×10^{-6}	6.39×10^{-8}	137%	6%
3.01	6.93	7.18	255.50	7.83	1.23×10^{-6}	3.78×10^{-8}	129%	4%
4.06	7.03	7.23	259.23	16.73	1.25×10^{-6}	8.07×10^{-8}	129%	8%
6.08	7.02	7.29	137.29	13.63	6.63×10^{-7}	6.58×10^{-8}	67%	7%
10.26	7.09	7.39	235.79	27.02	1.14×10^{-6}	1.30×10^{-7}	118%	13%
14.78	6.95	7.41	150.93	59.54	7.28×10^{-7}	2.87×10^{-7}	74%	29%
24.32	7.06	7.47	221.27	60.57	1.07×10^{-6}	2.92×10^{-7}	107%	29%
48.14	7.06	7.88	287.35	16.84	1.39×10^{-6}	8.13×10^{-8}	138%	8%
997.44	7.28	8.82	219.80	16.64	1.06×10^{-6}	8.03×10^{-8}	110%	8%

Table C.16. Kinetic and equilibrium data output from ICP-OES at $C_t = 0.07$ M, $I = 0.09$ M, $pH^{\circ} = 7.0$, $T = 25^{\circ}\text{C}$.

Time (hours)	pH initial	pH final	[Pb ²⁺] (ppb)	Std Dev. (ppb)	[Pb ²⁺] (M)	Std Dev. (M)	[Pb ²⁺] Recovery (%)	Std Dev. (%)
0.00	-	6.81	227.88	4.10	1.10×10^{-6}	1.98×10^{-8}	108%	2%
0.06	-	6.93	233.22	11.98	1.13×10^{-6}	5.78×10^{-8}	110%	6%
0.53	6.92	7.02	219.21	11.06	1.06×10^{-6}	5.34×10^{-8}	105%	6%
1.07	6.89	6.92	225.33	7.27	1.09×10^{-6}	3.51×10^{-8}	106%	3%
1.50	6.95	6.96	222.09	8.95	1.07×10^{-6}	4.32×10^{-8}	105%	4%
2.03	6.97	7.02	222.42	8.99	1.07×10^{-6}	4.34×10^{-8}	105%	4%
2.50	6.96	7.15	215.29	8.27	1.04×10^{-6}	3.99×10^{-8}	102%	4%
3.21	7.01	7.10	213.12	10.62	1.03×10^{-6}	5.13×10^{-8}	105%	5%
4.49	6.83	7.01	202.28	9.91	9.76×10^{-7}	4.79×10^{-8}	99%	6%
6.01	6.86	6.99	198.33	21.40	9.57×10^{-7}	1.03×10^{-7}	95%	11%
10.01	6.91	7.14	195.70	27.66	9.44×10^{-7}	1.34×10^{-7}	96%	14%
12.16	6.79	7.00	208.25	6.87	1.01×10^{-6}	3.31×10^{-8}	100%	3%
24.05	6.90	7.23	198.42	10.97	9.58×10^{-7}	5.30×10^{-8}	94%	5%
47.91	6.91	7.40	191.97	16.67	9.27×10^{-7}	8.04×10^{-8}	92%	8%
984.00	7.20	8.96	180.13	15.08	8.69×10^{-7}	7.28×10^{-8}	87%	8%

Table C.17. Kinetic and equilibrium data output from ICP-OES at $C_t = 0.14$ M, $I = 0.21$ M, $pH^\circ = 7.0$, $T = 25^\circ\text{C}$.

Time (hours)	pH initial	pH final	[Pb ²⁺] (ppb)	Std Dev. (ppb)	[Pb ²⁺] (M)	Std Dev. (M)	[Pb ²⁺] Recovery (%)	Std Dev. (%)
0.00	-	7.09	261.03	32.69	1.26×10^{-6}	1.58×10^{-7}	125%	16%
0.06	-	6.99	115.22	4.83	5.56×10^{-7}	2.33×10^{-8}	56%	3%
0.51	6.95	7.11	98.40	13.45	4.75×10^{-7}	6.49×10^{-8}	48%	7%
1.01	6.92	7.12	111.37	6.94	5.37×10^{-7}	3.35×10^{-8}	54%	2%
1.51	7.00	7.28	104.10	4.43	5.02×10^{-7}	2.14×10^{-8}	51%	2%
2.00	7.00	7.21	107.57	2.98	5.19×10^{-7}	1.44×10^{-8}	52%	2%
2.51	7.04	7.10	107.00	3.81	5.16×10^{-7}	1.84×10^{-8}	53%	2%
3.00	7.00	7.16	106.08	5.26	5.12×10^{-7}	2.54×10^{-8}	54%	3%
4.02	6.96	7.15	101.63	5.71	4.91×10^{-7}	2.75×10^{-8}	51%	3%
6.00	6.98	7.14	96.50	6.93	4.66×10^{-7}	3.35×10^{-8}	47%	3%
10.36	6.92	7.10	100.05	4.21	4.83×10^{-7}	2.03×10^{-8}	50%	2%
12.02	6.90	7.22	97.37	4.71	4.70×10^{-7}	2.28×10^{-8}	48%	2%
24.00	6.90	7.39	96.35	6.19	4.65×10^{-7}	2.99×10^{-8}	47%	3%
48.64	7.03	7.53	103.35	5.42	4.99×10^{-7}	2.61×10^{-8}	50%	3%
984.00	7.34	8.82	92.78	7.84	4.48×10^{-7}	3.78×10^{-8}	46%	4%

APPENDIX D. IODOMETRIC METHOD

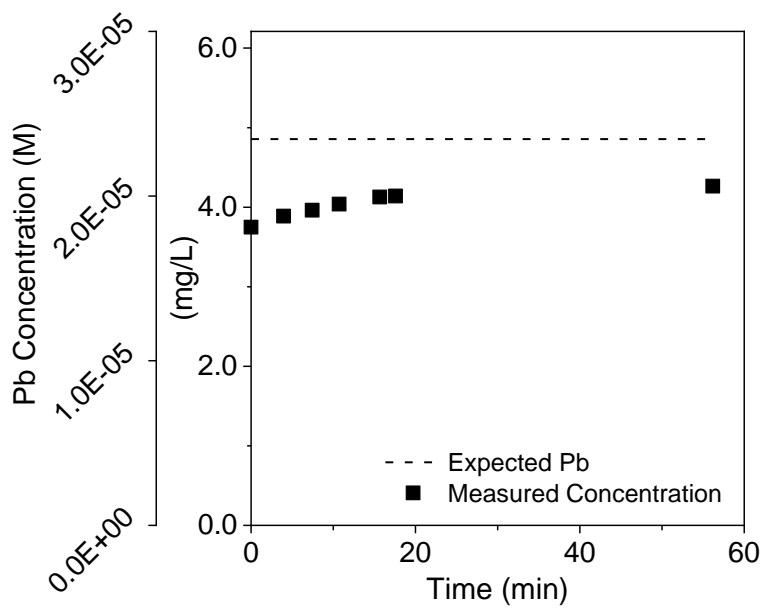


Figure D.1. Determination of $\text{PbO}_{(s)}$ via triiodide measurement using the iodometric method.
Experiment duration of 60 minutes to ensure full recovery of Pb over time.

Table D.1. Summary of results from iodometric method experiments. Organized by original mass added of $\text{PbO}_{2(s)}$. Average recovery ranged from $81\pm10.8\%$, excluding over-recovered samples.

Mass added (mg PbO_2)	Known [Pb] (mg/L as Pb)	Measured [Pb] (mg/L as Pb)	Known [Pb] (M as Pb)	Measured [Pb] (M as Pb)	Recovery (%)
0.01	0.01	0.05	4.18×10^{-8}	2.69×10^{-7}	644%
0.04	0.03	0.41	1.67×10^{-7}	2.24×10^{-6}	1339%
0.062	0.05	0.04	2.59×10^{-7}	2.10×10^{-7}	81%
0.062	4.30	3.44	2.07×10^{-5}	1.66×10^{-5}	81%
0.150	0.13	0.12	6.27×10^{-7}	5.79×10^{-7}	92%
0.431	1.38	1.08	1.80×10^{-6}	1.41×10^{-6}	78%
0.623	1.97	1.56	2.60×10^{-6}	2.06×10^{-6}	79%
2.000	1.74	1.43	8.36×10^{-6}	6.88×10^{-6}	82%
2.036	1.76	1.44	8.51×10^{-6}	6.94×10^{-6}	81%
2.054	1.78	1.55	8.59×10^{-6}	7.47×10^{-6}	87%
2.300	2.00	1.07	9.62×10^{-6}	5.12×10^{-6}	53%
2.335	2.02	1.89	9.76×10^{-6}	9.15×10^{-6}	94%
2.500	2.18	2.07	1.05×10^{-5}	9.95×10^{-6}	95%
3.727	3.03	2.29	1.56×10^{-5}	1.18×10^{-5}	76%
4.137	3.25	3.34	1.73×10^{-5}	1.78×10^{-5}	103%
5.620	4.86	4.27	2.35×10^{-5}	2.06×10^{-5}	88%
6.566	5.31	5.03	2.74×10^{-5}	2.60×10^{-5}	95%
8.099	7.01	6.07	3.39×10^{-5}	2.93×10^{-5}	87%
8.142	7.05	5.97	3.40×10^{-5}	2.88×10^{-5}	85%
8.194	7.09	5.87	3.43×10^{-5}	2.83×10^{-5}	83%
9.959	8.63	7.76	4.16×10^{-5}	3.74×10^{-5}	90%
10.165	8.81	6.21	4.25×10^{-5}	3.00×10^{-5}	71%
10.342	8.91	7.37	4.32×10^{-5}	3.58×10^{-5}	83%
11.708	10.16	8.61	4.89×10^{-5}	4.15×10^{-5}	85%
12.020	10.41	6.00	5.03×10^{-5}	2.90×10^{-5}	58%
12.234	10.61	6.86	5.11×10^{-5}	3.31×10^{-5}	65%
12.463	10.79	7.76	5.21×10^{-5}	3.75×10^{-5}	72%
13.667	11.90	8.67	5.71×10^{-5}	4.16×10^{-5}	73%
15.105	13.09	10.83	6.31×10^{-5}	5.23×10^{-5}	83%
15.183	13.15	11.14	6.35×10^{-5}	5.38×10^{-5}	85%
17.348	15.05	12.01	7.25×10^{-5}	5.79×10^{-5}	80%